SPECTRAL ANALYSIS

CLASSIFICATION SONARS

A thesis presented for the degree of

Doctor of Philosophy

in Electrical Engineering

at the

University of Canterbury,

Christchurch, New Zealand

by

Dolf de Roos, B.E. (hons)

1986

ABSTRACT

Sonar target classification based on frequency-domain echo analysis is investigated. Conventional pulsed sonars are compared with continuous transmission frequency modulated (CTFM) sonars, and differences relating to target classification are discussed. A practical technique is introduced which eliminates the blind time inherent in CTFM technology.

The value and implications of modelling underwater sonars in air are discussed and illustrated. The relative merits of auditory, visual and computer analysis of echoes are examined, and the effects of using two or more analysis methods simultaneously are investigated.

Various statistical techniques for detecting and classifying targets are explored. It is seen that with present hardware limitations, a two-stage echo analysis approach offers the most efficient means of target classification.

A novel design for three-section quarter-wavelength transducers is presented and evaluated. Their inherently flat frequency response makes these transducers well suited to broadband applications.

The design philosophy and construction details of a Diver's Sonar and an underwater Classification Sonar are given. Sea trials reveal that using the Diver's Sonar, a blind-folded diver can successfully navigate in an unknown environment, and locate and classify targets; using the Classification Sonar, targets may be located and classified using either operators or computer software.

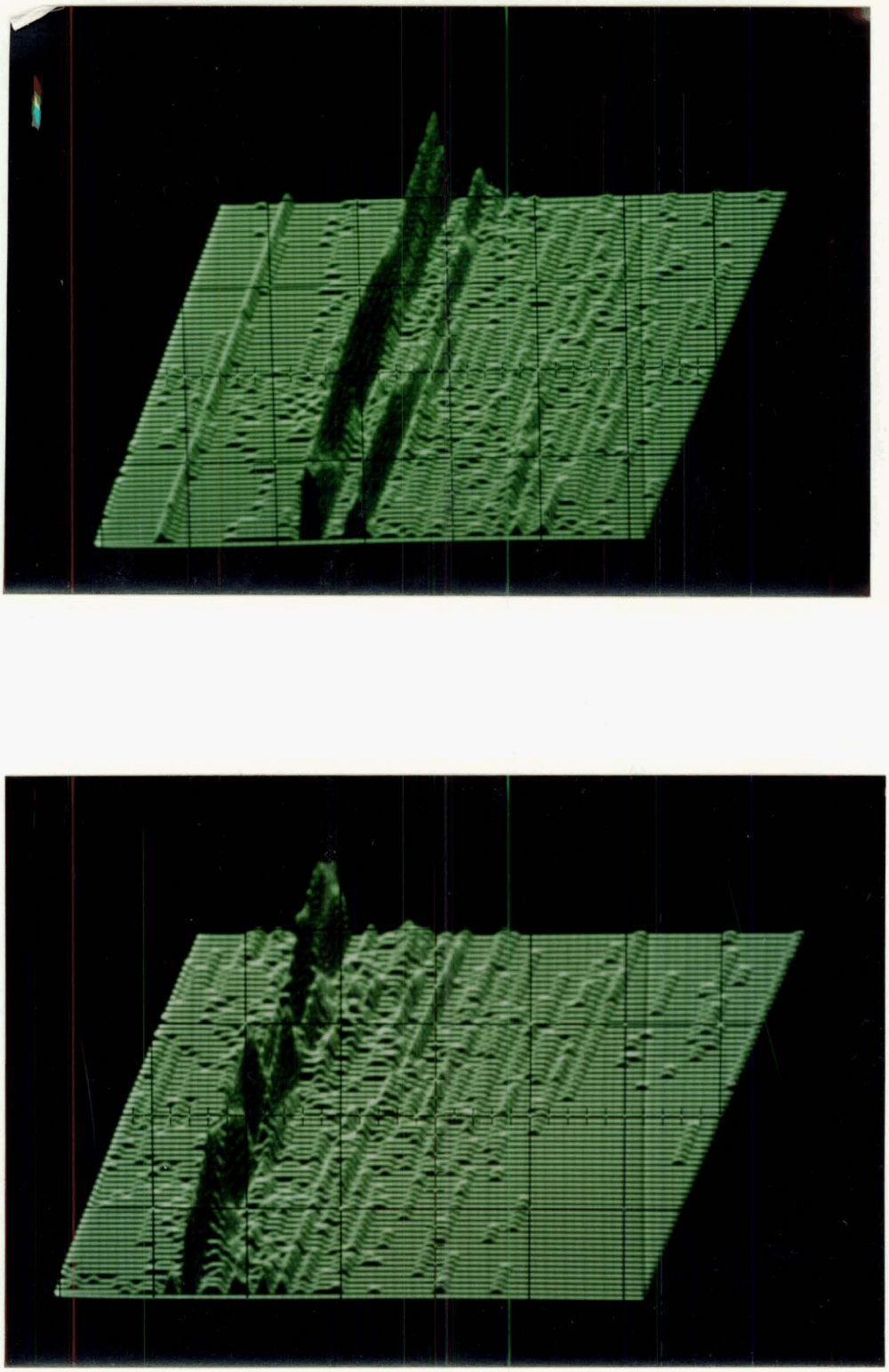

Figure 1 : Stack Plot displays showing the frequency responses of a -21dB sphere (top) and a scuba diver (bottom).

ACKNOWLEDGEMENTS

Firstly, I must thank my supervisor, Professor Leslie Kay, whose ideas and hypotheses sparked off my interest in this project. His intuitive grasp on the whole sonar field is extremely comprehensive and reflects the lifetime of dedication he has given it.

Professor Kay's propensity to extensive travel abroad has, however, resulted in a large part of my day to day contact being with my associate supervisor, Dr Peter Gough. With an uncompromising attitude towards relevance, Dr Gough has provided me with much-valued support and guidance.

Much of the experimental work and system development reported in this thesis could not have been carried out without the skills and enthusiasm of many individuals. Thanks are due to Art Vernon, the craftsman behind the diver's sonar transducers, who never complained about being given yet another design. Together we spent days on end in a shack known as the fish hut, testing a long succession of new transducer designs, and later calibrating and matching transducer elements and arrays.

I am particularly appreciative of the contributions of Mike Cusdin who designed and developed much of the sonar electronics referred to in this thesis. Mike's fifteen years of practical experience in building CTFM sonars is reflected in his engineering proficiency.

I would also like to thank my colleague Julian Sinton, with whom I shared the large ultrasonics laboratory and had many useful discussions. Julian put in a prodigious effort designing and constructing the computer

system used in the Classification Sonar.

Financial support during various phases of the research is acknowledged from the N.Z. Ministry of Agriculture and Fisheries, and from Edo Western Corporation (Salt Lake City, Utah).

Finally, I would like my family to know that their encouragement and support, not only for the duration of these studies but ever since I can remember, has always been tacitly appreciated and deeply valued, and I now take the opportunity to express my thanks to them.

PUBLICATIONS

During the course of the research leading to this dissertation, the following papers were published:

de Roos, A., Kay, L., Cusdin, M.J. & Vernon, A.N. (1981). **"A Sonar Aid for Divers using Binaural Displays"**, Ultrasonics International '81 Conference Proceedings, IPC Science and Technology Press, pp 171-175.

Kay, L., Kay, N., Sinton, J.J., de Roos, A. (1981). **"Characterization of Surface and Volume Structure using an Air Sonar with Auditory Display for the Blind"**, Ultrasonics International '81 Conference Proceedings, IPC Science and Technology Press, pp 38-42.

de Roos, Dolf, Cusdin, M.J., Kay, L. (1983). **"A Diver's Sonar with Auditory Display"**, Transactions of the Institution of Professional Engineers of New Zealand, Vol. 10, No. 2, July, pp 55-58.

Gough, P.T., de Roos, A., Cusdin, M.J. (1984). **"A Continuous Transmission F.M. Sonar with One Octave Bandwith and No Blind Time"**, Proc. I.E.E., Vol. 131, No. 3, Part F (Special Issue on Sonar Systems), June, pp 270-274.

Cusdin, Michael J. & de Roos, Adolf (1984). **"CTFM Sonar Enhances Diver's Eyes with Sound"**, Sea Technology, Vol. 25, No. 9, Sept., pp 44-46.

Cusdin, M.J., de Roos, A., Gough, P.T. & Sinton, J.J. (1984). **"A New Type of CTFM sonar with no Blind Time and a One Octave Bandwidth"**, New Zealand National Electronics Conference Proceedings, Vol. 21, pp 59-64.

Gough, P.T., Cusdin, M.J., de Roos, A. & Sinton, J.J. (1984). **"A High Speed Side Scan Sonar based on Wide Band CTFM"**, Proceedings International Conference on Developments in Marine Acoustics, (Sydney, Dec. 4-6), Australian Acoustical Society, pp 225-230.

CONTENTS

CHAPTER 1

INTRODUCTION

This thesis is concerned with systems and processing methods that have potential for improving the classification of objects using ultrasound. Four media are commonly probed by ultrasound : mammalian tissue (principally for medical diagnosis), solids (non-destructive testing), air, and water. The research detailed here is primarily concerned with the latter two. Although air sonars have been in limited use for some time, their use may soon increase dramatically as sonar systems are incorporated into robots. However, at present, the most common use of ultrasonics is with underwater sonars.

Underwater sonars for exploring the seabed generally operate in the high frequency range of 100-500 kHz and are consequently capable of providing useful information up to a maximum distance of around 400m (Flemming et al., 1982). They suffer severe limitations because of the physical properties of the sea as a propagating medium for sound - the only wave energy which can usefully propagate beyond a few metres. Furthermore, the aperture through which the sea and its boundaries are viewed is limited in practical systems to a few tens of wavelengths, and the bandwidth to a few tens of kilohertz, producing azimuthal and radial resolution elements of the order of 1m by 0.1m depending upon system parameters (Lee, 1979).

Although these sonars are described as having "high resolution" (Griffiths et al., 1978; Milne, 1980; Dybedal et al., 1985), practical systems for viewing the seabed for up to say 400m do not therefore provide a means for

identifying objects lying on the seabed. Even classifying them as belonging to a set of objects is difficult for distances much beyond 50m.

In areas where debris can be dumped, as in harbours, the problem of distinguishing between man's deposits and naturally occurring objects becomes exceedingly difficult. Nevertheless, for both civilian applications (e.g. salvage operations) and military applications (e.g. mine clearance), it is highly desirable that a means be found for making such a distinction.

Experiments have shown that the porpoise is capable of distinguishing between small objects at least better than man has so far managed (Busnel & Fish, 1980). This establishes that the physical means exists to an extent that man has not yet been able to exploit. Attempts to determine and emulate the essential features of the porpoise's sonar that enable fine discriminations have so far failed.

While many electronic sonars are based on pulse technology and therefore model the biological sonar of the porpoise, there is another class of sonars based on frequency modulation which more closely models the biological sonar of some species of bats. This thesis compares the two general classes of sonars, and shows how the FM system may be more relevant for target classification. Two sonars are described which have been built to test various hypotheses. The results of sea trials indicate that some progress has been made towards the goal of classification.

1.1 THESIS ORGANISATION

The thesis is divided into two parts. In Chapters 2 to 6, the theoretical aspects of sonar synthesis, echo processing and display interpretation are considered in relation to target classification. Chapters 7 to 10 detail the design, construction, and results of sonar systems built to test hypotheses and assumptions.

More specifically, Chapter 2 outlines the development of pulsed and CTFM (continuous transmission frequency modulated) sonars, and considers the influence of research into biological sonar systems on electronic sonar

design. This is followed by a comparison between pulsed, chirped, and CTFM sonars with respect to operating principles and practical limitations.

In Chapter 3, a technique is described which eliminates the blind time inherent in traditional CTFM sonars. Named 'dual demodulation', the technique is incorporated in sonars described in subsequent chapters.

In Chapter 4, the implications of modelling underwater sonars in air are considered, and examples are given of models used to check assumptions and help design sonars described elsewhere in the thesis. Chapter 5 compares visual, auditory and computer detection and classification of targets, and considers the consequences of using several processing methods simultaneously. Chapter 6 details the information required for target classification and studies various methods of processing this information.

In Chapter 7, a diver's sonar is described which can aid mobility and classify objects. The results of sea trials are presented.

Chapter 8 details a side scan sonar built to enable both operator and computer target detection and classification. The software written to provide automated detection and classification is outlined in Chapter 9, while Chapter 10 presents the results sea trials conducted in a harbour environment.

Concluding remarks and suggestions for further research are presented in Chapter 11.

CHAPTER 2

THE CTFM SONAR SYSTEM

2.1 INTRODUCTION

Although contemporary sonar (and radar) designs are predominantly based on pulsed technology, many other techniques have at some stage been popular. Early radars, for instance, were based on continuous wave interference (CW), and pulsed radars even encountered much scepticism in the mid 1930s when they were first proposed and tested (Skolnik, 1980).

Early sonars used pulses, but during the 1940s, when the war effort spurred intensive sonar research and development, CTFM systems became very popular. Kurie (1946) details eleven advantages of FM sonar systems over 'conventional' systems, some of which have at least partially lost their relevance (e.g. relative immunity from countermeasures) and others which are still relevant today (e.g. continuous and easily monitorable auditory outputs).

Work on FM sonars continued into the 1950s, but the emphasis shifted back to pulsed technology. This shift came about for two reasons. Firstly, significant advances had been made in pulsed radars, and many of the techniques were being applied to sonars (e.g. chirped pulses). Secondly, state-of-the-art electronics favoured pulse systems. Pulsed sonars operate in the time domain, and require accurate gating and timing mechanisms which were available at the time. FM sonars, on the other hand, operate in the frequency

domain, and require accurate and linear frequency modulators, and spectrum analyzers with narrow fractional bandwidth filters (or their equivalents). Adequate components were not generally available, and thus while many innovative ideas were postulated, they could often not be implemented. Consequently, FM sonars lagged behind those based on pulse technology.

Meanwhile, bat echo-location had been independently discovered by Griffin (Pierce & Griffin, 1938) and Dijkgraaf (Dijkgraaf, 1943; 1946). Early investigations of bat sonars did not so much influence engineering designs as justify the concept of a man-portable sonar system (Slaymaker & Meeker, 1948). However, the publication of "Listening in the Dark" (Griffin, 1958a) was followed by increased interest in the echolocating systems of bats, many of which use some form of FM sonar. While initial investigations concentrated on analysing bat sonar systems (e.g. Pye, 1960; Kay, 1962a; Kay & Pickvance, 1963), these studies inevitably led to hypotheses that if man's sonars were based on those of bats, comparable results should be achievable (e.g. Griffin, 1958b; Kay, 1962b). More recent research combines refinements of theories on the operation of bat sonars with the development of sophisticated bionic sonars. Such research may influence signal synthesis (e.g. Altes & Titlebaum, 1970; Escudie & Hellion, 1975), signal processing (e.g. Johnson & Titlebaum, 1976; Altes, 1976) or target classification (e.g. Skinner et al., 1977).

Lately there has been increased interest in CTFM sonars. Although various devices have been developed at the University of Canterbury over the last 20 years, such as blind aids (e.g. Kay, 1974), heart monitors (e.g. Kay et al., 1977), and fishing sonars (Do, 1977), CTFM technology is now being used in a number of applications such as diving (Ametek, 1978; de Roos et. al, 1981), side scanning (Gough et. al, 1984b) and robotics (Kay, 1985). The CTFM principle has similarly found new applications in radars (e.g. Neininger 1977; Clarricoats, 1977).

The reasons for the resurgence of interest in CTFM technology are diverse. A large contributing factor is that technology and electronics have caught up with theory - for example, the advent of extremely accurate and phase-controllable digital frequency synthesizers has enabled sophisticated demodulation systems that would not even have been attempted in the 1950's, while high speed digital FFT's have greatly improved spectral analysis.

The enhanced quality of CTFM sonar outputs resulting from current technology has enabled some of the inherent advantages of CTFM over conventional (pulsed) technology to be realised. For example, range resolution can be traded for response time, and targets can be observed continuously, two features no pulsed sonar can match. Nonetheless, there are still some disadvantages relative to pulsed sonars.

The remainder of this chapter compares CTFM sonars with pulsed sonars in terms of both theoretical capabilities and operational practicalities.

2.2 COMPARISON BETWEEN PULSED AND CTFM SYSTEMS

2.2.1 Operating Principles

There are many kinds of sonar technologies, although the differences are often very subtle. The present discussion considers three general systems: the short pulse sonar, the chirped linear FM pulse sonar, and the CTFM sonar. It is seen that while the output of the chirped linear FM pulse sonar appears similar to that of the (short) pulse sonar after demodulation, its demodulation process is functionally equivalent to that of the CTFM sonar.

Short pulse sonars radiate a repetitive train of pulsed tone, and measure the time delay between the transmission of a pulse and the detection of an echo to determine the range to a target. For a transmitted signal given by the real part of

$$s(t) = e^{j2\pi f_c t}.\mathrm{rect}[t/T_c - 1/2] \qquad (2.1)$$

for the period $0 < t < T$ and repeated every T seconds,

where f_c is the operating frequency,
T is the pulse repetition period, and
T_c is the pulse length,

the received echo from a single target at range R (with zero target velocity) is a delayed replica of the transmitted pulse given by

$$e(t) = As(t - 2R/c) \tag{2.2}$$

repeated every T seconds,
where A is a constant, and
c is the speed of sound.

The range to the target can be determined from the time delay between the transmitted pulse and the echo, since $R = c\Delta t/2$, where Δt is the time delay.

The received echo is passed through a narrowband filter (one whose bandwidth is small compared to the centre frequency) centred on the modulation frequency, which rejects the out-of-band noise and thus improves the signal/noise ratio. However, the range resolution, i.e. the ability to distinguish two targets not well separated in range, is improved by transmitting as short a pulse as possible. Typically, this pulse may be several tens of wavelengths long, but a lower limit of 8 or 10 wavelengths is often seen as a compromise between the desire for good range resolution and the ability of the bandpass filter to reject the out-of-band noise.

Since the average power radiated is proportional to the pulse length, as the pulse length is decreased to improve range resolution, the average power is decreased. As well, the total noise is now increased since the bandpass filter must be wider to pass the shorter pulse. To increase the average power radiated and yet retain the range resolution capability of a short pulse, the transmitted pulse can be chirped. The chirped pulse is many wavelengths long with the initial frequency either higher or lower than the terminal frequency; usually this frequency change is linear. In this case, the transmitted signal is the real part of

$$s(t) = e^{j2\pi(f_2 t - mt^2/2)}.\mathrm{rect}[t/T_c - 1/2] \tag{2.3}$$

for the period $0 < t < T$, and repeated every T seconds,
where f_2 is the initial frequency,
m is the sweep rate given by $m = (f_2 - f_1)/T$, and
f_1 is the terminal frequency.

For a decreasing frequency/time characteristic, $f_2 > f_1$. Now the received echo from a single target at range R (with zero target velocity) is a delayed replica of the chirp given by

$$e(t) = As(t - 2R/c), \tag{2.4}$$

for $0 < t < T$, repeated every T seconds.

There are two methods of processing echoes received from chirped sonars: matched filtering and correlation processing. Both methods, although considerably different in implementation, are equivalent in that both produce the same maximum possible S/N at their outputs (Wainstein & Zubakov, 1962).

A matched filter is described by

$$H(\omega) = S^*(\omega)\, e^{-j\omega\delta T} \tag{2.5}$$

and $$h(t) = s(\delta T - t) \tag{2.6}$$

where $H(\omega)$ is the frequency response of the filter,
$h(t)$ is its impulse response,
$S(\omega)$ is the transmitted signal spectrum,
$S^*(\omega)$ is its complex conjugate,
$s(t)$ is the transmitted signal waveform, and
δT is a delay required to realise the filter.

Matched filtering is most commonly implemented using the pulse compression receiver (Ohman, 1960) which has a frequency sensitive delay that retards the initial frequency by the length of the chirp while not retarding the terminal frequency at all. The process is intended to compress the chirp into an impulse. The output waveform y(t) of the matched filter is given by

$$y(t) = \int_{-\infty}^{\infty} h(\tau).e(t-\tau)\, d\tau \tag{2.7}$$

where e(t) is the received signal waveform. Using Equation (2.6) for h(t) and assuming the received signal is a replica of the transmitted signal

delayed by ΔT and diminished by a factor k, we obtain

$$y(t) = k\int_{-\infty}^{\infty} s(\delta T-\tau).s(t-\tau-\Delta T)\, d\tau. \tag{2.8}$$

Cook (1960) has shown that for a transmitted signal of unit amplitude and of the form of Equation (2.3), y(t) is given by

$$y(t) = kT\sqrt{m}\,\frac{\sin(\pi mtT)}{\pi mtT}.e^{j2\pi(f_2 t + mt^2/2 + 1/8)} \tag{2.9}$$

The envelope of the output pulse is seen to have a sinx/x form and the effective pulse width (measured at the -4 dB points) is $1/mT = 1/\Delta f$, where $\Delta f = f_2 - f_1$. Also, the peak power of the output pulse is $k^2T\Delta f$ compared with the peak input power which was k^2. The pulse compression filter has thus compressed the received pulse by a factor $T\Delta f$ and increased its peak power by the same factor.

The correlation receiver (Glisson & Sage, 1970) attempts to determine the cross correlation function of transmitted and received signals, $c_{tr}(\tau)$, given by

$$c_{tr}(\tau) = \int_{-\infty}^{\infty} e(t).s(t - \tau)\, dt \tag{2.10}$$

Assuming a particular received signal may be represented as before in the form

$$e(t) = ks(t-\Delta T) \tag{2.11}$$

we have

$$c_{tr}(\tau) = k\int_{\infty}^{\infty} s(t - \Delta T).s(t - \tau)\, dt. \tag{2.12}$$

This expression is seen to be of equivalent form to that of Equation (2.8), showing the equivalence of matched filtering and correlation processing.

The correlation receiver may be implemented in at least two distinct ways. The most general approach is to multiply the received signal separately by a number of delayed replicas of the transmitted waveform and to integrate (low pass filter) the outputs. An alternative and less cumbersome receiver may be used if a substantial overlap exists between transmitted and received signals. Such an overlap occurs if the length of the chirp is made equal to the pulse repetition period. The method involves the direct multiplication of the transmitted and received signals, and forms the basis of the traditional CTFM system.

If the transmitted signal is the real part of

$$s(t) = e^{j2\pi(f_2 t - mt^2/2)}, \qquad 0 \leq t < T \tag{2.13}$$

and repeated every t seconds to $\pm \infty$, the received echo from a single target at range R is

$$e(t) = As(t - 2R/c) + As(t + T - 2R/c), \qquad 0 \leq t < T. \tag{2.14}$$

From here, repetition every T seconds is assumed, and only the real parts of complex representations should be considered.

Let us now demodulate e(t) by multiplying it with a local oscillator which is a replica of s(t). Then low pass filtering the resultant signal gives

$$d(t) = Ae^{-j2\pi(T - 2R/c)mt}, \qquad 0 \leq t < 2R/c \tag{2.15a}$$

$$= Ae^{-j2\pi(2mR/c)t}, \qquad 2R/c \leq t < T. \tag{2.15b}$$

Note that in Equation (2.15b) a single target at a range R produces a single tone whose frequency 2mR/c is directly proportional to the range. This frequency is determined by passing the signal through a spectrum analyzer:

$$D(f) \approx f - 2mR/c \tag{2.16}$$

for large T where

$$D(f) = \int_{2R/c}^{T} d(t)e^{-j2\pi ft}\, dt \tag{2.17}$$

The CTFM system is illustrated in Figure 2.1, which shows a single target at a range R.

The demodulation process used in CTFM sonars makes analysis in the frequency domain appropriate. This contrasts with the time domain analysis of pulsed sonars outputs. Despite this difference, however, the systems are mathematically equivalent and identically constrained by system parameters. For example, system bandwidth determines the theoretical range resolution of all three classes of sonar. Furthermore, pulsed (or chirped) sonars and CTFM sonars with identical system parameters such as bandwidth, analysis time, centre frequency and transmitter output energy, will have identical capabilities in terms of range resolution, range accuracy, S/N and detectability.

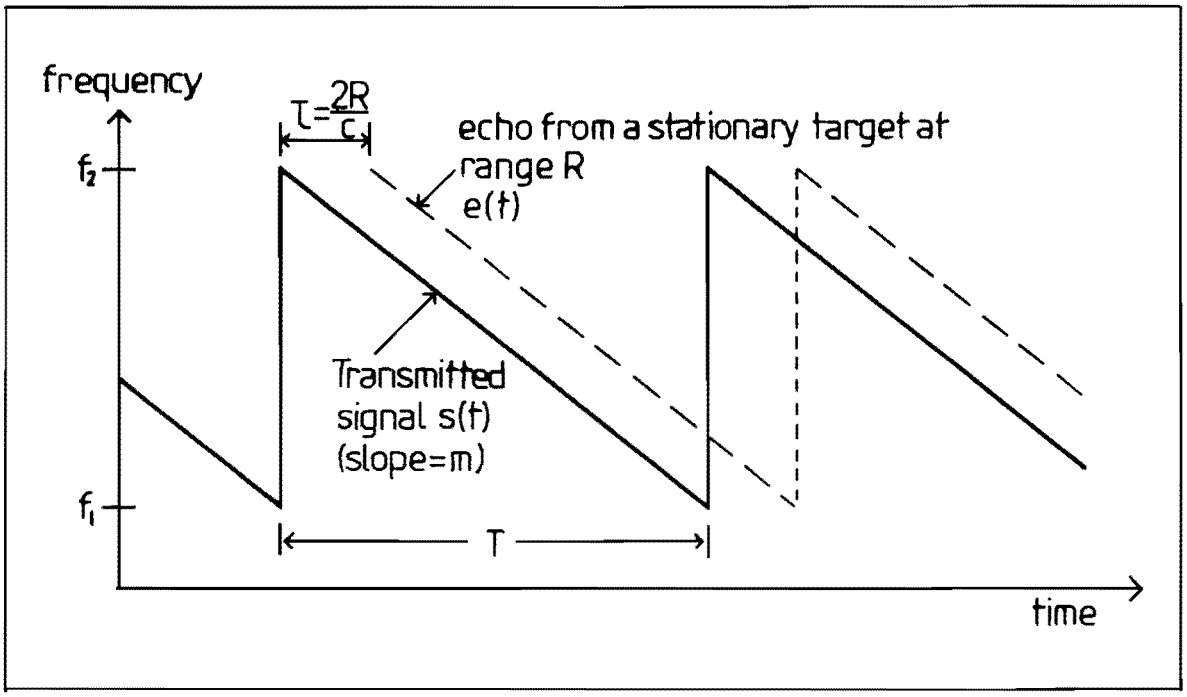

Figure 2.1 : CTFM Frequency-Time Characteristic

Differences in performance arise because some desired specifications or features may be more readily achieved using one particular system. Thus we are now considering practical limitations rather than theoretical capabilities. Many of these differences result from the fact that pulsed sonars transmit energy in a time which is short compared to the pulse repetition period, while CTFM sonars transmit continuously. Some of these differences are discussed in the following sections.

2.2.2 Transducer And Peak Power Constraints

Pulsed and chirped sonars require only one transducer, which is connected to the output of the transmitter power amplifier during pulse transmission, and to the input of the receiver pre-amplifier during reception. However, since CTFM sonars transmit and receive continuously, these sonars require two separate transducers. This requirement represents a severe limitation on CTFM systems in terms of both cost and transducer mounting logistics. Acoustic baffles may also be required to reduce crosstalk between the two transducers.

Since the transmitter duty cycle of pulsed sonars is small (typically 0.1%), all the radiated energy must be transmitted during a time which is short compared to the sweep repetition period, and so the peak power tends to be very high. However, the peak power that can be radiated underwater is limited by cavitation. Conversely, since the transmitted duty cycle of CTFM sonars is 100%, the average energy transmitted can be high using only moderate instantaneous power levels with no difficulties caused by cavitation.

Chirped sonars largely overcome the peak power limitations of pulsed sonars without the need for two transducers. However, since the entire chirp must be transmitted before the transducer can be switched to the receive mode, these sonars cannot provide full matched-filter demodulation for echoes received from targets within $cT/2$ metres range, where T is the length of the chirp. This short-range limitation gets worse as the duty cycle increases.

2.2.3 Transducer Beamwidth Considerations

Beamwidth is determined by aperture dimensions and wavelength. The beamwidth of a pulsed sonar is thus fixed by the size of the transducer and the frequency of operation. Furthermore, since pulsed sonars can operate using a single transducer, most (though not all) are operated in this manner, in which case the transmit and receive beamwidths are identical.

However, the operating frequency varies for CTFM and chirped sonars and the beamwidth changes correspondingly. For a CTFM sonar with a one octave transmitted frequency band, the beamwidths at opposite ends of the sweep differ by a ratio of 2:1. In some CTFM sonars, such changes in beamwidth are tolerated: these sonars usually have auditory displays, and sweep periods of less than around 250 ms, so that the ear integrates the output (e.g. Kay, 1974; de Roos et al., 1983). If the changing beamwidth is considered undesirable, methods of reducing the variation must be applied. Some sonars incorporate electronic networks which provide frequency selective shading of the transducer elements to alter the effective radiating aperture (e.g. Smith, 1972).

The beamwidths of a sonar's transmitter and receiver need not be the same. For example, scanning sonars may transmit using a broad beam, and receive using a narrow scanning beam to determine the direction to targets (alternatively, a broad-beam receiver may pick up echoes transmitted by a narrow scanning transmitter). Similarly, a side scan sonar using narrow transmitter and receiver beams may suffer from minimal overlap of the transmit and receive sectors owing to forward vessel motion. Making either beamwidth broader will increase the likelihood of receiving signals from the desired sector (at the expense of increased crosstalk and possibly noise, depending on which beam is broadened).

2.2.4 Range Ambiguities

Range ambiguities occur in repetitive echo locating systems as it can be difficult to determine which transmitted signal gave rise to a particular echo. In pulsed sonars, range ambiguities occur at multiples of the maximum range. Thus, a target displayed as being at a range R may in fact be at

$R + \ell cT/2$ where ℓ is a positive integer. One method of distinguishing between phantom targets and real targets in pulsed sonars is to operate with a varying pulse repetition frequency. The position of phantom targets on the display will then vary, while real targets will always appear in the same positions. Of course, more than one pulse repetition period is then required to resolve the ambiguities.

In CTFM sonars, range ambiguities can occur at ranges of $\ell cT/2 + R$ and $\ell cT/2 - R$, as the system demodulates echoes which are both higher and lower in frequency than the local oscillator signals. With traditional CTFM sonars, the maximum range tends to be much less than $cT/2$, and the extra transmission loss (due to absorption and spherical spreading) to phantom targets ensures that these targets are well attenuated. Chapter 3 introduces a CTFM demodulation system where the maximum range may be a large proportion of $cT/2$, and considers range ambiguities for these sonars.

2.2.5 Maximum Range Attainable

All active sonars are constrained by the general sonar equation, one form of which is given by

$$2TL = SL - (NL - DI) - DT + TS \qquad (2.18)$$

where TL is the one way transmission loss;
SL is the transmitted source level;
NL is the noise level
DI is the directivity index of the receiver;
DT is the detection threshold; and
TS is the target strength.

Recall that the average energy transmitted by a CTFM sonar may be greater than that transmitted by a pulsed sonar. The transmitted power level appears in Equation 2.18 as SL, and the greater SL generally available with CTFM sonars may be used to extend the maximum range. Gough et. al (1984b) show that for a state-of-the-art pulsed sonar can operating out to 400m, a comparable CTFM sonar with the same range resolution may operate out to 700m.

2.2.6 Trade-off Between Range Resolution And Response Time

The range resolution of a pulsed sonar is determined by the transmitted bandwidth, and to a first approximation equals $c/\Delta F$, where c is the speed of sound and ΔF is the bandwidth (Benjamin, 1966). Once the bandwidth and maximum range have been fixed, the range resolution and response time are also fixed.

The optimum range resolution attainable with a CTFM sonar is also $c/\Delta F$ (Gough et al., 1984a). However, a feature of any CTFM system is that range resolution is not determined by the form of the transmitted waveform. The outputs of CTFM sonars appear in the frequency domain, and hence must be analyzed using some form of spectrum analysis. Since the response time of a spectrum analyzer is proportional to the bandwidth of the individual bandpass filters, by making these filters less selective, they respond more rapidly. Less selective filters also encompass greater radial ranges, so that range resolution can be traded for speed of response. Thus, the full demodulated output of a CTFM sonar may be covered with a few wideband filters having a rapid response time, or many narrowband filters having a slow response. For example, the area observed by a sonar may be rapidly and continuously scanned; as soon as a target is detected, it may be examined in much greater detail, albeit less rapidly.

2.2.7 Target Classification Using Continuous Outputs

Differences in the duty cycles of pulsed and CTFM sonars are apparent in the displays of the sonar outputs. Consider a pulsed sonar with a transmitted bandwidth of ΔF. The sonar transmits this bandwidth in a short period $Tc = 1/\Delta F$, and repeats the pulse every T seconds, where $T>>Tc$. The echo received from any one reflecting point will also be Tc seconds long (ignoring any temporal spreading of the echo owing to target or medium characteristics). No more information is received from this target until another pulse is transmitted and an echo received. For example, a pulsed sonar with a 10 kHz bandwidth and a 400m maximum range will have a duty cycle of around 0.1% ; an echo lasting 0.1ms will be received approximately every second. A similar situation exists with chirped pulse sonars, for although the transmitted chirp may have a greater duty cycle (say 1%), the detected output (of the matched filter) will still be $1/\Delta F$ seconds.

CTFM sonars, on the other hand, transmit continuously and therefore receive echoes continuously from all targets. Consider a single target in the field of view of a CTFM sonar. If the target strength (TS) is just sufficient for the object to be detected with a single pulse of a pulsed sonar constrained by the same time-bandwidth product, then the continuous echoes received by a CTFM sonar will be weak, and detection will only occur using a narrow filter with a response time of one sweep period (Cook & Bernfeld, 1967). However, if the TS is greater than this minimum required for detection, then range resolution can be traded for response time. The target will then be detected after a shorter period, and hence observed more frequently within the same analyzer filter during a single sweep. Furthermore, if the response time of the analyzer filter in use is sufficiently short, and the TS of a target is sufficiently large so that detection is achieved within this filter response time, then observation (auditory or visual) of the target appears continuous.

There are two important benefits of a continuous display which can significantly improve target classification. Firstly, if a target exhibits characteristic motion, there are likely to be characteristic variations in echo strength and Doppler shifts. Continuous observation of these echoes may enable target identification. For example, the individual and group motions of fish comprising various schools are often characteristic of their species (Holliday, 1974). The ability to observe this motion (visually or aurally) provides additional information which may lead to school identification. Such identification may be impossible with the 'windowed' output of a pulsed sonar: by Shannon's sampling theorem, a pulsed sonar will only be able to reconstruct repetitive target motion if the period of the motion is less than half the pulse sonar repetition period. Furthermore, such reconstruction requires the echoes of several pulses; in contrast, the frequency of repetitive target motion detectable with a CTFM sonar is limited by the response time of the analysing filters, which, as was seen above, may be reduced to much less than a sweep period.

The second benefit of the continuous CTFM output is that the spatial frequency response of a target may be observed. Unless a target is an isotropic radiator with a frequency independent TS, its echo will vary during the sweep as the illuminating frequency changes. The variation of target strength with frequency is referred to here as frequency signature. Frequency

signatures are useful for target classification (Kay et al., 1981) using visual, auditory or electronic analysis. Although echoes from pulsed sonars constrained by the same time-bandwidth product will contain the same total information, this information is more difficult to analyze since it is all contained within a relatively short pulse echo. In comparison, the outputs of CTFM sonars are readily processed to generate 'stack plot displays' or spectrograms (see Figure 1, page ii), which are pseudo 3-dimensional representations of the the frequency signatures of targets. Such a display is described in Chapter 8 and extensively illustrated in Chapter 10.

2.2.8 Ambiguity Diagrams

Ambiguity diagrams are used to establish the ability of various waveforms to resolve range and Doppler uncertainties. The derivation of ambiguity functions for pulsed systems is well documented (e.g. Woodward, 1964; Skolnik, 1982). An introduction to ambiguity diagrams for linear FM sonars is given by Russo & Bartberger (1965). This work is extended to wide bandwidth systems by Kramer (1967), Bates (1971) and Sibul & Titlebaum (1981). A comprehensive derivation of ambiguity functions for wideband CTFM sonars is given by Do (1977).

2.2.9 Immunity From Interference

Active pulse and active CTFM sonars indicate the presence of a target upon the reception of an acoustic signal which is, within certain limits, a replica of the transmitted waveform. Consequently, any spurious signal received by the sonar which mimics the transmitted waveform will also be interpreted as a valid target. Echoes from unknown target-like objects will be detected with equal likelihood by both types of sonar. However, objects or phenomena which generate their own acoustic signals will be detected (i.e. considered valid targets) only if the signals they generate mimic the transmission of the sonar. While both impulsive sounds and linear frequency modulated sweeps occur in nature and man-made environments, there are several

factors which make pulsed sonars more susceptible to this kind of interference.

Impulsive noise frequently comprises wideband energy, some of which may readily intrude a pulsed sonar's receiver; linear sweeps must not only have energy across the CTFM sonar's operating bandwidth, but they must also sweep at precise rates and in the correct sense. Furthermore, impulsive phenomena are more prevalent in both nature and man-made environments. Consider the application of sonars to robots in an industrial environment. The sources of noise in such an environment are almost exclusively impulsive or of continuous frequency. Under these conditions, CTFM sonars are less likely to register phantom targets from spurious sources.

2.2.10 **Auditory Displays**

In contrast to animal sonar systems in which sonar echoes are processed by the auditory system, the primary displays of electronic sonars (and radars) have nearly always been visual. Auditory outputs are sometimes included in systems to provide confirmation of visual displays (Winder, 1975) or improve localization (Scorer & Watkins, 1977), but they are seldom used independently.

The major reason why auditory displays are seldom included in pulsed sonars is that human audition is limited by the precedence effect (Gardner, 1968) : if two clicks closely spaced in time are presented to a listener, two clicks may not be perceived. Instead, only the first click is heard, and this click inhibits perception of the second. With dichotic stimuli, a click pair will be heard as a single click if the delay between them is less than approximately 10ms. Since a 10ms time delay corresponds to a round-trip separation in range between two targets of 1.6m in air and 7.5m in water, the precedence effect limits auditory range resolution to these separations. Consequently, the precedence effect eliminates the possibility of using real-time auditory displays of sonar echoes in which object range is coded as delay. (By comparison, echo-locating bats can differentiate time lags between two echoes as small as 60us, corresponding to a distance between two targets of 1cm (Simmons, 1973)).

Time expansion of the auditory output can be used to overcome the precedence effect. This expansion may be configured to bring the received frequencies directly into the frequency band suitable for human perception. For example, the pulses emitted by the dolphin tursiops truncatus have been emulated and the received echoes time expanded by a factor of 50 to enable subjects to discriminate various targets (Martin & Au, 1978). However, time expansion is implemented at the expense of real-time analysis : expansion by a factor of 50 results in only 1/50th of all signals received being analysed.

The demodulated outputs of CTFM sonars, on the other hand, are ideally suited to auditory analysis. Mammalian auditory systems are modelled by a bank of filters (Altes & Reese, 1975; Neuweiler et al., 1980); Hunt (1972) describes narrowband filtering in the frequency domain as the signal processing adjunct to the human ear. Kay (1962b) has shown that range estimation is superior using frequency domain range coding compared to auditory estimates of delay using pulsed systems. Furthermore, two closely spaced targets are readily discerned using a CTFM sonar. For example, Roederer (1975) reports that two tones in the neighbourhood of 2,000 Hz must be separated by some 200 Hz to be discriminated. For a typical air sonar with a range code of say 1800Hz/m, this corresponds to a range resolution of around 11mm. Do & Kay (1977) report that a frequency separation of up to 40% is required to discriminate the tones; if the targets are placed closer together, the tones may not be separately discernible, but the resultant beat frequency will indicate the presence of the second target. In addition to providing range information, binaural CTFM displays can provide azimuth information, while the precedence effect degrades lateral localization in pulsed systems (Rowell, 1970).

Not surprisingly then, many CTFM sonars have auditory displays. While such displays are ideally suited to applications where vision is limited or non-existent, such as mobility aids for the visually impaired or navigational aids for divers working at night or in murky waters, they are also useful as additions to visual displays. The relative merits of visual and auditory displays are discussed in Chapter 5.

2.3 SUMMARY

Studies of mammalian sonar systems have influenced electronic sonar designs. While pulsed sonars operate in a manner similar to the biological sonars of many marine animals, CTFM sonars model those of various bats. FM sonar technology has lagged behind pulsed technology largely because adequate components were unavailable; now that most of the CTFM related operations can be adequately implemented electronically, some of the inherent advantages of CTFM sonars can be realised. These advantages may be summarised as follows:

1. Low instantaneous transmitted power levels ease transducer design constraints.

2. CTFM sonars may have a greater energy output which can result in a greater maximum range.

3. Whereas pulsed sonars have windowed outputs, CTFM sonar outputs may be perceived continuously, which can facilitate target classification.

4. Range resolution can be traded for analyzer response time.

5. CTFM sonars may be more immune to interference from typical spurious sources of noise.

6. CTFM outputs may be effectively processed aurally.

Against these advantages the following disadvantages must be noted:

1. Two transducers are required;

2. Beamwidth compensation may be necessary if wide bandwidths are in use.

CHAPTER 3

DUAL DEMODULATION

3.1 INTRODUCTION

Despite the fact that CTFM sonars transmit and receive continuously, the demodulated output corresponding to a single stationary target is not continuously present as a single frequency. The discontinuity arises because the transmitter must be periodically reset to its initial frequency.

Recall from Section 2.2.1 that the demodulated output of a traditional CTFM sonar for a single target at range R is given by

$$d(t) = Ae^{-j2\pi(T - 2R/c)mt}, \quad 0 \leq t < 2R/c \tag{3.1a}$$

$$= Ae^{-j2\pi(2mR/c)t}, \quad 2R/c \leq t < T. \tag{3.1b}$$

This situation is illustrated in Figure 3.1, where part (a) shows the transmitted and received signals, part (b) the demodulated signal, and (c) a possible amplitude versus time function. The discontinuity in the demodulated output is shown in Figure 3.1(b) as blank triangles in the frequency band from dc to f(max). Whenever the transmitter is reset, there are phase and amplitude discontinuities resulting in undesirable transients. Similar transients occur when the received echo changes from the lowest to the highest frequency. Furthermore, between these two occurrences, frequency is no longer directly proportional to the range of the target. These transients and demodulation

components are unwanted, and the usual procedure is to eliminate them by amplitude modulating the outputs of the VCO and the receivers in such a way that the amplitude is reduced to zero some time before reset, and increased again, in a controlled manner, some time after. Thus the output is blanked when reset occurs, resulting in a hiatus known as 'blind time' (or sometimes 'lost time').

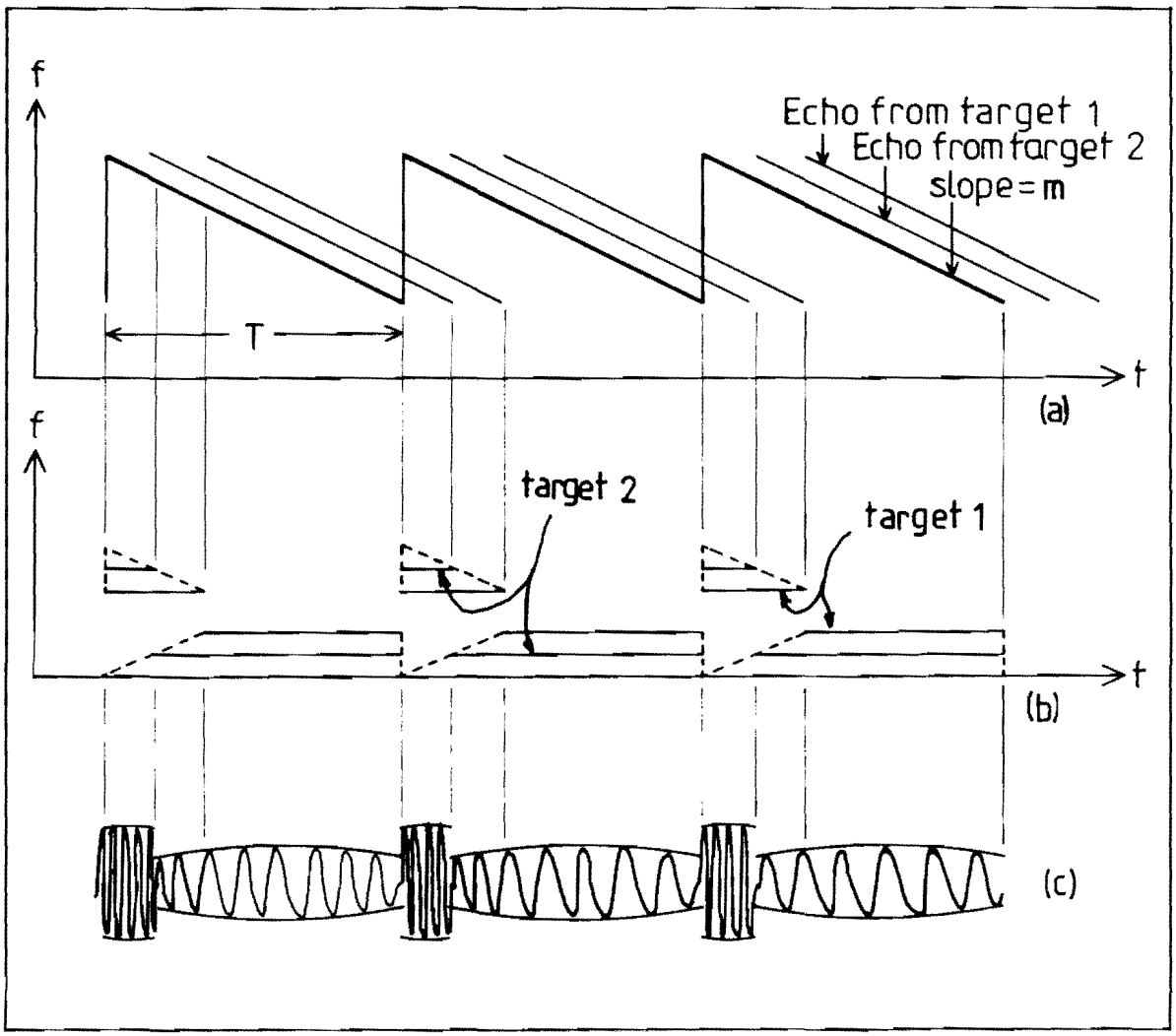

Figure 3.1 : Conventional CTFM system showing (a) transmitted and received signals, (b) demodulated signals, and (c) a possible amplitude versus time waveform of the demodulated output.

There are several disadvantages of blind time in the outputs of CTFM sonars. Firstly, while blanking may eliminate transients and unwanted demodulation components, the resulting hiatus is equivalent to a modulation of the signal at the sweep repetition rate. When analyzed aurally, the echo signal is heard as an interrupted tone, and the quality of this tone is degraded as the proportion of blind time is increased (Kay, 1980). While the modulation of the auditory output produced by blanking may be relatively unobtrusive with sweep repetition periods greater than around 200 ms, for shorter range devices (such as children's blind aids), the modulation becomes intrusive, and perception of the sweep rate may mask the desired target sounds (Hodgson & Boys, 1977).

Secondly, implementing the blanking usually involves using a series of timing circuits and a multiplier. These circuits may require considerable trimming for adequate suppression of the reset induced signal discontinuities.

Thirdly, the proportion of the transmitted sweep which must be blanked will depend on the maximum range at which the sonar has been set to operate, as the blanking must cover both the transmitter flyback and the received echo flyback for targets out to the maximum range. Consequently, for small maximum ranges (i.e. where Rmax is much less than cT/2), blind time is less noticeable than for large maximum ranges (when Rmax becomes a significant portion of cT/2) in which case the sonar may be blind for a large portion of its sweep repetition period. This is one of several reasons why the demodulated bandwidth of practical CTFM sonars has tended to be limited to some 10% of the transmitted bandwidth.

Fourthly, there may be an adverse effect with the sudden application of the signal D(t) to spectrum analyzers. Many analyzers comprise banks of high Q-factor bandpass filters which are somewhat underdamped to achieve maximum selectivity. The sudden application of the signal D(t) may produce unwanted transients in all of the bandpass filters, and these transients can mask a weak signal.

Finally, blind time degrades the range resolution. The sweep period T results in an output spectrum line spacing of 1/T Hz. If the demodulated output produced by a single target is available for a complete sweep period, the spectrum corresponding to this target will have a sinx/x envelope with the

zeros spaced apart by 1/T. Furthermore, two targets are considered to be resolved if there is a 3 dB dip between the spectral components corresponding to the targets. Consequently, if the demodulated outputs of two targets are available for an entire sweep period T, the targets will be resolved if they are spaced apart by 2/T. This result is apparent when the two frequencies are centred on spectral lines of the line spacing, but holds true in general. However, as a result of blanking, the demodulated outputs are available for less than an entire sweep period. Recall that blanking is effectively implemented by multiplying the sonar outputs with a rectangular function. In the frequency domain, this multiplication corresponds to a convolution with a sinc function, the effect of which will be to broaden the spacing between the zeros of the sinc function corresponding to the target (Kay, 1980). Consequently, the resolution will be reduced to 2/(T-b), where b corresponds to the length of the blanking pulse.

Not surprisingly, then, attempts have been made to reduce or eliminate blind time. Hodgson & Boys (1977) describe a merged sweep system in which the demodulated outputs of two temporally interlaced sweeps are weighted such that when one oscillator is being reset, the second is at the centre of its sweep and given full weighting. Similarly, Boys et al. (1978) describe both a multiple sweep technique and a 'balanced envelope-random phase' technique. In the multiple sweep technique, a comb of frequencies is swept through the transmit bandwidth, and the reset of any one frequency sweep tends to be masked by the demodulated outputs resulting from the remaining sweeps. However, the technique is difficult to implement, the demodulated bandwidth is limited to a proportion of the transmitted bandwidth determined by the number of frequencies in the comb, and the ability of an operator to perceive target motion is unclear, since at any instant the Doppler shifts are different for each sweep. The balanced envelope-random phase technique is interesting in that the transmitter begins each sweep from a random frequency. Since the phase of the output signal is dependent on the starting frequency, the output is randomly phased from one sweep to the next. Consequently, the line spacing of the output spectrum completely disappears, and the spectrum becomes continuous. However, while this technique will reduce the amplitude discontinuity at the sweep reset for stationary targets, a phase discontinuity will still exist. None of these systems has progressed past the theoretical or experimental stage.

The only previous operational CTFM system without any blind time was the Delta-Cobar sonar developed during the early 1940s (Kurie, 1946). An operator would monitor the sonar's auditory output, which would produce two tones for a target during the sweep, as given by Equations (3.1a) and (3.1b). These tones are shown as having frequencies fa and fb in Figure 3.2. The operator would vary the sweep period T until the auditory output was heard to have a single frequency during the entire sweep. Under these conditions, fa = fb in Figure 3.2, and T = 4R/c in Equation (3.1a), where R is the range to the target being examined, thereby equating Equations (3.1a) and (3.1b). The range of the target could then be read off a calibrated sweep period dial. However, as there would only be a continuous and constant frequency for targets in a single range annulus, the exception of the Delta-Cobar system is rather academic.

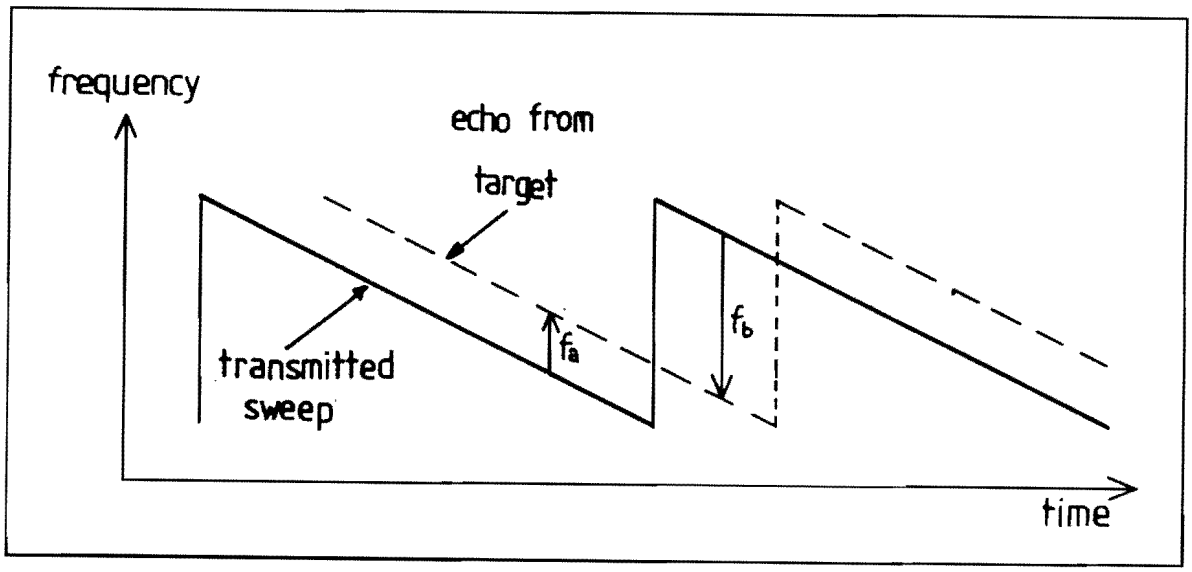

Figure 3.2 : The transmitted sweep period of the Delta-Cobar sonar is varied until fa = fb.

3.2 DUAL DEMODULATION

Consider a sonar system using the same transmitted signal s(t) and the same received signal e(t) as given in equations (2.13) and (2.14). However, instead of demodulating e(t) by s(t), let us use two demodulators with two local oscillators having outputs $L_1(t)$ and $L_2(t)$ where

$$L_1(t) = e^{+j2\pi(f_1 + kmT)t} . e^{-j2\pi mt^2} \tag{3.2}$$

and

$$L_2(t) = e^{+j2\pi(f_1 + \{k-1\}mT)t} . e^{-j2\pi mt^2} \tag{3.3}$$

where $0 < t < T$ and k is any integer such that $k \geq 2 - (f/mT)$. If $D_1(t)$ is the output from the first demodulator and $D_2(t)$ the output from the second demodulator, then

$$D_1(t) + D_2(t) = \sum_{i=1}^{M} A_i \; e^{-j2\pi(\; |k|mT \; - \; |k-1|2mR/c)t} \; + G(t) \tag{3.4}$$

for all t, where G(t) comprises all signals outside the frequency band $|k|mT$ to $|k-1|mT$, and is usually filtered out. Note that there is now no blind time and Rmax is only limited by the sweep repetition period T so that Rmax may extend out to cT/2. Of course, there may be good reasons for limiting the useful range to much less than cT/2, such as range ambiguities, and spectrum analyzer capabilities.

The demodulated frequency associated with zero range is $|k|mT$, while that associated with the maximum range Rmax = cT/2 is $|k-1|mT$. Hence for all positive integer values of k, the range will be reversed with respect to demodulated frequency, with zero range at a higher frequency than the maximum range. Furthermore, for all values of k other than zero and one, the demodulated output will not be at baseband (DC to +mT). In these situations, the outputs can be brought down to baseband by a third demodulator with a fixed local oscillator at

$$f = |k-1|mT \qquad \text{for } k \geq 2 \tag{3.5a}$$

$$= |k|\,mT \qquad \text{for } k \leq -1. \tag{3.5b}$$

Alternatively, the spectrum analyzer can cover the demodulated frequency band if this is more convenient.

3.2.1 Range Ambiguities

It was shown in Section 2.6 that whereas range ambiguities in pulsed sonars occur at multiples of the maximum range, so that a target displayed as being at a range R may in fact be at $\ell cT/2 + R$, where ℓ is an integer, range ambiguities in traditional CTFM sonars may occur at ranges of $\ell cT/2 + R$ and $\ell cT/2 - R$, as the system demodulates echoes which are both higher and lower in frequency than the local oscillator signals. Furthermore, recall that in traditional CTFM sonars, since the maximum range Rmax tends to be a small portion of cT/2 (to keep the blind time small), the range corresponding to the first ambiguity (cT/2 - R) is much greater than the displayed range R, and the extra transmission loss ensures that the phantom target is well attenuated.

However, in dual demodulation CTFM sonars, where Rmax can be a significant portion of cT/2, the signal strengths of phantom targets can be comparable to those of real targets. It is possible to eliminate range ambiguities at ranges of cT/2 - R. For example, using narrow bandpass filters, cascaded mixers and single sideband techniques, circuits can be designed to force the system to use only echoes above (or below) the local oscillator. These techniques will reduce the range ambiguities to those of pulsed sonars at the expense of circuit complexity.

3.3 PRACTICAL EXAMPLES

Recent advances in digital frequency synthesis have made interlaced or multiple local oscillator techniques feasible. More specifically, the advent of repeatable, linear and phase-controllable swept frequency generators make the interlaced dual demodulation system described above quite practical.

The first sonar built to evaluate the technique sweeps down from 100 kHz to 50 kHz (one octave) in a sweep period T which is user selectable.

This transmit sweep also doubles as the first local oscillator L_1, so that k of equations 3.2 and 3.3 is zero. The second local oscillator L_2 is synthesized to join onto the end of L_1, and sweeps down from 50 kHz to 25 kHz as shown in Figure 3.3(a). Since $L_1(t)$ is phase matched to $L_2(t)$, there is no phase discontinuity at the point where D_2 takes over from D_1. The received echoes are demodulated directly to baseband (DC to 25 kHz) as shown in Figure 3.3(b), and the signals are fed to a spectrum analyzer. Rmax has been limited to 0.5cT/2 in order to reduce range ambiguities. A block diagram of this sonar is shown in Figure 3.4.

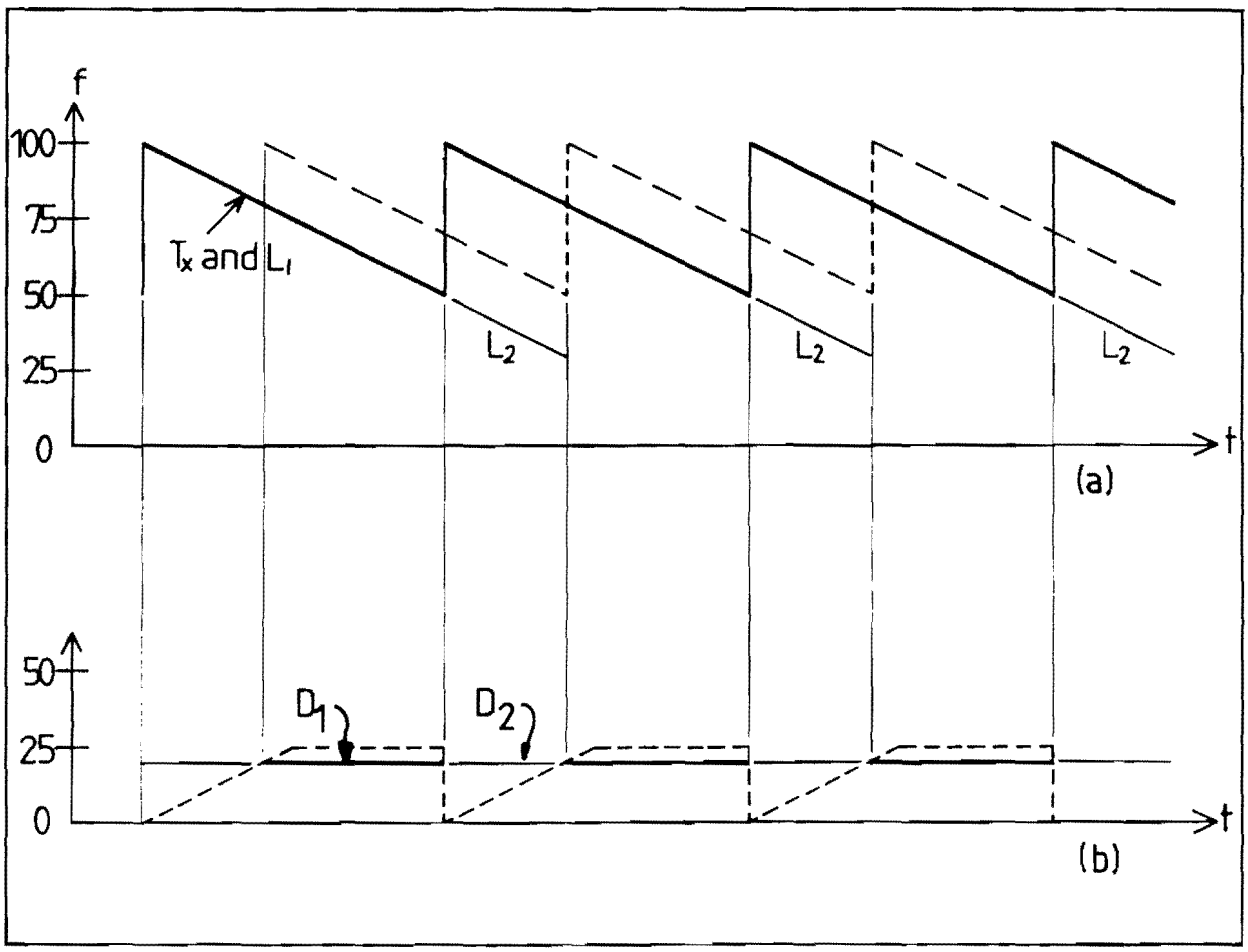

Figure 3.3 : Dual demodulation system with k = 0 showing (a) transmitter and local oscillator signals and (b) demodulated signals.

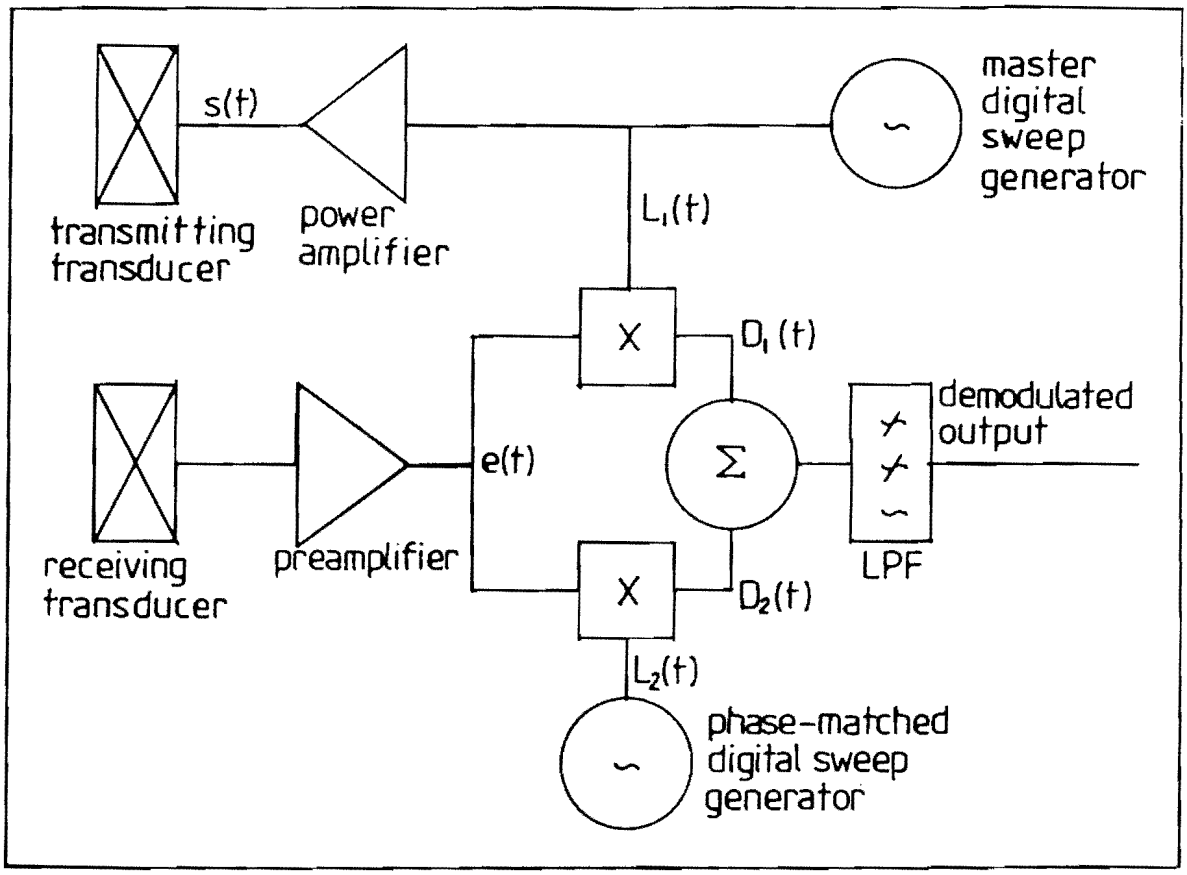

Figure 3.4 : Block diagram of dual demodulation system.

A focussed, high resolution scanning air sonar has also been developed using dual demodulation. As with the previous sonar, the parameter k of equations 3.2 and 3.3 is zero, but now the transmitter and first local oscillator L_1 sweep down from 200 kHz to 100 kHz, while the second local oscillator sweeps down from 100 kHz to DC. Further, the maximum range is made equal to cT/2, as the sonar is intended for use at a robot work station, and it is assumed that there are no objects beyond the maximum range to give rise to phantom targets. (Echoes from objects beyond the maximum range would in any case be relatively weak as a result of being out of the beam's focus.)

The third dual demodulation sonar that has been built is an underwater side scan sonar. In this sonar, $k = 4$, so that the two demodulator sweeps are

of a considerably higher frequency than the transmitted sweep, as shown in Figure 3.5(a). One of the reasons for this choice of k is that the demodulated outputs, shown in Figure 3.5(b), fall outside the transmitted bandwidth, thereby reducing any feedthrough frequency components. This sonar forms the basis of the Classification Sonar described more fully in Chapter 8.

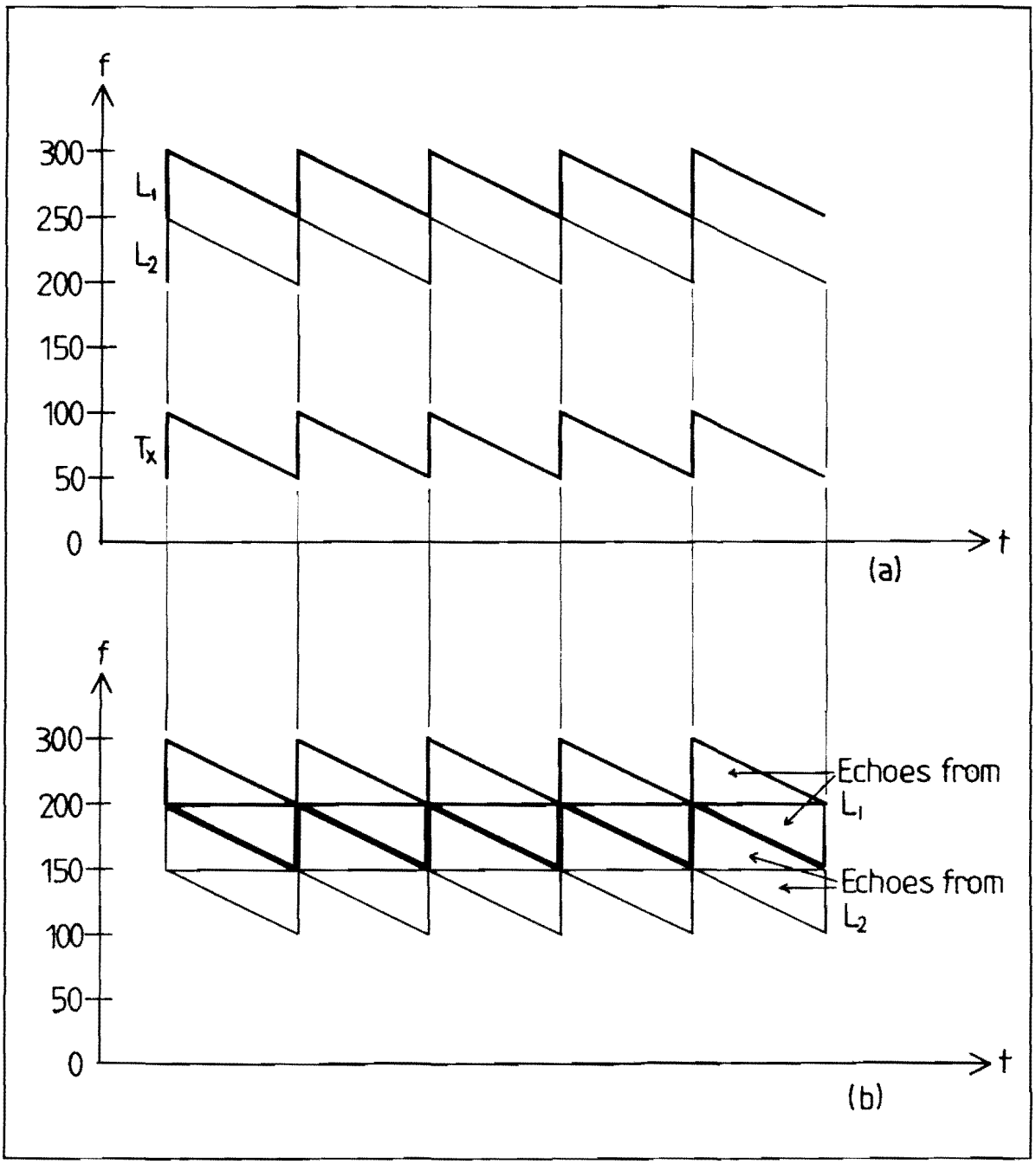

Figure 3.5 : Dual demodulation system with k = 4 showing (a) transmitter and local oscillator signals and (b) demodulated signals.

3.4 SUMMARY

The blind time inherent in traditional CTFM sonars results in amplitude and phase discontinuities which adversely affect auditory analysis of sonar outputs and electronic spectrum analysis. Furthermore, blind time degrades range accuracy and resolution.

While previous attempts at eliminating blind time have not resulted in practical sonars, recent advances in technology have enabled a viable technique to be implemented. This technique has resulted in the development of a number of sonars which have subsequently been used to provide the bulk of the experimental results presented in this dissertation.

CHAPTER 4

AIR MODELLING

4.1 INTRODUCTION

While sonars are most commonly associated with underwater devices, the use of sonars in air goes back a long way - indeed, the first patent relating to sonars was for an air application (Richardson, 1912). However, the advantages of sound as a propagation source over light are much less in air than they are in water. The attenuation of sound, for instance, is two orders of magnitude greater in air than it is in water; conversely, light is barely attenuated in air, but propagates poorly in water. Similarly, while factors reducing aquatic vision (e.g. silt) hardly affect the propagation of sound in water, atmospheric conditions that reduce vision, such as rain, dust and fog, do impair the propagation of sound. This impairment is illustrated by echolocating bats, which turn back on fog as if it were a solid wall (Pye, 1971). Not surprisingly then, air sonars are most frequently employed where vision is impossible or difficult.

One use of air sonars is as mobility aids for the blind or partially sighted (e.g. Kay, 1974). Such devices have been developed at the University of Canterbury for the last 20 years. Early devices constituted simple obstacle indicators (Kay, 1964), while recent devices incorporate binaural displays and provide sufficient auditory information to enable target classification (Kay et al., 1981).

Another use for air sonars is robotic sensing. While optical sensors can provide good angular resolution, they tend to suffer from relatively poor range resolution (Jarvis, 1983). Sonars, on the other hand, have

comparatively poor angular resolution, but accurate range resolution. Hence, a combined system using optics for angular resolution and sound for range resolution may be useful. Sonars may also be useful in robotics applications where adequate lighting is difficult to provide, where objects are optically transparent, or where background objects confuse the optical processor (Marsh et al., 1984).

There is, however, a further use for air sonars, namely to model underwater sonar systems. Underwater trials are usually expensive and difficult to control, while air modelling can be versatile, and the cost is usually small compared to the value of information acquired. Much less physical space is required (distances must be scaled down in the model), and trials are not dependant on swimming pool, vessel, or crew availability, harbour board authority, or favourable weather conditions. However, the literature does not suggest that air sonars are often used for this purpose - most sonar modelling is analytic or mathematical, rather than physical. Nonetheless, Smith (1972) tested his sonar in air to confirm performance prior to sea trials, while Cram and Staveley (1977) used a scale model air sonar to model radar systems.

This chapter considers some of the factors involved in air modelling, and illustrates these with some practical examples.

4.2 SYSTEM ADAPTATIONS FOR AIR OPERATION

Sound waves are propagated pressure and density fluctuations in the medium caused by particle motions. For small amplitudes, the general wave equation can be expressed as follows:

$$\nabla^2 p - \frac{1}{c^2} \frac{\delta^2 p}{\delta t^2} = 0 \qquad (4.1)$$

where $p = p(x,y,z,t)$ is the dynamic pressure,
$c = c(x,y,z)$ is the speed of sound, and
∇^2 = the Laplacian operator.

The simplest description of the sound field is the solution of the wave equation in one dimension (x) as a sinusoidal plane wave represented by

$$p(x,t) = p_0.\sin(2\pi x/\lambda - 2\pi ft + \phi) \qquad (4.2)$$

where p_0 is the amplitude of the pressure fluctuations,
λ is the wavelength,
f is the frequency, and
ϕ is the phase shift.

This equation can also be expressed as

$$p(x,t) = p_0.\sin(kx - \omega t + \phi) \qquad (4.3)$$

where $k = 2\pi/\lambda$ is the angular wave number and
$\omega = 2\pi f$ is the angular frequency.

While these relationships apply in air as well as in water, there are some fundamental differences in wave transmission between air and water which are now considered.

The speed of propagation of a physical disturbance in a medium is largely dependant on the density of the medium. Water is considerably more dense than air, and thus the speed of sound in water is much greater than it is in air. Tables are available giving the speed of sound as functions of humidity, temperature, pressure, salinity, etc (e.g. Weast, 1981). For the purposes of the discussion to follow, it is assumed that the speed of sound in air is 300 m/s, and that in water it is five times greater, at 1500 m/s.

As a result of this difference in speed, the maximum range attainable so as to avoid primary range ambiguities (cf. section 2.2.4) in air will be one fifth as great as it is underwater, (for a given sweep period for CTFM sonars, or pulse repetition period for pulsed sonars), all other things being equal. The slower speed of sound in air is one of several factors limiting the maximum range attainable using air models.

There are two sources of transmission loss associated with sonars: spherical spreading and absorption. The attenuation due to spherical

spreading is the same underwater as it is in air, and is derived by simple geometry to be 6 dB per doubling of distance for a one-way transmission path.

The attenuation due to absorption varies considerably with such factors as temperature, pressure, and (in water) salinity. In both air and water, absorption increases dramatically with increasing frequency, and thus the operating frequency severely limits the maximum range attainable. However, at 80 kHz and 20°C, the absorption of sound in water is typically 0.02 dB/m, while in air under the same conditions it is 2.9 dB/m, or 24 times as great. The absorption of sound in air is the greatest factor restricting the maximum range attainable with air sonars.

The slower speed of propagation and higher absorption of sound in air reduce the maximum range of an air sonar compared to that of the underwater sonar being modelled. In modelling an underwater CTFM sonar in air, the sweep rate is usually increased to achieve a comparable demodulated bandwidth. By maintaining the demodulated bandwidth, it is possible to use the same spectrum analyzer used for the underwater sonar being modelled. However, the shorter sweep period will broaden the line spacing in the analyzer output, and the analyzer must now be able to capture the data in a shorter time.

For any periodic disturbance,

$$c = \lambda f \tag{4.4}$$

where c is the speed of propagation,
λ is the wavelength, and
f is the frequency.

Thus for a given frequency of operation, a decrease in speed results in a corresponding decrease in wavelength. If a target is encompassed by n wavelengths underwater, then that same target will be encompassed by 5n wavelengths in air (assuming no change in frequency of operation). If it is desired to retain a given number of wavelengths across a target, then for a fixed frequency of operation, the model of the target will have to be scaled down by a factor of five. Alternatively, the centre frequency can be altered, but a choice must then be made between maintaining the original bandwidth or maintaining the proportion of an octave over which the transmitter sweeps. The former is important in scaling range accuracy and resolution, and the latter may be necessary to avoid harmonics. In practice, target size and centre frequency may be adjusted simultaneously.

A further factor to be considered in modelling underwater environments in air is the relative characteristic impedance of targets and the propagating medium. The extent to which some of the incident sound penetrates the target depends on the impedance mismatch between the target and the medium. If there is no mismatch, there will be no reflection and the target will be acoustically transparent. Conversely, a large mismatch results in most of the incident energy being reflected.

Since the characteristic impedance of air is orders of magnitude less than that of typical targets, most of any incident sound is reflected, and thus received echoes are caused by reflecting points on the surface of the target. In water, however, the characteristic impedance of the medium is much closer to that of many typical targets. As a result, there is considerable target penetration by the incident sound, some of which is reflected by discontinuities within the target (i.e. where there are further boundaries between materials of different characteristic impedance). The reception of echoes from within a target may facilitate the identification of that target. For example, the characteristic impedance of fish flesh is so similar to that of water that the echo from the water-flesh interface is very small. Most of the sonar echo originates from the flesh-air interface created by the swim-bladder, an air-sac used by most species of fish for breathing (Tucker, 1967).

Although background noise and reverberation are generally not modelled in air, they can be considerable in water (especially the sea). Hence, results using air models that take no account of background noise or reverberation should be interpreted with due caution.

Since some of the parameters discussed (speed of sound, wavelength, absorption, transmitted bandwidth, sweep rate, characteristic impedances) are not scaled in the same proportion in going from water to air, and further since some phenomena behave differently in the two media (e.g. absorption and reverberation) it is impossible to devise an air sonar which models the underwater environment accurately in all respects. For instance, if the maximum unambiguous range and number of wavelengths across a target are modelled accurately, then one must accept a relatively higher rate of absorption with increasing range in the model. Similarly, if it is desired to preserve the dynamic range between echo strengths from targets at the nearest

and furthest ranges, then the maximum range of the air model has to be reduced. Hence, any air model will be a compromise, with some parameters being scaled more accurately than others.

Finally, while most of the underwater sonar electronics can be used in the air model if desired, the underwater transducers are totally unsuited for use in air. The most common underwater transducer element is a piezo-electric ceramic, clamped between two sections of material used to modify the characteristics of the element and to improve coupling to the medium. The condenser transducer (Kuhl et al., 1954) typically used in air comprises a grooved metal back-plate covered with a sheet of mylar, the outer layer of which is coated with a thin layer of conducting material. Since air transducers are completely different to underwater transducers, the transmitter power amplifier and receiver pre-amplifiers must also be replaced.

4.3 EXPERIMENTAL AIR MODELS

Various air models were used to derive results presented elsewhere in this thesis. Some of these are described to illustrate the modelling process.

4.3.1 Fish School Classification

State-of-the-art sonars used by fishermen do not provide easy recognition of fish species. A recent study reports that 50% of commercial fishermen consider the major problem with their sonars to be a lack of species identification (Kanciruk, 1983). Any success at identifying targets is based largely on sonar operators' familiarity with fishing zones and their knowledge of the habits of species sought, such as school velocity and swimming depth. Hence fishermen would greatly benefit from sonars that could distinguish between different schools of fish. A number of attempts have been made at making such discriminations (e.g. Holliday, 1972, Deuser et al., 1979).

In order to investigate fish school recognition using CTFM technology, an underwater fish finding sonar was modelled in air. The model was

configured to sweep from 100kHz to 55kHz in 80ms, giving a range code of 3400Hz/m, and a range accuracy of 7.3mm. A binaural receiver was used with the two receiver transducers splayed 15 degrees either side of the transmit transducer.

Since it is not the water-flesh interface but rather the flesh-air interface at the swim bladder that gives the predominant echo from fish, the models comprised plastercine blobs representing the swim bladders. Three schools of fish were modelled, each school comprising fish of a given size. The number of fish in each school was varied so as to present the same cross sectional area to the sonar. All three schools were 250mm in diameter, and viewed from 1.5 metres a mean audio echo frequency of 2.55 kHz was produced. The plastercine blobs were suspended on single threads and could rotate independently, resulting in random orientation with respect to other fish in the school. Thus, many characteristics of the individual fish and their schools, such as extent of lateral body displacement with propulsion and temporal uniformity in direction change were not modelled.

When the fish were in motion - even very slight motion - the different schools were readily identified by seven subjects in one session. When the fish were perfectly still, some practice was required but this needed no more than 30 minutes. Once the characteristics of the three schools became apparent, they could be memorised and retained. By modelling the swim bladders in air, a much more controlled and manageable experiment was possible than would have been the case using live fish underwater.

4.3.2 Rough Versus Smooth Characterizations

During the conceptual and early developmental stages of the Classification Sonar described in Chapters 8, 9, and 10, some basis for target characterization was sought to enable an initial investigation of possible classification strategies. A design goal was that the sonar be able to distinguish man-made objects from those occurring naturally. Objects of interest could thus include pipelines, car-bodies, oil drums, sunken vessels, and mines.

Had sea trials been attempted to determine the most useful approach to distinguishing man-made objects from others, the exercise would not only have been time consuming and costly, but would have required an underwater sonar sufficiently flexible to incorporate design features suggested by the trials. Instead, an air model of the underwater Classification Sonar was used. This air sonar was the first dual demodulation sonar described in section 3.3, which swept from 100 to 50 kHz in a user selectable sweep period. Initial experimentation suggested that the most useful discrimination criterion (in terms of both operator and computer characterization capability) was that man-made objects have essentially smooth surfaces with relatively few reflecting points, while naturally occurring objects are generally rough with many reflecting points.

A series of experiments was then designed to evaluate the usefulness of this rough/smooth criterion. By modelling various targets in air, it was possible to check the viability of this approach rapidly and in a controlled environment for auditory, visual and computer analysis methods. Furthermore, air modelling enabled the development and refinement of characterization algorithms prior to the completion of the underwater Classification Sonar; both areas could thus be developed simultaneously.

The man-made targets to be modelled included a sunken spherical buoy and a variety of mines. Since the characterization criterion required a high resolving power, the most important parameter to model accurately was the number of wavelengths across the targets. Fire extinguisher cylinders, which come in a wide variety of shapes and sizes, can be reasonable models of mines. They are generally smooth, and, after the handles have been removed, have few protrusions.

Rough targets are easy to model. A rocky sea-bottom was modelled by using a pile of pebbles, and a rocky or coral outcrop by pine cones (both open and closed). Other models included rods and plates covered in wood chips.

4.4 CONCLUSIONS

Of all the uses of air sonars, modelling the underwater environment is one deserving greater attention. While the parameters involved cannot all be scaled in the same proportion, modelling is a practical and useful method of implementing ideas without requiring great expense or time, and of predicting underwater sonar performance.

CHAPTER 5

VISUAL, AUDITORY, AND COMPUTER TARGET RECOGNITION

5.1 INTRODUCTION

Of the five definitive senses available to man, vision, hearing, and touch have been used to interpret information provided by sonars. Furthermore, the increasing complexity of computers has enabled sophisticated detection and classification algorithms to be used to analyze sonar outputs. This chapter compares the merits of these analyzers and considers the effect of simultaneously using several.

5.2 SENSORY ANALYSIS

The most common displays for sonars (and radars) are visual. The continuing preference for visual displays comes about largely for ergonomic and commercial reasons: they provide a useful output, operators are familiar with them, new operators are readily trained, and hence manufacturers continue producing them. There are, however, several alternatives.

The development of ultrasonic mobility aids for the blind required an alternative to visual displays. A number of systems have been built based on human somatosensory (touch) perception (e.g. Bach-y-Rita, 1969; Brabyn et al., 1981). A matrix of vibrators is typically strapped onto some part of the body (usually the abdomen), one dimension of the matrix corresponding to the

range, and the other dimension to the azimuth of the environment being sensed. While these systems do work, there are severe limitations imposed by the finite number of vibrator elements on axial and lateral resolution.

The more common alternative or addition to a visual display is an auditory display. The human auditory system is a particularly good analyzer for signals in the frequency domain, in a band extending from several hundred hertz to around 8 kHz (Plomp, 1964). We can perceive frequencies beyond these limits, and young people in particular can hear sounds above 15 kHz, but their ability to analyze these signals is limited. Auditory displays are also used in systems other than sonars to improve or augment analysis. In particular, radars sometimes include an auditory display (e.g. Scorer, 1977) as an aid to target detection or classification. Some of the relative merits of the two main sensory inputs used to analyze sonar signals (visual and auditory) are now considered.

There are tasks which can readily be performed visually but which are difficult to perform aurally, and vice versa. For example, it is relatively easy to perceive aurally when detonation (or pre-ignition) has occurred in a vehicle engine whereas the same phenomenon cannot readily be displayed and observed visually (Haber & Wilkinson, 1982). Similarly, harmonic musical chords (or false notes within such chords) are much easier to discern aurally than visually (Roederer, 1975). A further example is provided by speech. Not only is speech easily understood aurally, but it is usually possible to identify the speaker, assuming the speaker's voice is familiar to the listener. Such identification is possible even if the voice is heard out of environmental context, or if the voice is heard over a band limited channel such as a telephone. Visually, speech recognition is very difficult (reference is made not to the reading of text, but rather the observation of visual displays depicting the vocalized sounds such as time waveforms or frequency spectra). Machines are still having difficulty distinguishing more than a few words spoken by one person in a good acoustic environment (Beuter, 1985).

There are also instances where phenomena are more readily discerned visually. For example, using vision, humans can identify a wide variety of faces. While there is no auditory analogue, no computer can (yet) match this performance (Haber & Wilkinson, 1982).

When it is claimed that certain information is more readily perceived using one particular sense, that does not mean that the information is absent when a less successful sense is used to analyze the information. Rather, one of two effects is taking place. Either that particular sense is simply better adapted to record, analyze and thus perceive the information (just as peripheral vision notices flicker more readily than foveal vision), or the equipment being used as the link between the phenomenon and the sensory input cannot cope with the volume of information.

Early investigations into auditory and visual detection of signals are relevant to analysis techniques applied to CTFM sonar outputs. Garner & Miller (1947) found that the ear integrates acoustic energy linearly with time up to 200ms, such that a 10 fold decrease in duration results in a 10 dB loss in sensitivity; for durations greater than 200ms, the change is slight, and integration is considered complete at 1 second. This integration effect is used when the ear is used to analyze CTFM sonar outputs, which have sweep periods typically ranging from 40ms (in air) to 1 second (in water). Tanner & Swets (1954) proposed a theory of visual detection in which human operators are assumed to make threshold judgements between two probability distributions, "noise alone" and "noise plus signal". This theory was confirmed by Sherwin et al. (1956) who also demonstrated a similar phenomenon with audition. Such threshold judgements are also invoked electronically in sonar and radar systems. Sherwin et al. further compare human detection using audition with electronic detection, and find that human observers consistently out-perform electronic detectors. This author records similar results in the next section.

More recently, Swets et al. (1977) studied the task of passive-sonar operators who must detect and identify complex underwater sounds or visual representations of them. They concluded that temporal integration of sensory information is fundamental to detection and identification. The outputs of CTFM sonars are well suited to such integrations.

Visual displays have one distinct advantage over all other sensory mechanisms : when a signal appears on the display, it can be referred to by physically pointing at it. All operators or observers thus know they are considering the same target or phenomenon. In using auditory displays, however, while it is possible to say: "That's the signal of interest, the one

you hear now", and even to go to great length to describe the sound, there is no guarantee that it is the same sound that others hear or pick out as being the important sound. This uncertainty gets progressively more noticeable as the information contained in the auditory output becomes more complex.

Another advantage of visual displays lies in the fact that most deteriorations of eye sight owing to the natural ageing process do not noticeably affect one's ability to observe and interpret displays. Near and far sightedness, for instance, can be compensated by wearing glasses, while an inability to refocus as quickly as a child will not impair display interpretation. However, natural deteriorations in hearing do significantly affect the quantity and quality of useful information perceived. The most common deleterious effect on hearing with advancing years is a loss of high frequency sensitivity. This loss has two detrimental effects. Firstly, the bandwidth available to display information is limited. Accordingly, the frequency corresponding to the maximum range in blind aids has typically been set to 5 kHz to enable most potential users to perceive the maximum range. However, most people can hear beyond 5 kHz, and are thus deprived of extra bandwidth, which could be used to extend the maximum range or increase the sweep rate. Secondly, loss of high frequency sensitivity may impair auditory target classification by preventing the perception of high frequency Doppler shifts.

There are advantages of auditory displays over visual displays. For instance, to detect a particular target or phenomenon on a visual display with continuously varying information requires constant observation of the display, making other tasks (such as vessel navigation) difficult. Using an auditory display, it is possible to perceive the echoes from a particular kind of target while still engaged in some other activity. Furthermore, auditory displays make use of the vast and as yet poorly understood signal processing mechanism of the human auditory system (Moore, 1983).

Bearing in mind that the signals transmitted and received by sonars are already acoustic in nature, the signals fed to the ears can be minimally processed, and thus contain all or most of the information present in the echoes from targets. Much of the processing can thus take place in the brain. On the other hand, in systems using visual displays, nearly all of the processing has already taken place when the signals are displayed. The

displayed information may therefore not include all the information contained in the original echo.

Unfortunately, it is difficult to objectively quantify the performance of the human auditory system (and hence auditory displays) since we are dealing with psycho-acoustics rather than a purely scientific discipline. However, auditory displays can be used for remarkably fine discriminations (Kay et al., 1981).

An alternative to choosing between an auditory and a visual display is to use both. Miller (1956) has shown that increasing the number of variable attributes of a display mechanism increases the channel capacity (the number of absolute levels that can be discerned), albeit at a decreasing rate. This result applies even if the attributes are varied together in perfect correlation. While it may be debatable whether the addition of an auditory display to a visual display increases the total information presented to the operator or merely presents the same information in another form, in either case Miller claims the channel capacity will be increased. Winder (1975) confirms this by reporting operational results which indicate that the simultaneous utilization of both audio and video displays, assuming each has a comparable recognition differential, can increase the effective system recognition differential by as much as 6 dB.

5.3 COMPUTER RECOGNITION

The preceding comparison of the two sensory inputs most suited to sonar signal analysis omitted altogether to mention the major disadvantage of these systems, namely the element of human fatigue. Fatigue as it relates to sonar target classification is a condition of reduced awareness brought about by the repetitive nature of a task, or the absence for long periods of targets of interest. Consequently, it would be convenient if these tasks could be relegated to machines.

While computers do not suffer from fatigue of the kind described above, they are presently not as capable as fresh human operators at discriminating between certain targets. One possible reason why human

operators can still surpass computers in this area is that humans use several decision processes simultaneously, and may, subconsciously or otherwise, adapt the processes invoked to suit the task. Computers, however, are pre-programmed to invoke a given set of tests, and while these tests may be comprehensive and adaptable to some extent, state-of-the-art computer software does not yet fully model what is known of human perception mechanisms. Nonetheless, computers can be expected to approximate the performance of human operators working with a visual display, as the data used to make decisions are usually extensively pre-processed and identical for both decision mechanisms. The potential performance of computers relative to a human operator using an auditory display is less certain, however, as it is not yet known exactly what kind of processing takes place in the brain, and therefore if this processing can be matched. No doubt computer performance will improve with increasing processing power and algorithm sophistication.

Until computers can be shown to match and exceed human performance, in which case human interpretation of sonar outputs will no longer be necessary, computers can still perform a very useful task. For instance, they may be programmed to ignore detected targets if some characterization criterion does not exceed a threshold; if this threshold is exceeded, then the computer can alert a human operator who is then given the task of making a decision as to the importance of the target in question. If the work load is shared between the computer and human operator in this manner, the incidence of human fatigue may be reduced.

5.4 EXPERIMENTAL COMPARISONS BETWEEN VISUAL AND AUDITORY DISPLAYS

5.4.1 Auditory Versus Visual Classification Of Fish Models

To compare visual and auditory recognition capabilities of three schools of fish, an air model was constructed (cf. Chapter 4) comprising three clusters of plastercine blobs suspended on thin threads. The first cluster comprised 8 blobs (with blob diameters of 40 mm), the second 16 blobs (28 mm) and the third 32 blobs (10 mm). Inter-blob spacing was approximately two blob diameters for each cluster, and each target cluster was 250mm in diameter. Since the total cross sectional areas of the three clusters were identical, the time averaged energy reflected by each cluster was constant.

To provide the auditory display, the demodulated output of the sonar was presented to the subjects through headphones. With the centre of the targets placed 1.5m from the sonar, the mean audio echo frequency was 2.55 kHz. The visual displays comprised time envelopes presented on an oscilloscope, and frequency spectra presented by a 64-channel spectrum analyzer.

Six subjects were used to attempt identifying the clusters. When the targets were in motion - even very slight motion - the different clusters were readily identified aurally by all subjects in one session. When the targets were perfectly still, some practice in listening to each cluster was required, but this needed no more than 30 minutes. Once the different characters of the three clusters became apparent they could be memorised and retained.

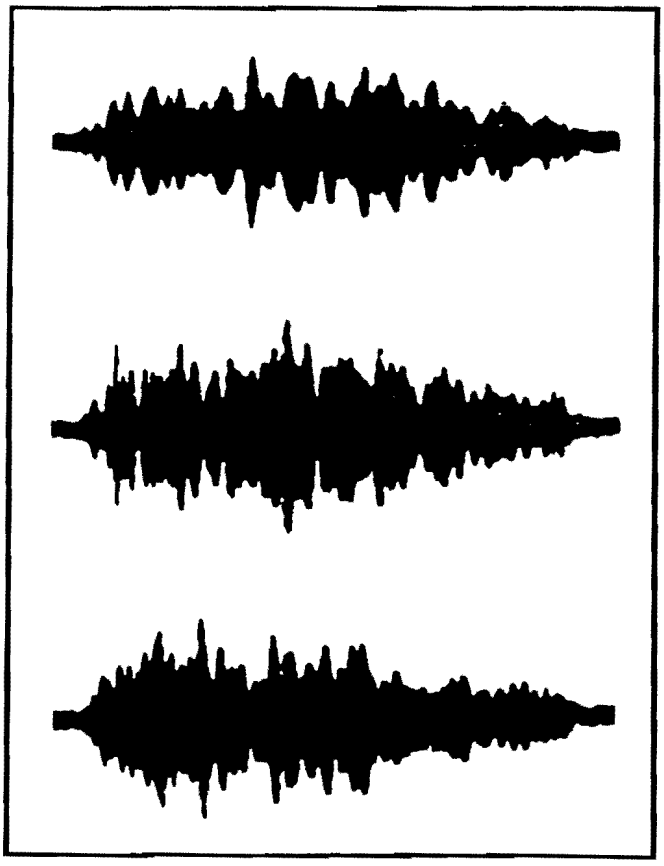

Figure 5.1 : Auditory envelopes of three target clusters.

The auditory envelopes produced by each of the three clusters are reproduced in Figure 5.1. It can be seen that they are difficult to distinguish visually, and the targets cannot be discriminated using these envelopes alone. The differences lie in the frequency domain, but even when the frequency spectra are plotted, the differences are not obvious. It appears that the human ear is better able to analyze the frequency spectrum of the sonar output than the spectrum analyzers used in the experiments. These results do not indicate that fish will generally be more readily identified aurally; rather, the particular targets, experimental set-up and displays favoured identification in this manner. Other forms of visual displays (temporal or spatial) may provide useful information.

5.4.2 Auditory, Visual, and Computer Rough/Smooth Classification

A major design objective of the Classification Sonar described in Chapters 8, 9, and 10 was that man-made objects be distinguishable from naturally occurring objects. Air modelling had led to the hypothesis that characterization would be possible if the "smoothness" of an object was used as an indication of its likelihood of being man-made (cf. Chapter 4). To determine the validity of this hypothesis and to investigate different methods of interpreting the sonar outputs, air models of rough and smooth targets were constructed.

Four "rough" (natural) targets and four "smooth" (man-made) targets were modelled. The rough targets comprised a sheet of gravel, an open pine cone, wood chips randomly glued onto a 30cm length of 2cm diameter dowling rod, and wood chips randomly glued onto a 30cm length of 8cm diameter tubing. The smooth targets comprised a 9cm diameter spherical sheet-copper ball, and three fire extinguisher canisters of lengths 30, 38 and 43cm, and diameters 10, 11 and 13cm respectively. The targets and sonar were configured so that the centre frequency of the demodulated output spectrum was 1,725 Hz.

Tape recordings were made of the targets so that all subjects would be presented with identical information. The targets were chosen and oriented randomly, and the recording level normalised to remove amplitude as a classification cue. One recording was used to train subjects : the first 20

targets were preceded by a statement indicating whether the target to follow was "smooth" or "rough", while the next 20 targets were followed by similar statements. Subjects played this tape once prior to each of the four trials. The second recording contained no verbal feedback; subjects were presented with 40 targets selected at random, and were asked to choose whether each target was smooth or rough.

Six subjects were used. In the first trial, the subjects were presented with the auditory signals through a pair of headphones. Table 1 gives the number of correct rough/smooth classifications for each subject. In the second trial, conducted several days later, the same recordings were used, but the display was visual. The recordings were analyzed by a Nicolet Scientific Corporation model 444 Mini Ubiquitous Spectrum Analyzer which displayed the spectra of the targets. Trials 3 and 4 repeated the first two, with the exception that noise was added to the outputs corresponding to the targets. The added noise had a 3 dB-down bandwidth of 960 Hz centred on 1725 Hz, and its intensity was such that the total noise energy in this band equalled the total signal energy of the target (i.e. 0dB S/N). It is seen in Table 1 that the added noise degraded performance somewhat, although the number of correct responses still averaged better than 80%.

Subject No.	Audio no noise	Visual no noise	Audio 0dB S/N	Visual 0dB S/N
1	31	40	27	32
2	31	37	33	35
3	35	39	35	37
4	36	39	33	36
5	37	40	36	35
6	39	40	37	36

Table 1 : Operator Performance on Rough/Smooth Classification Experiment (correct classifications out of 40 randomly selected targets).

When asked which factors were used in classifying the recordings, all subjects agreed that with the auditory display, 'purity' of sound was the prime consideration - a smooth target tended to have a single dominant frequency which appeared constant during a sweep, while a rough target sounded like a mixture of frequencies whose relative amplitudes varied continuously. Similarly, in considering the visual display, subjects reported looking for a dominant spectral component, the presence of which was used as a basis for deciding the target was smooth. Two of the subjects further reported that with smooth targets, the dominant frequency is often followed by a band of frequencies of noticeably low energy. This is consistent with the frequently noted phenomenon that a target is often not merely detected because of the echoes from the target per se, but because of the lack of echoes from the "shadow" cast by the target (Flemming et al., 1982).

From the data collected, it is presumptuous to infer any relative advantage of one display mechanism over another, as there are many uncontrolled variables. For example, subjects 1 and 2 of Table 1 were the only subjects with no prior experience listening to the auditory outputs of CTFM sonars, and this no doubt affected their auditory performance. (These same two subjects did have considerable experience analyzing visual displays). However, the data establish that the rough/smooth criterion hypothesized as being useful in discriminating between man-made and natural objects is valid, at least with air models using human perception.

The recordings described above were also analyzed by a computer to determine whether the decision process could be automated. Computer analysis requires specific recognition criteria to be isolated so that they may be programmed into the computer. The criterion used here was that the smooth targets have a frequency component that is dominant for the duration of the sweep. Three algorithms were tested sequentially:

1. The amplitude of the dominant peak is at least α times that of any other peak during a sweep, where α is a constant;

2. There are no more than η secondary peaks exceeding A/ℓ in the frequency spectra averaged over one sweep, where η and ℓ are constants and A is the amplitude of the maximum peak;

3. The dominant peak in the output corresponding to the start of sweep remains the dominant peak for the duration of the sweep.

The constants listed above were adjusted to optimise computer performance. The results are presented in Table 2, and indicated that automatic classification based on the rough/smooth criterion should be possible.

Computer Algorithm No.	No noise	Noise
1	36	34
2	39	38
3	37	31

Table 2 : Computer Performance on Rough/Smooth Classification Experiment (correct classifications out of 40 randomly selected targets).

5.5 CONCLUSIONS

The most common output displays of sonars and radars are visual. However, despite this preference for visual displays, there are many tasks which can be more readily performed using auditory displays. Furthermore, using an auditory display in addition to a visual display can improve the channel capacity.

While computer algorithms are not yet as capable as human operators at making some fine target discriminations, computers are not prone to fatigue. In addition, there are already instances where computers can perform characterization tasks beyond the capability of human operators, and it is reasonable to expect that as algorithms gain sophistication, the need for humans to interpret sonar outputs will diminish.

CHAPTER 6

ECHO PROCESSING FOR TARGET CHARACTERIZATION

6.1 INTRODUCTION

The detection and classification of targets in a noisy environment on the basis of their acoustic echoes is a formidable problem. An optical image will generally be preferable to an acoustic image because of the smaller wavelengths involved, and hence the greater potential resolution. However, sonars tend to be used where vision is restricted, and in these situations ultrasonics often constitute the only practical imaging tool.

Sonar operators often search for small objects at great distances. Such tasks can be difficult using vision in air. For example, it may not be easy to visually identify a football on a beach at 200m, and yet an analogous performance is frequently expected of a sonar operating underwater. Furthermore, acoustic echoes may not be received from all parts of an object; for perfectly smooth targets, unless the surface is perpendicular to the direction of the incident beam, echoes will only be received from surface discontinuities (such as edges or corners), or, if there is any target penetration, from interior discontinuities. Sometimes information may be gained about a target not from echoes from the target itself, but rather from the lack of echoes from the background area masked by the target.

This chapter discusses the statistics of sonar echoes, and shows how a knowledge of these statistics can influence the choice of processing techniques and subsequent display mechanisms used to attempt target detection

and classification. Various statistical analysis methods are compared as a background to the detection and classification algorithms invoked in the Classification Sonar (Chapters 9).

Many descriptors are used, often loosely and interchangeably, to describe the information gained by a sonar about an object. The use of some descriptors is defined for this thesis as follows:

Detection : awareness of the presence of an object or suspected target; nothing is known about the nature of the object.

Characterization : with no a priori information about objects in the environment, objects may be characterized as having certain features.

Classification : with a priori information about objects in the environment, objects may be classified as belonging to one of a finite set of possible targets.

Recognition : when targets and their acoustic echoes are known, recognition occurs when echoes are recognized as coming from a known target.

Identification : when it is not known what targets may expected, identification takes place when echoes carry sufficient information to determine what the target is.

Thus, as defined above, classification and recognition apply when the sonar is searching for known targets, while characterization and identification apply to unknown targets. Detection covers both cases.

6.2 DETECTION STRATEGIES

In the absence of backscatter, the detection of signals would pose few if any problems. The presence of backscatter in the output of a sonar forces a decision to be made as to whether a received waveform comprises noise alone,

or noise plus the wanted signal. Such a decision process is illustrated in Figure 6.1, which shows the sampled outputs of a bank of contiguous filters connected to the demodulated output of a CTFM sonar (Figure 6.1 may also be considered to represent the output of a pulsed sonar). Detection is usually based on establishing a threshold and considering a target to be present if this threshold is exceeded. The dashed line in Figure 6.1 represents a threshold which is exceeded only at point A. Hence, a target is considered present at A by definition. However, it is possible that the high amplitude of this filter was caused by noise alone, in which case a false alarm would have occurred. Conversely, noise may have destructively interfered with the echo from a true target at B, resulting in the signal amplitude failing to exceed the threshold. Hence the threshold must be chosen judiciously, as increasing the threshold will reduce not only the probability of a false alarm but also the probability of detection. These parameters are more readily illustrated with reference to probability density functions.

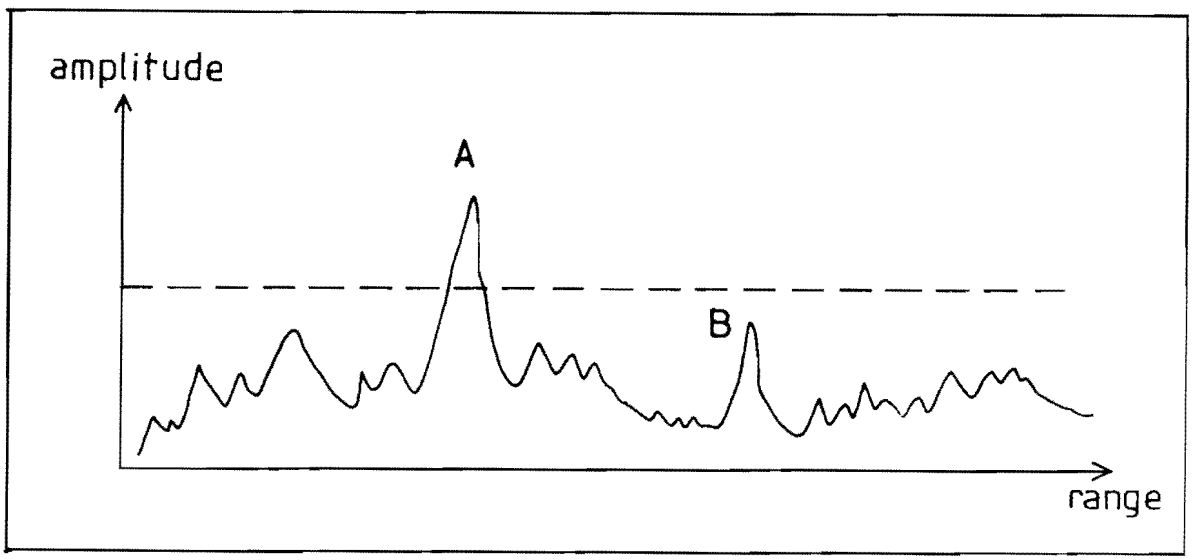

Figure 6.1 : Target detection based on a threshold level.

The sources of backscatter and noise (e.g. thermal noise and sea-state noise) in a sonar may each be represented by gaussian statistics. The probability density function of a gaussian distribution is defined by (Marcum, 1960)

$$p(x) = \frac{1}{\sqrt{2\pi\psi_0}} e^{-x^2/2\psi_0} \tag{6.1}$$

where ψ_0 is the variance, the mean value of x is taken to be zero, and the parameters have been normalized to ensure that

$$\int_{-\infty}^{\infty} p(x)\, dx = 1 \tag{6.2}$$

Furthermore, according to the Central Limit Theorem, the probability density of the sum of these statistically independent signals will also be gaussian. Thus, the probability density of the backscatter and noise sources prior to spectrum analysis will be gaussian.

Now if a gaussian signal is passed through a narrowband filter (one whose bandwidth is small compared to the centre frequency), as occurs with spectrum analysis, the probability density of the envelope is shown by Rice (1944) to be

$$p(R) = \frac{R}{\psi_0} e^{-R^2/2\psi_0} \tag{6.3}$$

where R is the amplitude of the envelope of the filter output. Equation 6.3 is known as the Rayleigh probability density function.

The probability that the noise envelope will exceed a threshold ν is

$$\begin{aligned} P(\nu < R < \infty) &= \int_{\nu}^{\infty} \frac{R}{\psi_0} e^{(-R^2/2\psi_0)}\, dR \qquad (6.4) \\ &= e^{-\nu^2/2\psi_0} \\ &= P_{fa}. \end{aligned}$$

Recall that a target is considered present whenever the envelope exceeds the threshold. Since the probability of a false alarm is the probability that the noise will cross the threshold, Equation 6.4 gives the probability of a false alarm, denoted P_{fa}.

6.2.1 Peak Detection

Consider next a sine wave of amplitude A to be present in addition to the noise at the input to the narrowband filter, and let the frequency of the sine wave be within the band of the filter. Then the output of the envelope detector has a probability density function given by (Rice, 1944)

$$p(R) = \frac{R}{\psi_0} e^{\frac{\left(-(R^2+A^2)\right)}{2\psi_0}} I_0(RA/\psi_0) \qquad (6.5)$$

where $I_0(Z)$ is the modified Bessel function of zero order and argument Z. Equation 6.5 is known as the Rician probability density function.

For large Z, an asymptotic expansion for $I_0(Z)$ is

$$I_0(Z) \approx \frac{e^Z}{\sqrt{2\pi Z}} \left(1 + \frac{1}{8Z} + \ldots\right) \qquad (6.6)$$

When the signal is absent, A = 0, and Equation 6.6 reduces to the Rayleigh function of Equation 6.3. The Rayleigh function is thus a particular case of the Rician function.

The probability of detection is then the probability that the envelope R will exceed the threshold ν, i.e.

$$\begin{aligned} P_d &= \int_\nu^\infty p(R)dR \\ &= \int_\nu^\infty \frac{R}{\psi_0} e^{\frac{\left(-(R^2+A^2)\right)}{2\psi_0}} I_0(RA/\psi_0)\, dR \end{aligned} \qquad (6.7)$$

This is not readily evaluated, but an approximation, valid when $RA/\psi_0 >> 1$ and $A >> |R-A|$, and terms in A^{-3} and beyond can be neglected is (Rice, 1944)

$$P_d = \frac{1}{2}\left(1 - \text{erf}\,\frac{\nu - A}{\sqrt{2\psi_o}}\right) + \frac{e^{\left[-(\nu-A)^2/2\psi_o\right]}}{2\sqrt{2\pi}\,(A/\sqrt{\psi_o})}$$

$$\times \left[1 - \frac{\nu - A}{4A} + \frac{1+(\nu-A)^2/\psi_o}{8A^2/\psi_o} - \ldots\right] \qquad (6.8)$$

$$\text{where erf } Z = \frac{2}{\sqrt{\pi}} \int_0^Z e^{-u^2}\, du.$$

This process is illustrated graphically in Figure 6.2. The probability density function for noise alone (Equation 6.3) is plotted along with that for signal plus noise (Equation 6.6), with $A/\psi_o = 3$. A threshold of $\nu/\sqrt{\psi_o} = 2.5$ is shown. The area under the Rician curve to the right of the threshold indicates the probability of detection, while the corresponding area under the Rayleigh curve indicates the probability of a false alarm. If the threshold is increased to reduce the probability of a false alarm, the probability of detection is also reduced. Families of curves exist to illustrate the relation between probabilities of detection, probabilities of false alarms, and signal to noise ratios (e.g. Skolnik, 1982).

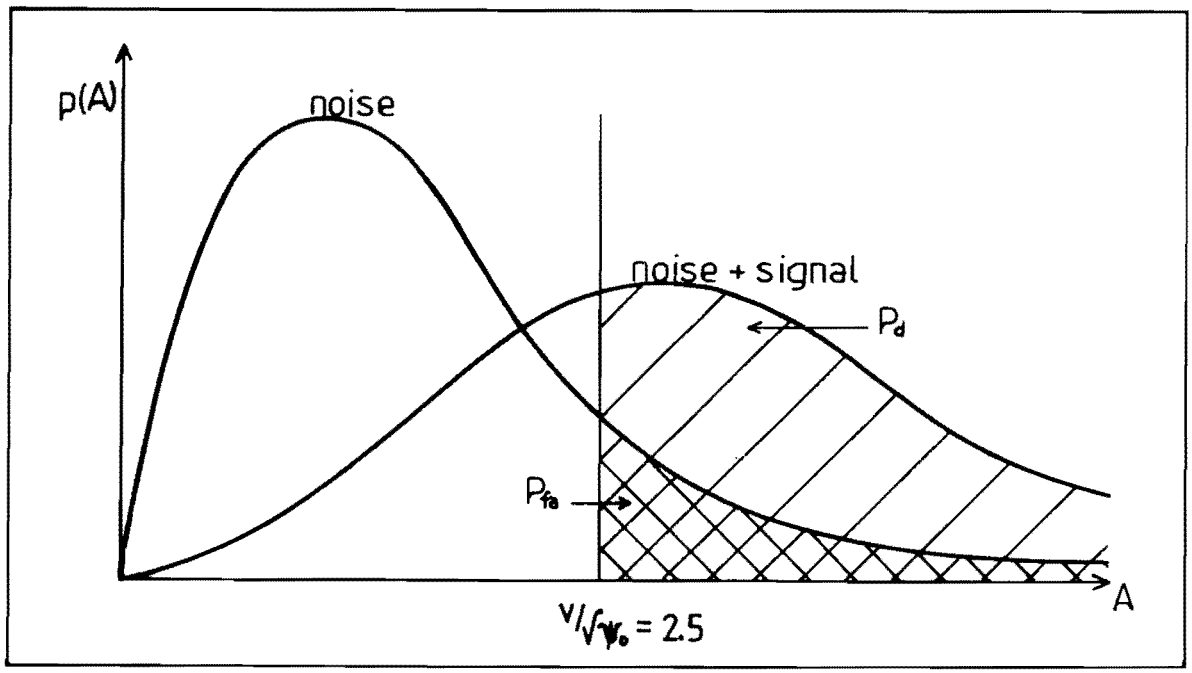

Figure 6.2 : Probability density functions of Rayleigh and Rician distributions; the threshold level determines P_d and P_{fa}.

The relationship between P_d, P_{fa}, and S/N as shown in Figure 6.2 applies to a single output sample only. If more than one sample is received from a particular sector, there are two general methods of processing the extra data: integration, and probability density analysis.

Integration involves combining the samples (typically by averaging the amplitudes) to improve the S/N. Using coherent integration (where phase information is preserved), the integration of n pulses, all with the same S/N, results in an integrated S/N (power) n times that of a single sample. If the same n pulses are integrated by an incoherent integrator, the resultant S/N would be less than n times that of a single sample (Marcum, 1960). However, although incoherent integration is not as efficient as coherent integration, it is generally used more often since in many applications it is simpler to implement (Skolnik, 1982).

Nonetheless, the relatively slow velocity of propagation of sound can result in considerable changes in the positions of targets and/or the sonar between samples to make each sample unique and thus render integration inappropriate. For example, a pulsed side scan sonar with a three degree beam and travelling at 20 knots cannot possibly get more than one return from each sector. Consequently, integration tends to be restricted to radar devices.

However, recall from section 2.7 that in a CTFM sonar, range resolution may be traded for response time. Many samples may thus be obtained from a CTFM sonar in the same time that it takes a comparable pulsed sonar to receive one pulse echo. Assume for instance that a pulsed and CTFM sonar are operating under identical conditions over the same transmitted bandwidth and maximum range. They will then have the same range resolution, and will receive a sample from each range cell once every pulse repetition period or sweep period. The pulsed sonar cannot receive samples more frequently than this, even if the range resolution is degraded (by lengthening the pulse). However, if the range resolution in the CTFM sonar is degraded by a factor of say 10 (by broadening the bandwidths of the filters in the spectrum analyzer), then the filter response times will be correspondingly shortened, and 10 times as many samples will be received during each sweep period. Each sample will now correspond to an annulus of seabed 10 times wider than previously, and so the S/N will be $1/\sqrt{10}$ of what it was previously.

The 10 samples may be integrated, and assuming ideal (coherent) integration, the S/N will be what it was originally, i.e. the same as for the pulsed sonar. However, instead of being integrated, the samples may be analyzed statistically using techniques based on probability density functions such as hole detection and maximum likelihood estimation.

6.2.2 Hole Detection

Consider again the probability density functions corresponding to a Rayleigh distribution and a Rician distribution with arbitrary mean, as shown in Figure 6.2. We have seen that for a single sample a common detection strategy is to compare the sample to a threshold level, and to consider a target to be present whenever this threshold is exceeded. When many samples are available, several options exist in addition to integration. For example, a target may only be considered present if all samples exceed a threshold, or if any one or several samples exceed the threshold. Similarly, instead of considering a relatively high amplitude threshold, as in Figure 6.2, Kay (1960) has shown that we may now consider a relatively low amplitude threshold, and assume a target to be present only if this low threshold is exceeded by every sample. Such a low threshold is illustrated in Figure 6.3.

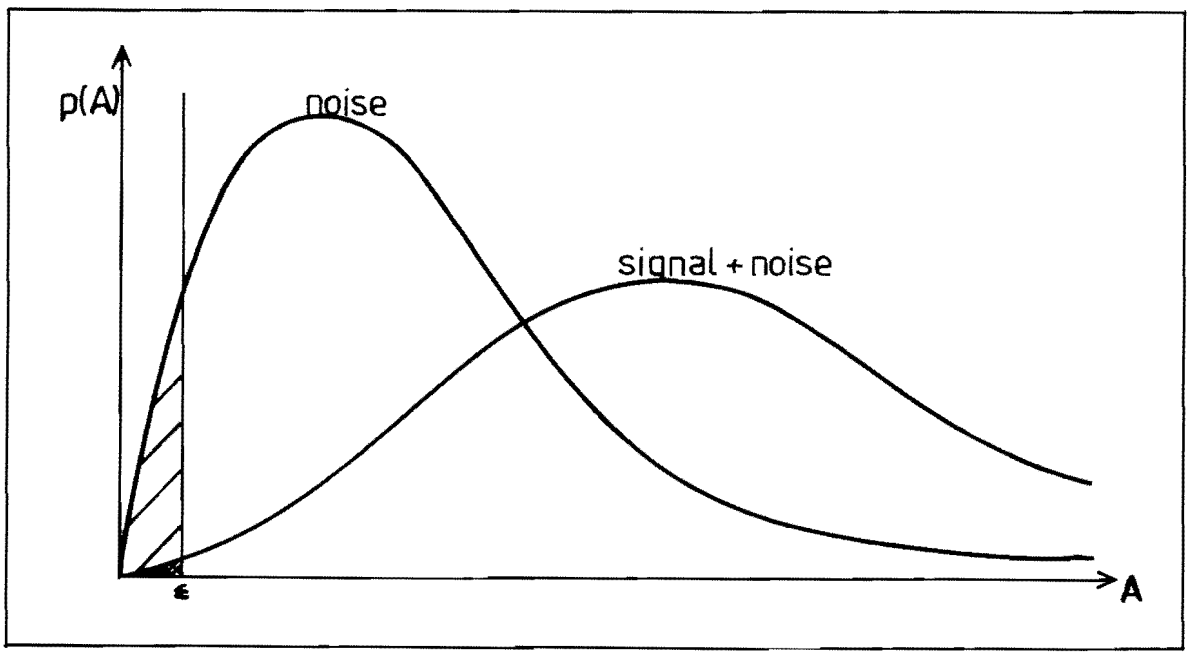

Figure 6.3 : Probability density functions of Rayleigh and Rician distributions with a low amplitude threshold ε.

Notice that the area to the left of ε under the Rician curve is much less than the corresponding area under the Rayleigh curve. In other words, the probability of low amplitude echoes from a range cell encompassing a target is extremely low. When many samples from contiguous range cells are viewed on an A-scan display, this low probability of small amplitude signals (whenever a target is present) shows up as a gap extending from the base line to the lowest amplitudes present for that particular range cell. These gaps have the appearance of holes on the display, and hence the detection of targets based on noting the absence of low level signals is referred to here as hole detection.

The probability of detection using hole detection is then the probability that no samples from the parent (Rician) distribution fall below the threshold, i.e.

$$P_d = \left[\int_{\varepsilon}^{\infty} \frac{R}{\psi_0} e^{\frac{(-(R^2+A^2))}{2\psi_0}} I_0(RA/\psi_0)\, dR \right]^n \qquad (6.9)$$

where n is the number of samples taken. The value of ε will normally be determined by the number of samples available and the desired P_d. For instance, using 20 samples and with a desired $P_d = 0.8$, the area to the right of ε in the parent Rician distribution must equal $(0.8)^{1/20} = 0.989$. With ε established, the probability of a false alarm can then be determined as follows:

$$P_{fa} = \left[\int_{\varepsilon}^{\infty} \frac{R}{\varepsilon} e^{(-R^2/2\psi_0)} dR \right]^n \qquad (6.10)$$

For small values of ε, the integral inside the square brackets in Equation 6.10 may be substantial, and consequently hole detection using a single samples is inappropriate. However, since P_d is always greater than P_{fa} for any n and ε, then as n increases, P_{fa} will diminish more rapidly than P_d. For example, if the integral of Equation 6.10 is 0.7, then for $n = 20$, $P_{fa} = 7.8 \times 10^{-4}$.

The figures drawn above of Rayleigh and Rician probability density functions have all been normalised according to Equation 6.2. However, the backscatter from two different areas of seabed, one relatively smooth, the other rough, can result in considerably different average amplitudes, even though both parent distributions may have the Rayleigh distribution shape. Similar variations in absolute amplitudes may occur with samples from Rician distributions. Consequently, when looking for average or peak values on an A-scan display, it may be difficult to distinguish the samples produced by an area of strong backscatter without a target, from an area of weaker backscatter with a target. In looking for holes, however, only one would be found in the above two situations, as illustrated in Figure 6.4. A similar technique is used by Newhouse et al. (1982) to detect flaws in solid materials. Examples of hole detection are given in Chapter 10.

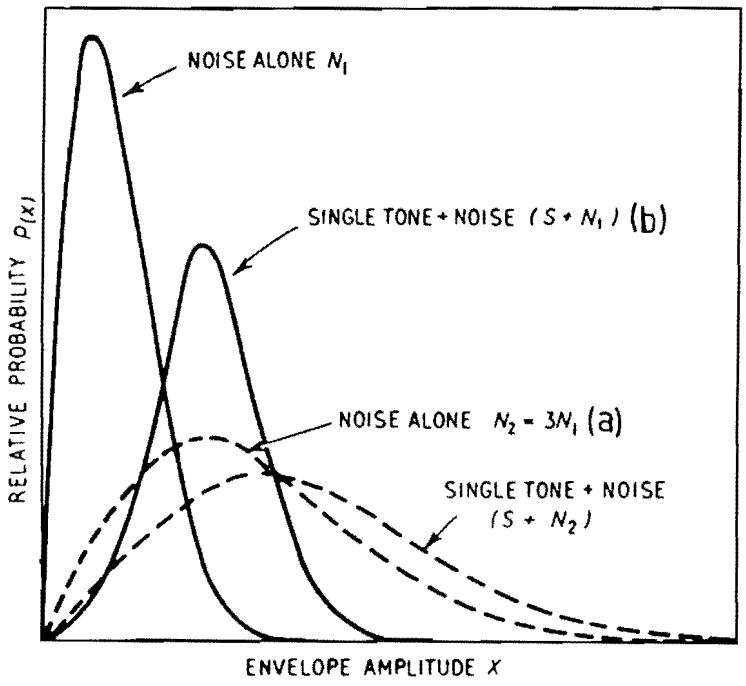

Figure 6.4 : Non-normalised probability density functions of (a) strong backscatter without a target, and (b) weak backscatter with a target.

6.2.3 Maximum Likelihood Detection

The peak detection and hole detection techniques outlined above consider high amplitude and low amplitude samples respectively from the probability density function. A more rugged system may use samples both below ε and above ν. In the limit, the amplitude of each sample may be considered in determining whether a target is present. One of the best known techniques which uses the amplitude of each data point is the Maximum Likelihood Estimator.

The Maximum Likelihood Estimator sets up two hypotheses, namely:

H_1 : the samples are produced by a Rician distribution with unknown signal amplitude A and noise variance ψ_0;

H_0 : the samples are produced by a Rayleigh distribution.

Let $R_1, R_2, \ldots R_n$ be n random samples with density functions

$$f(R_i, A, \psi_0) = \frac{Ri}{\psi_0} e^{\frac{\left(-(R^2+A^2)\right)}{2\psi_0}} I_0(RA/\psi_0) \tag{6.11}$$

Then the joint density function is

$$L(A,\psi_0) = f(R_1,R_2,\ldots R_n;\ A,\ \psi_0), \tag{6.12}$$

and because the R_i are mutually independent,

$$L(A,\psi_0) = f(R_1;A,\psi_0) \times f(R_2;A,\psi_0) \ldots . f(R_n;A,\psi_0). \tag{6.13}$$

Note that $L(A,\psi_0)$ is a function of A and ψ_0 only, and call it the likelihood function, i.e.

$$L(A,\psi_0) = \prod_{i=1}^{n} f(R_i;A,\psi_0) \tag{6.14}$$

Then the values of A and ψ_0 for which $L(A,\psi_0)$ is a maximum are called the maximum likelihood estimators of A and ψ_0 (i.e. those values of A and ψ_0 which define the probability density function most likely to have generated the data points $R_1, R_2, \ldots R_n$).

The maxima are determined by taking the natural logarithms of both sides of equation 6.14:

$$\ell n\ L(A,\psi_o) = \sum_{i=1}^{n} \ell n\ f(R_i;A,\psi_o) \qquad (6.15)$$

$$= \sum_{i=1}^{n} \ell n\ R_i - \ell n\psi_o - \frac{1}{2\psi_o}.(R_i^2+A^2) + \ell n\ I_o(AR_i/\psi_o).$$

The maxima will occur when equation 6.15 is equated to zero, i.e.

$$\frac{\partial}{\partial A}\ \ell n\ L(A,\psi_o) = \sum_{i=1}^{n} \left(\frac{-A^2}{\psi_o} + \frac{I_1(ARi/\psi_o)}{I_o(ARi/\psi_o)}\frac{Ri}{\psi_o} \right)$$

$$= 0 \qquad (6.16)$$

Equation 6.16 is solved to yield

$$A = \frac{1}{n}\sum_{i=1}^{n} R_i.\frac{I_1(ARi/\psi_o)}{I_o(ARi/\psi_o)} \qquad (6.17)$$

Similarly,

$$\psi_o = \frac{1}{2n}\sum_{i=1}^{n} R_i^2 - \frac{A^2}{2} \qquad (6.18)$$

Since both A and ψ_o are unknown and dependent, they are estimated iteratively, with each estimate of one parameter being used to determine the next estimate of the other. The iterations continue until $(A_{n+1} - A_n)$ and $(\psi_{o_{n+1}} - \psi_{o_n})$ are less than some predetermined limit. The hypothesis H_o can then be tested.

Because all sample points are used to determine the likelihood of a target being present, the maximum likelihood function is more rugged than either peak detection or hole detection discussed above, which consider only the number of samples above or below certain limits. Furthermore, the technique automatically compensates for variations in the reverberation level, and can be modified to provide a constant false-alarm probability (Cable, 1977). However, the manner in which the samples must be processed makes the method computationally demanding, and for many systems which must operate in real-time, prohibitive.

6.3 CLASSIFICATION STRATEGIES

While techniques and systems for the detection and localisation of targets have become sophisticated, relatively little research has been directed to the problem of discriminating between several potential targets. Some attempts at target discrimination have been made by analyzing echoes in the time domain (e.g. Hoffman, 1971), but most of the research has involved analysis in the frequency domain. Chestnut et al. (1979) postulated that in order to recognise a target, the system must analyze the frequency response of that target, and further that the system must have a wide bandwidth. In a subsequent paper, Chestnut & Floyd (1981) developed an aspect-independent sonar target recognition method based on frequency response analysis using a pulsed sonar.

Diverse frequency domain classification techniques have been investigated. Energy spectrum analysis has been proposed as a model of animal sonar processing (Johnson & Titlebaum, 1976), while Skinner et al. (1977) studied a classification technique based on a power series expansion of the target transfer function. Robertson (1980) characterized signals using high resolution spectral analysis, and Smith (1981) concluded that the maximum entropy method of spectral analysis has several advantages over other methods.

Since the classification of a target conveys more information about the target than mere knowledge of its presence, it follows that classification requires more information from a target than detection. Such additional information will result from a higher S/N ratio. For example, Do (1977) has found that in using audition to analyze the outputs of a CTFM underwater sonar, the S/N required for classification is 10 dB above that required for detection.

This section considers two general classification strategies : high range resolution analysis and frequency analysis.

6.3.1 High Range Resolution Analysis

The classification of targets based on high resolution echo processing is equally valid for comparable pulsed and CTFM sonars. Several criteria may be used as a basis for classification decisions.

The first criterion considers the amplitude of each reflecting point on the target, either in absolute terms, or relative to other reflecting points or background noise. For example, consider a rectangular target illustrated in Figure 6.5. For the angle of incident ultrasound indicated, the echo from the leading corner (labelled A) can be expected to be greater than that from corner B, which will in turn be greater than the echo from the trailing corner C, while D will in all probability not show at all. Hence, the classification of an unknown target as the rectangular shape illustrated in Figure 6.5 may be partially conditional upon the correct ranking (and possibly acceptable proportioning) of the received echo strengths.

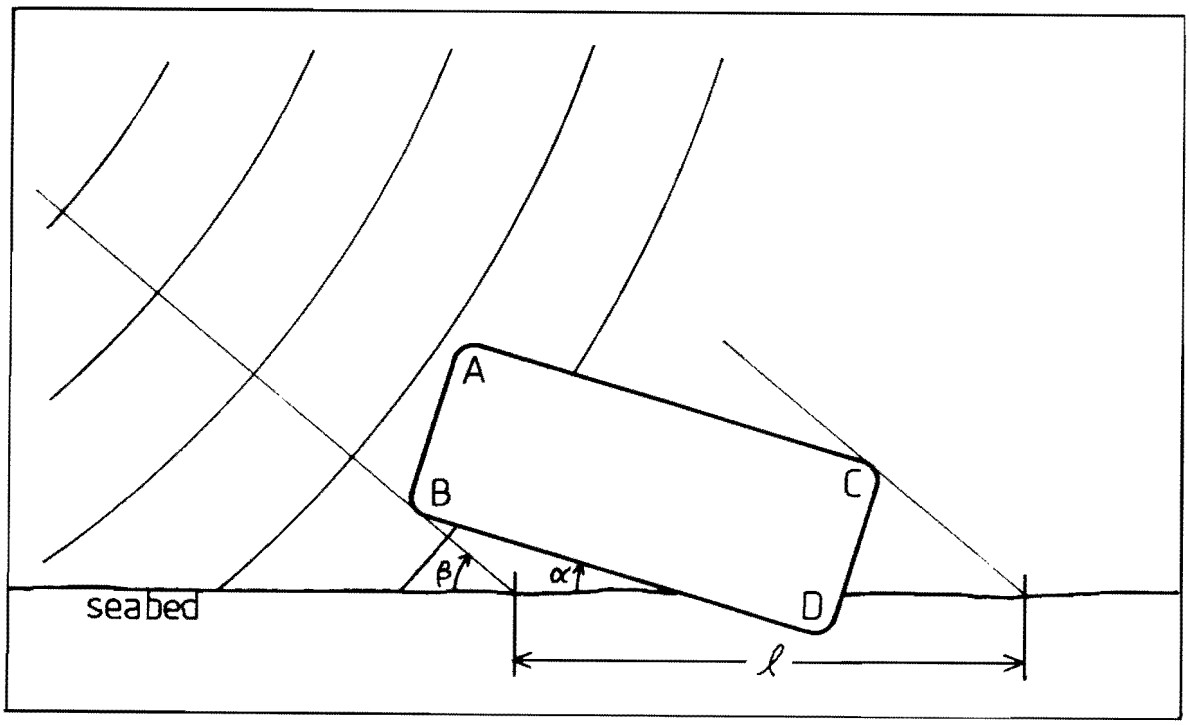

Figure 6.5 : Cross-section of target on seabed; backscatter from seabed is masked for an extent 'ℓ'.

If the target is on or near the seabed, additional information may be inferred, not from echoes from the targets per se, but from a lack of echoes from an area of seabed masked by the target. The extent to which this effect will be apparent will depend on the area of the target "shadow" compared to the plan projection of a resolution cell on the seabed. In Figure 6.5, the seabed is masked from the sonar for a distance labelled 'ℓ', which may include several range annuli past the end of the target. For such a void to be apparent, there must be noticeable backscatter from the seabed in the absence of targets. The masking of background seabed by targets is particularly noticeable on maps produced by side scan sonars, and some excellent examples are given in Flemming et al. (1982).

For targets which have only a single reflecting point (e.g. a perfect sphere or an infinite wedge), echo amplitude analysis is the only aid to classification. Most real targets, however, have more than a single reflecting point, and in addition to analyzing the echo strengths of these reflectors, their spatial distribution can provide extra information useful for classification. Consider again the rectangular target in Figure 6.5. The separation in range between points A and B is $\omega.\sin(\beta-\alpha)$, where ω is the actual distance between A and B, α is the inclination of the target relative to a horizontal seabed, and β is the angle of incident radiation. Similarly, the separation in range between points A and C is $\rho.\cos(\beta-\alpha)$, where ρ is the distance between A and C. Consequently, for every aspect of the target relative to the sonar, there is a fixed relationship between the separations in range between A and B, and A and C, namely

$$AB/AC = \omega/\rho \tan(\beta-\alpha) \qquad (6.19)$$

Hence if the shape and dimensions of the target are known a priori, measurement of the spatial distribution of the reflecting points may substantiate or refute recognition of the target; if recognition has occurred, the spatial distribution may then serve to establish one of two possible (and ambiguous) aspects of the target as shown in Figure 6.6. Alternatively, if the shape and dimensions are unknown, the spatial distribution of the reflecting points merely places constraints on the possible shape and aspect of the target.

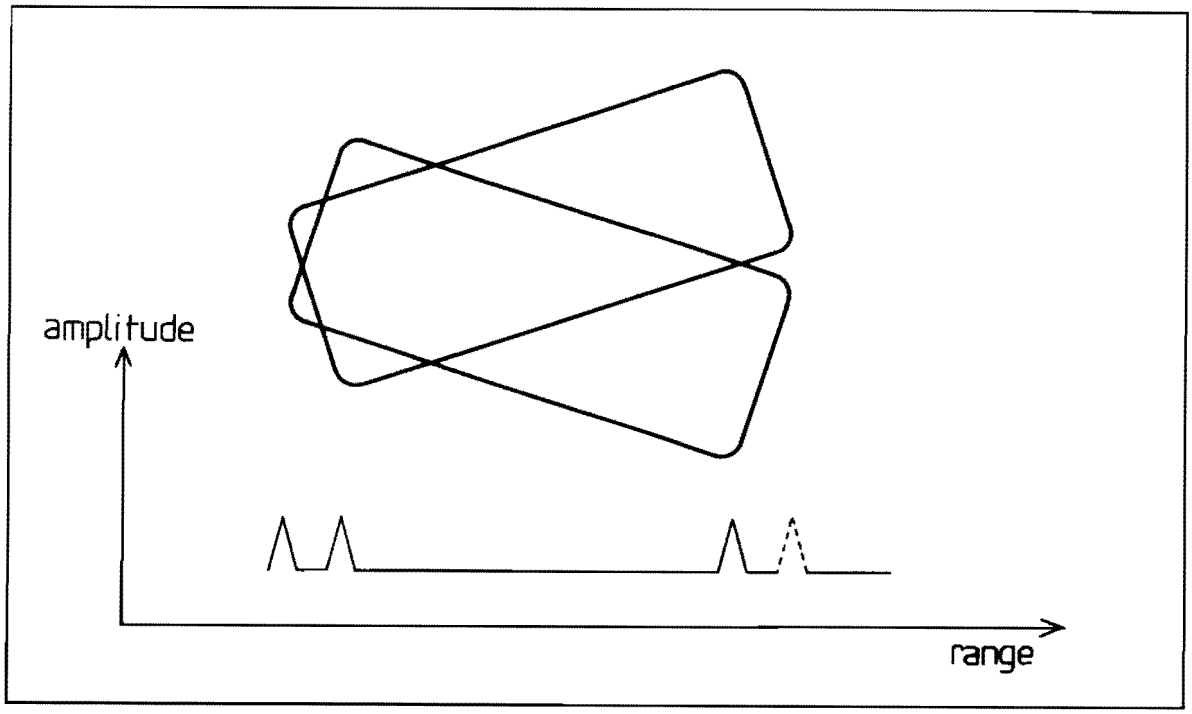

Figure 6.6 : Two possible aspects of a target given the echo structure shown.

Instead of attempting to associate each echo with a reflecting point, and thus undertaking some crude, uni-dimensional imaging of the object, more general characterization strategies may be invoked. For example, in Chapter 4 it was shown that a promising criterion for distinguishing between man-made and naturally occurring objects is to observe the 'smoothness' of an object. If the echoes from an object have relatively few major peaks with amplitudes considerably greater than the average echo strength, the object is likely to be smooth, and man-made. If, on the other hand, the echoes have many peaks, all of approximately the same amplitude, the object is likely to be rough, and therefore naturally occurring. Thus, this rough/smooth criterion considers the number of echoes and their amplitudes, but not their spatial distribution or their amplitude ranking within that distribution.

Various methods can be devised to implement the rough/smooth criterion. For instance, the amplitude of the peak echo compared to the average amplitude surrounding this peak will tend to be large for smooth objects. Similarly, the number of secondary peaks that exceed say half the amplitude of the primary peak will be smaller for smooth objects than rough

objects. Alternatively, the mean echo strengths from range cells surrounding a target may be compared to the median. The few large amplitude peaks associated with smooth objects will increase the mean, with almost no effect on the median. These methods and others have been implemented in the Classification Sonar detailed in Chapter 8. Their theory of operation and practical usefulness are discussed in Chapter 9.

6.3.2 Frequency Response Analysis

An alternative to high resolution analysis is to observe the frequency signature of a target. Frequency signatures are readily portrayed using stack plot displays (see Figure 1, page (ii), and section 2.2.7). A stack plot (or spectrogram) provides a convenient signal representation by portraying a waveform as a non-negative function of instantaneous frequency and time. Stack plot displays are useful for the spectral decomposition of data having a time-bandwidth product which is too large for an available Fourier transform device. The outputs of many CTFM sonars fall into this category. For such data, a sequence of Fourier transforms is obtained by shifting a window function across the data and calculating a Fourier transform for each new window position. The stack plot retains only the magnitude of each Fourier transform and discards the phase, but little information is destroyed by this process (Altes, 1980).

A stack plot is generated either by bandpass filtering or by Fourier transformation of a time-windowed signal, and plotting the resultant spectral components. Usually, frequency (corresponding to range) is plotted on the x-axis, echo-amplitude on the y-axis, and time on a slant axis. In the case of CTFM sonars, it is convenient to generate one stack plot from each transmitted sweep, so that each stack plot displays the frequency response of a target to the transmitted frequency band. The resultant image is a 3-dimensional representation of the frequency response of objects in the sonar's field of view.

Stack plot displays are a useful tool for target classification. Construction details of a stack plot display generator are given in Chapter 8, and numerous stack plot images are included in the results of sea trials of a Classification Sonar presented in Chapter 10.

6.4 SUMMARY

Many techniques are available to process sonar echoes and attempt target detection and classification. While some of these techniques apply equally well to both pulsed and CTFM sonars, others work best in conjunction with one particular kind of sonar. Thus, hole detection is ideally suited to the multiple outputs available from a CTFM sonar during each sweep, and constitutes a detection strategy which is useful visually and computationally.

Similarly, while frequency response analysis is invoked with pulsed sonars, the outputs of CTFM sonars can readily be processed in this manner. The resulting stack plot displays form a very useful classification tool for these sonars.

CHAPTER 7

DIVER'S SONAR FOR TARGET RECOGNITION

7.1 INTRODUCTION

An early diver's sonar, made using discrete transistors, was first described in 1961 (Colldeweih et al.), although the unit was originally produced in the 1950's using vacuum tubes. The sonar operated on the CTFM principle, and allowed a diver to detect an obstacle ahead of him as far away as 120m by listening to the auditory output. The unit resembled a searchlight in appearance, and was sufficiently bulky to require the diver to hold it with both hands. More recently, Ametek (Straza Division) and Edo Western Corporation have marketed diver's sonars similar to the Colldeweih et al. sonar (models DHS-2 and 384A respectively), although the bulk had been reduced to enable operation and manoeuvring with one hand, and the maximum range (of the Ametek sonar) had been extended to 200m (Milne, 1983). All these sonars suffer from a number of drawbacks, however. Firstly, single channel operation prevents direction information being coded in the sonar output; the sonars have to be aimed at a target to determine the target's presence and bearing. Consequently, two or more targets at different bearings cannot be perceived and localized simultaneously. Secondly, the transmitted bandwidths of around 0.2 of an octave (95 to 116 kHz for the Ametek sonar and 160 to 200 kHz for the Edo sonar) are relatively narrow, and hence target characterization is restricted (cf. Chapter 6). Thirdly, since at least one of the diver's arms is used to manoeuvre the sonar, the diver is handicapped in performing any additional tasks.

Shorrock and Woodward (1984) further criticise the Colldeweih et al. sonar (and by implication the Ametek and Edo sonars) by pointing out that it does not measure the range to an object, but merely gives an audible indication which undergoes subjective assessment by the diver. While that observation is correct, all mammals navigate successfully using either vision or echolocation, on land or underwater, with only a subjective assessment of the distances to objects. Furthermore, blind humans can navigate using ultrasonic blind aid devices without an objective measurement of the range to objects (e.g. Kay, 1974). This author believes that knowledge of the exact distance to an object will often be of considerably less use than some knowledge of what the target may be, for if it is a target of interest, the diver will usually want to approach (or avoid) it (and his subjective assessment of range will be sufficiently good to permit this), while if the target is of no interest, then knowledge of its presence and approximate range will suffice for navigation.

Shorrock and Woodward then describe a pulsed sonar rangefinder developed to give a digital readout of the range to the nearest target in a single beam. This device still does not provide characterization ability, or the ability to simultaneously detect and track targets at different ranges and/or bearings. It appears that the primary aim of the Shorrock and Woodward sonar is to measure the range to a target. Such a facility can also be provided by CTFM sonars, as indicated by their reference to their own CTFM rangefinder.

Milne (1980) describes a rangemeter sonar which can fix an operator's position by triangulation of the measured slant ranges to three seabed transponders. This sonar thus addresses itself only to the task of determining absolute position.

Hicks and Hollien (1983) look at diver navigation using sound from a different perspective. Claiming that 'traditional' approaches to overcoming visual limitations underwater (tethered diving, and use of a compass combined with dead reckoning) are only marginally successful, they propose a system whereby divers use their natural ability to perceive and localize sound underwater. Linear arrays of transducers are energised by computer controlled pulses to insonify the environment. Since diver's perception of these sounds varies according to the diver's position relative to the transducers,

navigation is possible. While this system has the advantage that divers are not encumbered with electronic equipment, navigation can only take place where transducers have previously been placed, and no detection, let alone classification, is possible of objects in the environment.

The primary aim of the sonar described in this chapter is to provide a diver with target classification capability under conditions of poor or zero visibility. In addition, it is desirable to simultaneously display to the diver multiple objects in his field of view, thereby enhancing object detection and navigation. Since air modelling of the diver's sonar had already been undertaken using blind aids, the basis for achieving these aims had been established. The remainder of this chapter describes the transducer element design, signal processing, physical construction, and sea trials.

7.2 TRANSDUCER ELEMENT DESIGN

CTFM and pulsed sonars impose different demands on transducer design. Firstly, CTFM sonars require two separate transducers: one for transmission, and one for reception. Secondly, although the transmitted bandwidths of a pulsed and CTFM sonar may be identical, the pulsed sonar operates at a single frequency, and its transducers may therefore be tuned to resonate at that frequency with a high Q, whereas the CTFM sonar sweeps through its full bandwidth and thus its transducers must have a repeatable and reasonably flat response over the entire frequency range.

The standard transducer design is based on the 'sandwich' principle developed by Langevin in 1917 to control the characteristics of a piezoelectric element, in particular the fundamental resonant frequency. In one form of this design, a piezoelectric ceramic (typically lead-zirconate-titanate) is sandwiched between two quarter wavelength blocks which determine the resonant frequency, control the bandwidth, acoustically couple the element to the medium, and provide a high mechanical impedance to the rear face of the element. Cady (1949) developed a rigorous theory to explain the performance of three-section sandwich transducers of arbitrary dimensions.

Since ceramics are weak in tension, a compressive prestress is normally applied to the transducer by means of a high-tensile steel bolt, which also improves the electrical and mechanical coupling between the faces of the components. However, one of the problems with this construction method is that the steel bolt affords multiple propagation paths for acoustic energy within the transducer. Through shear forces acting along the thread boundaries, energy may transfer between the bolt and transducer components several times, the velocity of propagation changing according to the density of the medium. Hence the desired acoustic signal may be corrupted (during both transmission and reception) by interfering signals caused by a multiplicity of propagation paths.

Pulsed sonars are largely immune to these corruptions : any destructive interference arising from secondary propagation paths at the operating frequency will merely reduce the peak sensitivity. Furthermore, the dimensions of the steel bolt may be trimmed to minimise the deleterious effect.

In CTFM sonars, however, this corruption is more evident. The transmitted frequency is continuously changing, and since the wavelength at any given frequency depends on the density of the propagating medium, the secondary path lengths (in terms of wavelengths) are also continuously changing, some combinations resulting in constructive interference, and others in destructive interference. As a result, the response of the transducer element varies during a sweep, giving rise to wide fluctuations in the sensitivity of the transducer element with frequency.

In an effort to reduce or eliminate the secondary propagation paths, two alternative sandwich transducer construction methods were investigated. The first method involved using adhesives to join the component parts, thereby entirely eliminating the bolt, while the second method involved a bolt which was an integral part of the front matching element.

7.2.1 Adhesive Construction

The use of adhesives in transducer construction had been investigated in the early 1970's (Smith, 1972), but subsequent advances in adhesive technology warranted further research. Accordingly, two adhesives were evaluated: epoxies and cyanoacrylates. With both types of glue, fine metal filaments must be mixed with the adhesive material to provide electrical conductivity between the piezoelectric ceramic and the matching elements. Without these filaments, the adhesive layers act as dielectrics and coupling to the ceramic is capacitive only.

Numerous transducer elements were constructed using epoxy adhesives with a variety of cure temperatures and times. The sensitivity of each element was then measured after prescribed time delays. Figure 7.1 gives an example of the frequency response of a randomly selected transducer element. The solid line shows the frequency response after 24 hours, and the broken line shows the response after 7 days. The difference between these two plots highlights the problem of using epoxy adhesives: the frequency response is not stable with time. The deterioration in sensitivity continues after seven days, albeit at a slower rate.

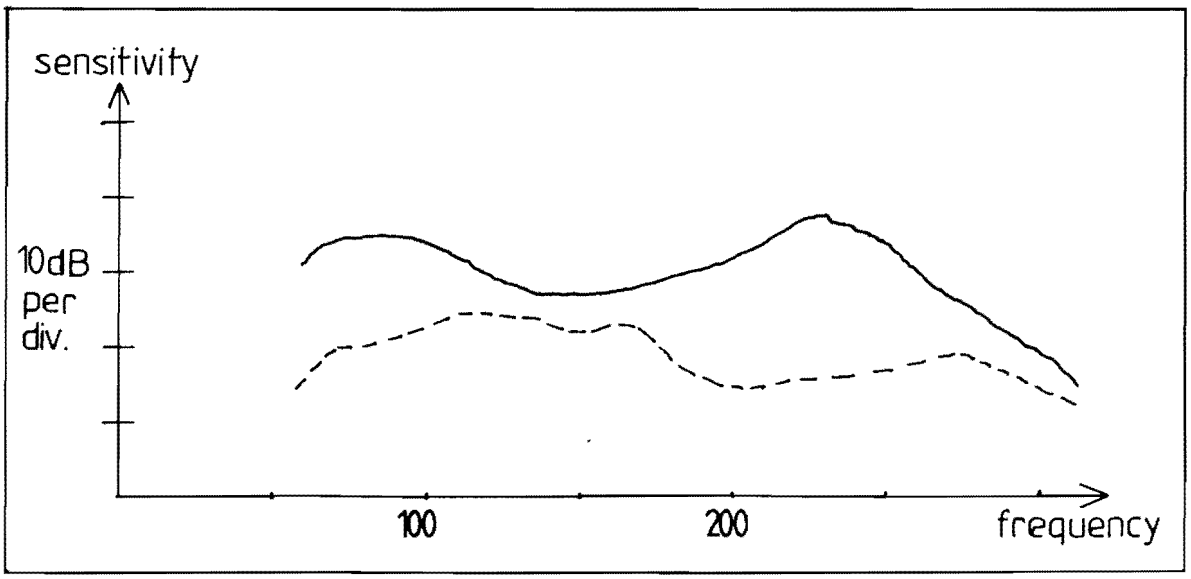

Figure 7.1 : Frequency response of a transducer element constructed using epoxy adhesives. Solid line shows response after 24 hours; broken line shows response after 7 days.

Many transducer elements were also constructed using several 'Loctite' cyanoacrylate adhesives. Figure 7.2 shows the frequency response of an element constructed in this manner. It is seen that the response is very flat over the desired frequency band. However, these adhesives require perfectly flat and smooth surfaces to effect a reliable bond, and the need to add metal filaments for electrical conductivity precludes these conditions. As a result, these elements tended to disintegrate after rigorous testing.

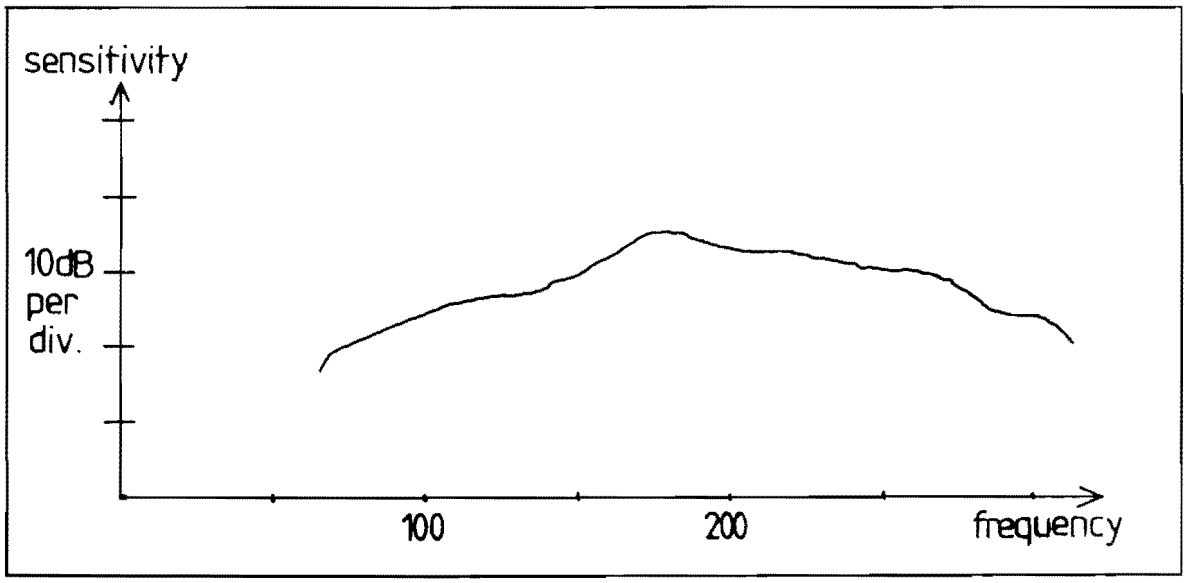

Figure 7.2 : Frequency response of a transducer element constructed using a cyanoacrylate adhesive.

One further disadvantage of using adhesives to join the constituent parts of transducer elements is that no tension can be applied to the components. Placing the transducer element under tension improves both the electrical and mechanical coupling between the components.

7.2.2 Bolt Construction

The second transducer construction method designed to reduce the multiple propagation paths that result from the steel clamping bolt involves making the bolt an integral part of the front matching element. As far as the author is aware, this is a novel approach.

An exploded cross-section of this transducer is given in Figure 7.3. The cylindrical projection from the front face now takes the place of the steel bolt. The piezoelectric crystal, the brass rear matching element, and an insulating washer are placed over the aluminium shaft, and a nut is tightened on the threaded end of the aluminium shaft. This nut allows the tension mentioned above to be applied to the transducer.

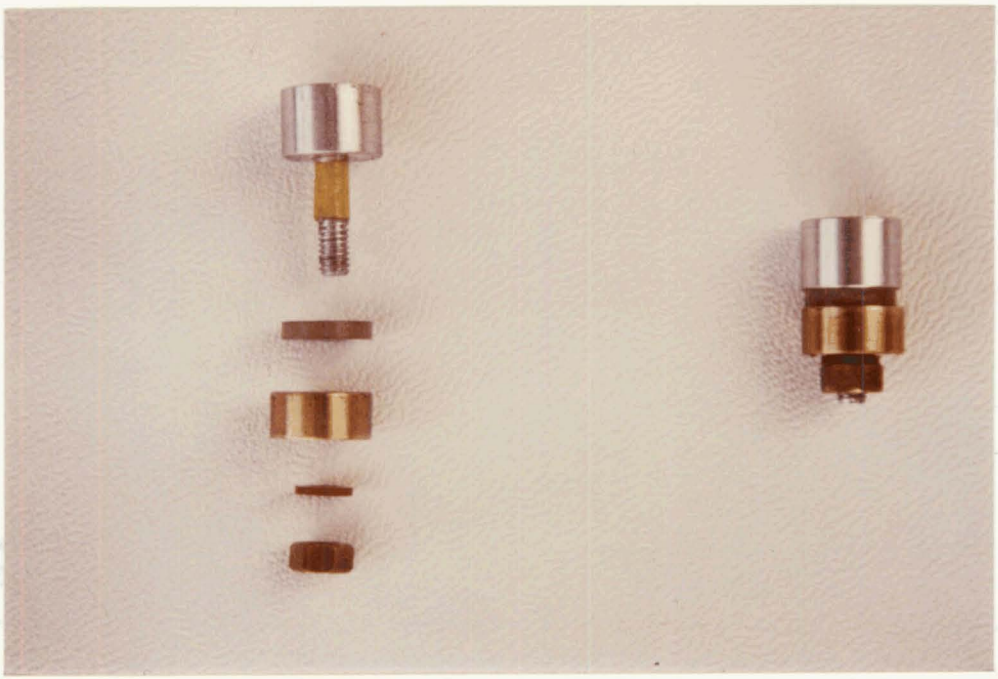

Figure 7.3 : Photograph of transducer elements with integral bolt showing from the top: aluminium front section with shaft; piezoelectric ceramic; brass rear section; washer; and nut.

The aluminium shaft does create a path for some acoustical energy, thereby enabling some secondary propagation. However, the energy in these secondary paths will be much less than in a transducer clamped with a steel bolt. Consider a transducer element operating as a receiver. There are now no shear forces acting to inject any of the energy incident on the front matching section into the aluminium shaft. Ignoring minimal diffraction effects, the only energy entering the aluminium shaft is that portion of the energy incident on the aluminium front matching section which falls within the projection of the shaft on the front surface. A converse situation applies for a transducer element operating as a transmitter.

The response over the operating frequency range is further smoothed by operating the transducers off resonance. This 'out of band' operation is not possible with conventional pulsed sonars, where the transmitted signal is generated by shock excitation of the crystal (Boys et al., 1978).

The frequency response of an aluminium shaft transducer is given by the solid line in Figure 7.4. The broken line shows the frequency response of a conventional steel-bolted transducer element. It is seen that the aluminium shaft element has a much flatter frequency response; furthermore, this response is stable over time.

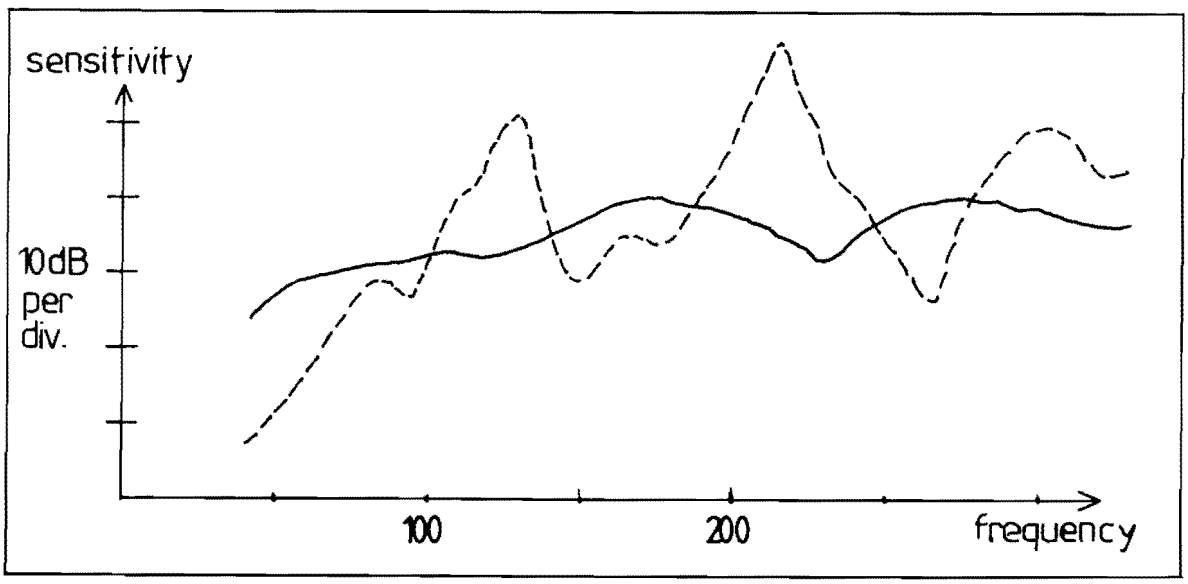

Figure 7.4 : Frequency response of integral bolt transducer element (solid line) compared to that of a conventional steel bolt transducer element.

7.2.3 Array Configuration

Once the transducer element design was optimised to give an acceptably flat frequency response, a small batch was produced. Thirty elements were used to make four arrays of the required beamwidths. The transmitter and two side channel receiver arrays comprise three transducer elements in a vertical column, resulting in 14 degree beamwidths vertically and 53 degrees horizontally (3dB down at the centre frequency). The centre channel receiver array comprises a 7 by 3 matrix of elements, resulting in 14 degree beamwidths vertically and 7 degrees horizontally. This array is shown in Figure 7.8.

Note that although the beamwidths vary during the frequency sweep, no beamwidth compensation was considered necessary (cf. section 2.2.3). This is because the longest sweep period of the diver's sonar (corresponding to a maximum range of 40m) is 800 ms, while the shortest sweep period is 100 ms. These sweep periods are sufficiently short that the ear integrates the output corresponding to the varying beamwidth (Rowell, 1970). The beamwidths of blind aids are similarly left uncompensated (Kay, 1974).

Each array is housed in an aluminium casing, the front face of which is made of 3mm thick neoprene. The neoprene is in contact with the front faces of the transducer elements. A silicon rubber vulcaniser is used to ensure good acoustical coupling between the neoprene and the transducer elements.

7.3 SIGNAL PROCESSING

The diver's sonar was developed before dual demodulation (see Chapter 3) was successfully implemented and before digital frequency synthesis was incorporated in sonars at the University of Canterbury. Hence the prototype diver's sonar is based on the conventional CTFM system as described in section 2.2, and uses analogue frequency synthesis.

The choice of operating frequency is always a compromise between several conflicting factors. For example, the higher the operating frequency, the greater the attenuation of the signal in the medium (thus restricting the range), but the smaller the size of the transducer array required to give a certain beamwidth. Further constraints are imposed by the frequency response attainable with transducer construction. An operating frequency of 165 kHz to 230 kHz was chosen.

Whereas previous underwater CTFM sonars with an auditory display had one receiver channel (Colldeweih et al., 1961; Milne, 1983) or two (Smith, 1972), the present diver's sonar is equipped with three receiver channels. Two of these channels are wide beam side channel receivers whose outputs are fed respectively to the right and left ear to provide an inter-aural amplitude difference (I.A.D.) for lateral localization (see section 2.2.10). The third

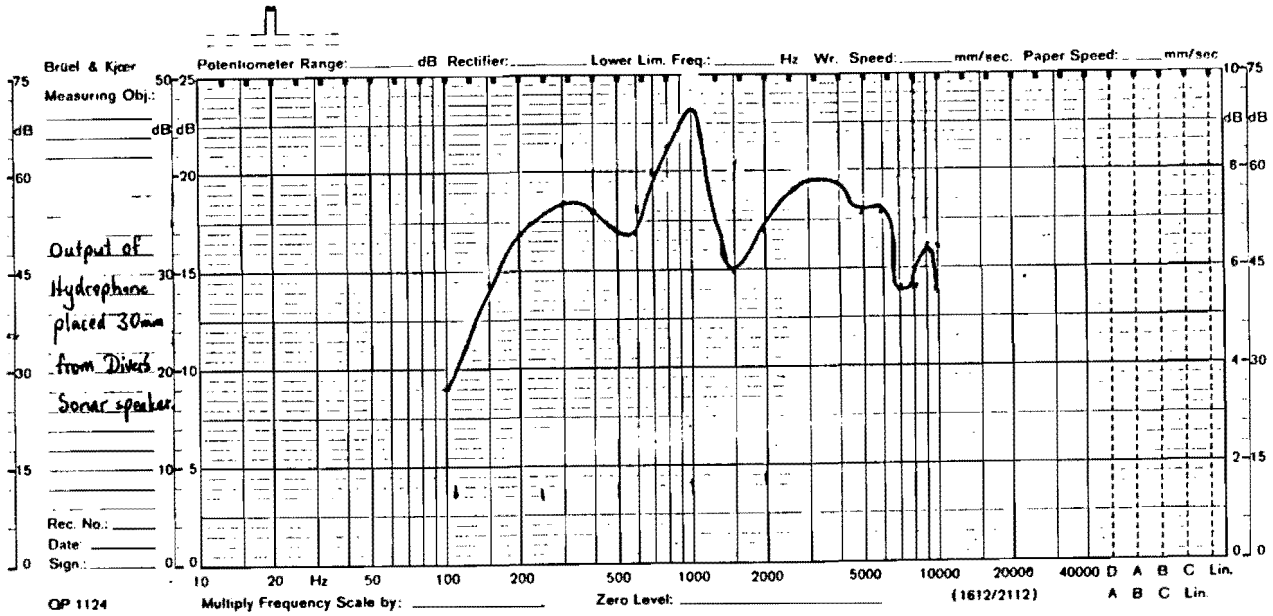

Figure 7.5(a) : Frequency response of a flat signal after transmission through the diver's sonar audio output chain.

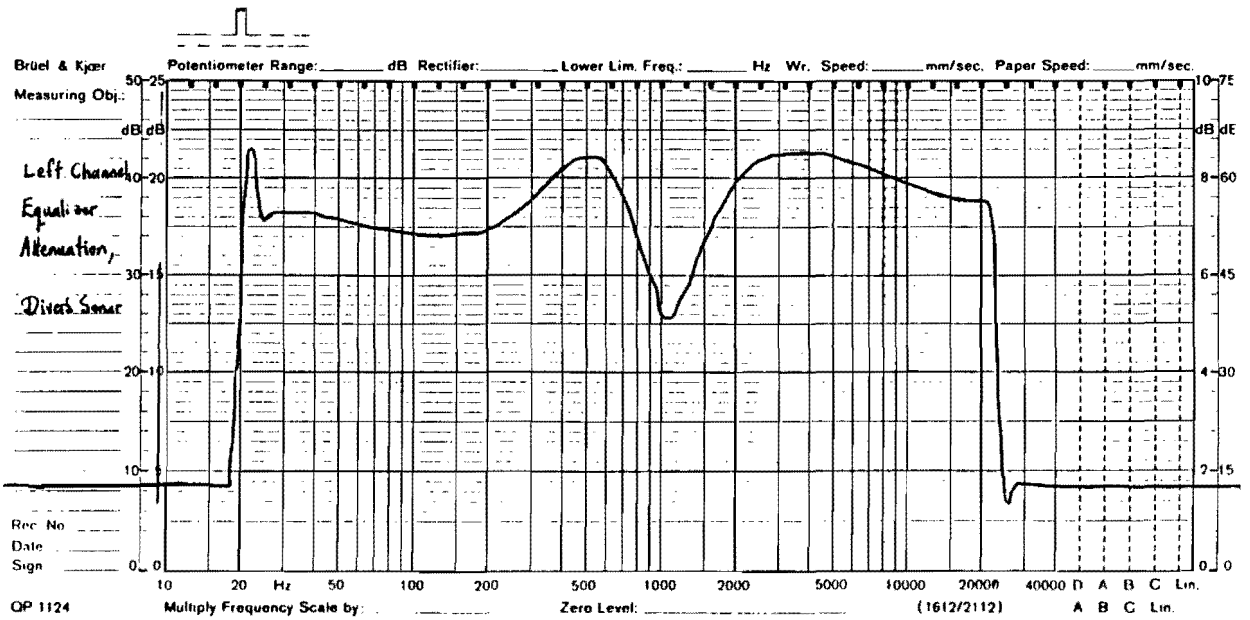

Figure 7.5(b) : Frequency selective attenuation provided by the third equalizer network to equalize acoustic losses.

receiver is a narrow beam centre channel receiver used to enhance lateral resolution (Kay, 1981).

Three forms of equalization have been incorporated to maintain linearity throughout the sonar-medium-diver system. The first equalizer counteracts the increased attenuation of higher frequencies in the medium, and takes the form of a high pass filter in the transmitter output stage. The second equalizer compensates the attenuation owing to absorption and spherical spreading that increases with range, and takes the form of a high pass filter connected to the output of the demodulator. Although absorption varies with such factors as temperature and salinity, the overall attenuation can be adequately predicted and compensated.

Unlike the first two equalizers, which have been incorporated in previous CTFM sonars developed at the University of Canterbury, the third equalizer is unique to the diver's sonar. The need for this equalizer arises because the auditory output of the sonar is transmitted to the diver's ears by miniature air speakers housed in metal capsules with the sound waves coupling to the water through a neoprene cover. Considerable frequency selective attenuation occurs in the transmission chain from the sonar electronics to the diver's ears. A plot of the received signal, as recorded by a calibrated hydrophone placed 30mm from a speaker in response to a flat input signal to the speaker, is reproduced in Figure 7.5(a). The frequency response of the equalizer network designed to counteract this attenuation is reproduced in Figure 7.5(b).

The combined effect of these three equalizers is to ensure that the amplitude of the auditory output at the diver's ears is determined solely by target strength.

One important feature of the CTFM system is that reflections from objects of different shapes and densities are different, and after processing can be perceived as having come from different objects. Thus the tonal quality or timbre of the audio signal allows for characterization of targets (cf. section 2.2.10). Therefore, as with other CTFM sonars, upon detecting a target, the diver has information regarding its range (audio pitch), direction (I.A.D.) and character (timbre).

Figures 7.6(a), (b) : Side and front view of Diver's Sonar head gear.

To eliminate the auditory outputs caused by distant objects which are of no interest, a low pass filter is incorporated to attenuate all audio frequencies above 5 kHz, which corresponds to the maximum detection range on any range scale. The maximum range can be altered by varying the length of the transmission sweep.

7.4 PHYSICAL CONSTRUCTION

The diver's sonar is packaged in two separate parts interconnected by waterproof cables. One part comprises a standard full-face scuba diving mask and helmet modified to provide mounting for the transducer cluster and speakers, as shown in Figure 7.6. The entire transducer cluster can be tilted

vertically, and the splay angle of the two side channel receivers can be adjusted independently. The splay angles were adjusted so that the psycho-physical perception of the direction to a target at a fixed bearing was identical to the sensation provided by blind aids. Experiments have shown that enhanced lateral localization is achieved when the I.A.D. is slightly exagerated (Brabyn, 1978). Physically, this resulted in splay angles of 15 degrees.

The auditory output of the sonar is fed to the ears by two speakers housed in waterproof containers and held in position over the ears by two rods attached to the dive mask. The speakers should not make physical contact with the diver's head as then the resulting bone conduction would fuse the signals from the two side channels and destroy the I.A.D. (Bauer & Torick, 1965).

The second part of the sonar consists of the electronics canister, which is mounted adjacent to the air tank on the diver's back pack as shown in Figure 7.7. This canister houses a 6 A-hr rechargeable battery pack (providing 9 hours of normal use), and all of the electronics except for the receiver pre-amplifiers which are housed in the transducer casings. Three controls are provided on the canister. An on-off/volume control switches power to the sonar and enables the audio output level to be adjusted. The second control is a continuously variable range selector, which allows the maximum range to be decreased from 40m to 5.6m. This change is effected by increasing the sweep rate, which in turn changes the range coding. Decreasing the maximum range enables distracting objects beyond any target(s) of interest to be deleted from the auditory output. The third control on the electronics canister is a switch which enables the outputs of the two broad-beam side channel receivers to be turned off (monaural/trinaural selector). This switch is useful in confined spaces where environment boundaries produce distracting echoes. Note that since the sonar is mounted in part on the diver's back pack and in part on his mask, his limbs remain free to provide stability and mobility or to perform any other task.

Specifications of the diver's sonar are given in Appendix I.

Figure 7.7 : Side view of diver using sonar showing transducer cluster mounted on dive helmet and electronics canister mounted adjacent to air tank.

7.5 TRIALS

The trials were designed not so much to establish the capabilities of the diver's sonar independently, but rather to measure the extent to which the operation of the diver's sonar mimics that of the blind-aids in air. The rationale behind this emphasis is that the number of subjects available and capable of undertaking scuba dives is limited, while the capabilities and limitations of the blind aids are well known. Knowledge of the extent of similarities between blind aids and the diver's sonar would save conducting numerous analogous experiments.

Brabyn (1978) details exercises useful in evaluating mobility. These exercises include approaching objects, shorelining (moving parallel to a wall or line of poles) and slaloming. His laboratory evaluations of various blind aids include quantitative measurements and plots of positions, velocities and

rms deviations from "ideal paths" (Brabyn et al., 1978). While the facilities available for the diver's sonar trials did not permit such quantitative studies, the tasks were repeated to qualitatively compare performance. Furthermore, divers with blind aid experience could describe the perceived difficulty of the task in water relative to air.

During all trials, a long (100m) cable connected the diver to colleagues on the surface, providing two-way voice communications, monitoring of the sonar's auditory output, and recording capabilities for future reference and analysis.

Initial trials were carried out in an olympic sized diving pool. Test targets such as spheres, tri-planes and suspended poles were placed at various depths and positions in the pool, and divers were required to locate and approach them. These tasks were performed with both competence and confidence.

A slalom course was assembled comprising 5 aluminium poles 1.45m in length and 19mm in diameter, suspended 1m below the surface and spaced roughly 2m apart. Since the target strength of a pole when viewed obliquely is much less than when viewed perpendicularly, the diver had to ensure an approximately perpendicular angle of approach. However, when this condition was met, the slalom course was readily negotiated by a blind-folded diver. Although this may seem a trivial task, it should be noted that mobility while suspended in a fluid environment differs from conventional ambulation in that there is no physical feedback from a fixed reference point.

To test target classification capability, two identical 10 litre paint tins were positioned on the bottom of the pool. One tin was filled with water, the other with sand. The diver's task was to locate the tins and identify their contents by analysing the sonar outputs. In eight trials involving random diver-target distances, the contents of both tins were identified without error. Furthermore, during the trials, the auditory outputs of the sonar were recorded, and subsequently played to 5 subjects. These subjects likewise correctly identified the contents of the tins. All subjects (including the diver) reported that the hollow (water-filled) tin gave a compound echo comprising several frequency components, while the sand-filled tin sounded pure and almost bell-like.

The above-mentioned trials were conducted using subjects with air-sonar experience. All subjects reported experiencing sensations very similar to those using the Trinaural blind aid. To determine the necessity for air sonar experience for competent and confident use, an able scuba-diver with no sonar experience donned the equipment. Only upon entering the water was it explained that audio pitch was proportional to distance. After no more than 20 minutes of familiarisation, the blind-folded novice successfully negotiated the slalom course. While targets could readily be located and approached during the initial trial, confidence in classifying these targets required several training sessions.

Other trials were conducted in a harbour environment. In shallow waters, performance was considerably degraded by tidal swells, which altered the position of the diver relative to targets. Under these conditions, divers felt continually disorientated. However, in steadier seas, divers reported sensations comparable to those with air sonars. In one sea trial conducted in Norway, several subjects were asked to identify targets chosen at random from a rope, a metal chain, a smooth pontoon pole and a pontoon pole covered in marine growth. The targets were each about 4cm in diameter, and placed 10m from the sonar. The task seemed trivial : subjects identified the targets without error.

In another trial, conducted in England, four experienced navy divers were given up to 2 hours training using a trinaural air sonar before spending up to 3 hours underwater. After one hour of training (both on land and in the water), divers were able to distinguish between the following targets from a range of 10m in poor (0.5m) visibility: lobster pots, oil drums, scaffold poles, rocks, jetty and mines. After a short training period, a diver put down within 30m of a target could quickly locate the target, even in zero visibility. With more training, a specific target could be selected from several objects lying on the seabed. The general technique adopted by the divers was to use the sonar in the trinaural mode until the desired target was detected. The sonar would then be switched to the monaural mode and the range scale adjusted during the approach to the target.

7.6 DISCUSSION

An ultrasonic sonar with auditory display has been developed which gives divers information on the range, direction and character of objects within its field of view. Initially conceived as an underwater version of the technically successful blind aids, the sonar is intended for use under conditions of reduced or zero visibility which often prevail during non-recreational dives.

The prototype was produced during 1980 and 1981 before either digital frequency synthesis or dual demodulation was incorporated in our CTFM sonars; performance should be improved by adding these features.

One criticism is that the equipment becomes uncomfortable on the head, neck and shoulders during prolonged dives. However, in keeping with typical prototype development, the sonar has greater bulk than production versions would require. Furthermore, no audio transducers which couple directly into the water were available at the time of construction, and the method used to generate the audio output is very inefficient. Consequently, a 10 W output stage was required, necessitating a large capacity battery to enable useful dive durations. A more efficient audio output stage would ease battery requirements and enable a lighter and better balanced sonar to be produced.

Divers could not wear a hood for warmth as it would interfere with the perception of the audio output. Some divers reported that when their head and ears became cold, their confidence at performing tasks dropped off.

Furthermore, divers commented that the narrow vertical beamwidth limited their ability to hold contact on a target. One solution could be to make the vertical beamwidth user-adjustable, either independently through a fourth user control, or in conjunction with the monaural/trinaural switch such that in the trinaural (search) mode it is wide, and in the monaural (locate) mode it is narrow.

The diver's sonar can be considered a bionic sonar for three reasons. Firstly, the one octave bandwidth swept frequency transmission and correlation processing model the sonars of many species of bats. Secondly, whereas most electronic sonars have a visual display as their sole or main output, the

diver's sonar has only an auditory display, thereby modelling the perception mechanism of animal sonars. Thirdly, with the sonar strapped onto the diver's back and head, the sonar becomes an integral part of the diver without restricting movement or the use of his hands or feet.

All divers were impressed by the speed with which they gained the experience necessary to perform useful tasks. Many commented that the useful advantages of this sonar compared with others they had used was that their limbs remained free to perform normal tasks, and that target characterization was possible.

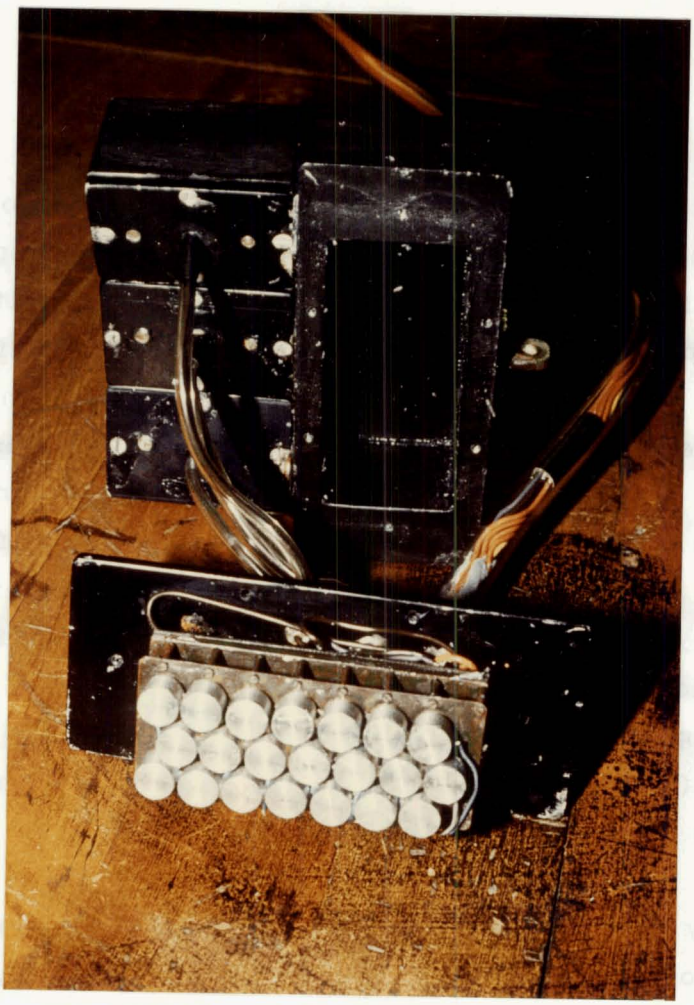

Figure 7.8 : Centre channel receiver transducer array and housing.

CHAPTER 8

CLASSIFICATION SONAR

8.1 INTRODUCTION

Commercial applications of sonar hardware developed during World War II, primarily in connection with submarine warfare, led to the observation that high frequency sound reflections from the seabed appeared to show a consistent correlation between signal intensity and seabed lithology (Flemming et al., 1982). Specific experiments aimed at utilizing this phenomenon for mapping the surface of the seabed were conducted by Chesterman et al. (1958), and led to the development of the first operational side scan sonar (Tucker & Stubbs, 1961). By the late 1960s, the concept of side scan sonar began to receive world wide acceptance, and today the applications of side scan sonar are very diverse. These applications include geological, hydrographic and engineering surveys, mineral exploration, cable and pipeline location, underwater archaeology, the detection of gas leaks, oil rig surveys, studies of iceberg scouring and the location of sunken objects such as ships, planes and lost torpedoes (Milne, 1980). An excellent overview of the development of side scan sonars is given by Somers & Stubbs (1984).

The primary aim of the side scan Classification Sonar described in this chapter was to provide a means of examining the seabed, so as to enable the detection and subsequent classification of man-made objects. In particular, it was desired to bring to the operator's attention specific targets or groups of targets such as drums or mines.

This chapter describes the sonar's theoretical performance based on the design specifications, outlines the electronic and physical construction, and details the operational facilities. The following two chapters discuss the detection and classification algorithms and present the results of trials using the sonar.

8.2 SPECIFICATIONS AND THEORETICAL PERFORMANCE

Three general design specifications were initially established, namely that the sonar be able to operate out to 200m, that the sonar be able to perform its task with a forward vessel speed of 20 knots, and that the minimum detectable target have a TS of -25 dB. Other often conflicting constraints contributed to the final specifications, which are given in Appendix II.

Based on these specifications, it was possible to calculate the performance of the Classification Sonar for a variety of sea-state and seabed conditions and diverse targets. While there is always a margin of error in any prediction of performance because of uncertainties in many factors, such as backscatter from the seabed, volume reverberation, and sea-state noise, predictions provide useful feedback during the design stages and serve as a useful guide in devising experiments to test the sonar. Appendix III details the expected performance for two different sets of conditions. It is shown that with the specifications given in Appendix II, and assuming the system is seabed reverberation limited rather than sea state noise limited, the sonar should detect at 200m a -28 dB target on a mud seabed, or a -8 dB target on a rock seabed using the low resolution filter bank. Using the high resolution filter bank, the sonar should detect a -37 dB target on a mud seabed and a -17 dB target on a rock seabed.

8.3 ELECTRONIC DESIGN

A general system block diagram of the Classification Sonar is given in Figure 8.1. There are three major subsystems: the CTFM sonar front-end, the spectrum analyzer, and the computer. Each subsystem generates signals required to implement the sonar displays.

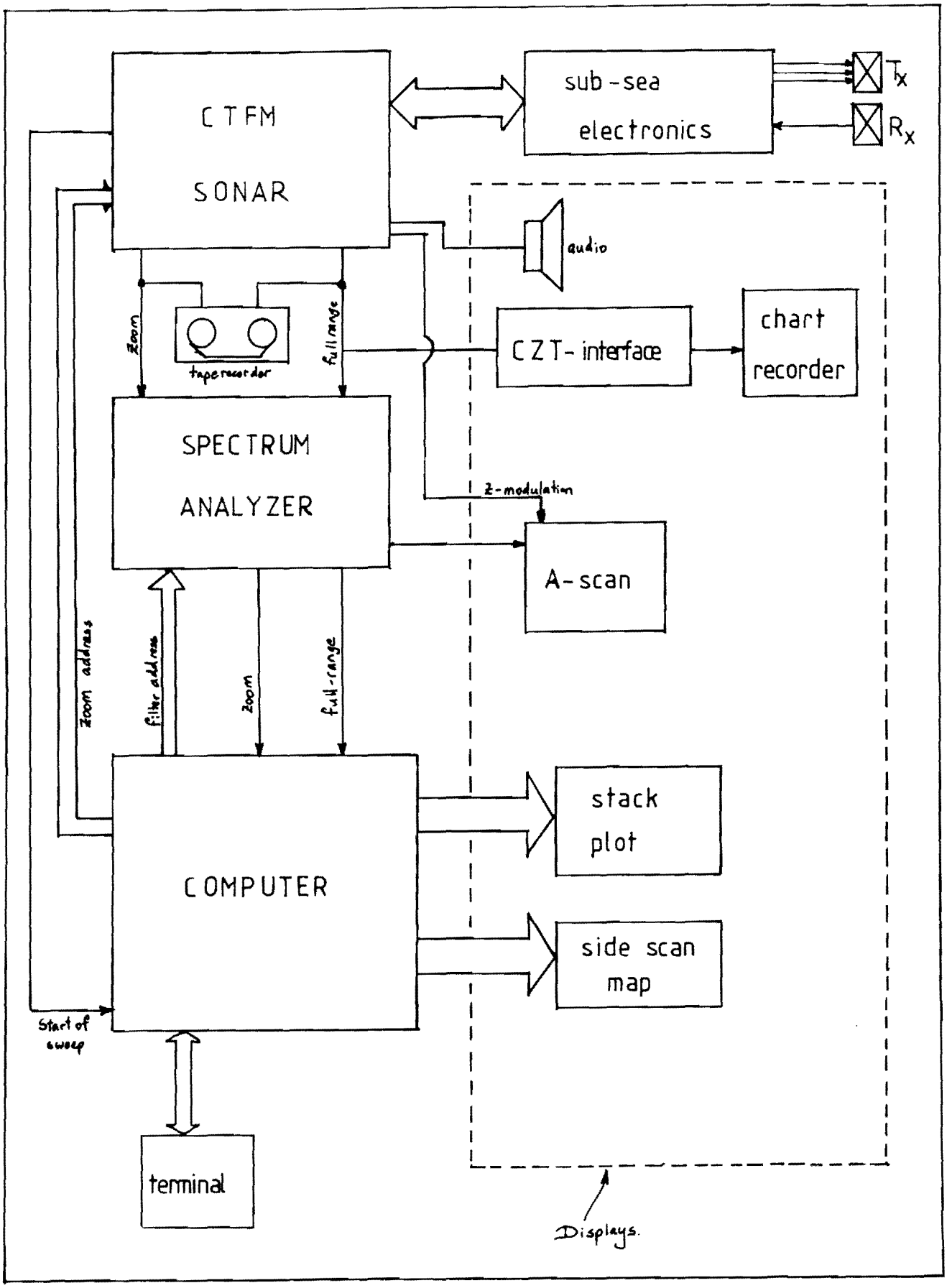

Figure 8.1 : System block diagram of Classification Sonar.

8.3.1 The CTFM Sonar Front-end

The CTFM sonar front-end comprises the electronics required to generate and equalize the transmitted signal, receive and demodulate any echoes, and provide a zoom (range expansion) capability and audio output. A block diagram of the front-end is given in Figure 8.2.

The sonar incorporates dual demodulation as described in Chapter 3, with the parameter k of Equation 3.2 set to four. The transmitter is set to sweep linearly from 100 to 50 kHz with a sweep repetition period of 533ms. Consequently, the two IF demodulators sweep from 300-250 and 250-200 kHz respectively. The transmitter and demodulator sweeps are generated using standard direct digital synthesis techniques.

The received waveform is amplified, filtered, and fed to the balanced demodulators. The wanted outputs from these demodulators (i.e. the difference frequencies between the local oscillator sweeps and echoes from targets up to the maximum range), fall in the frequency band from 175 to 200 kHz, providing a continuous demodulated output for all signals up to the maximum range.

The allocation of frequency bands is illustrated in Figure 8.3. By configuring the dual demodulator with parameter k of Equation 3.2 set to four, the demodulated echoes of interest fall outside either the transmitter or local oscillator frequency bands, thereby avoiding problems resulting from the direct break-through of oscillator signals into sensitive receiver electronics. However, there are still undesirable signals left at frequencies outside the band from 175 to 200 kHz; these unwanted components are filtered out with the IF filter module. The filter has an elliptical function with notches at 150 and 200 kHz to attenuate the two strong crosstalk components at these frequencies (i.e. the constant frequency differences between the transmitter and the two local oscillators). Furthermore, the slope of this filter is tailored to provide 50dB of range equalization. The echoes are then brought down to baseband by multiplying them with a local oscillator fixed at 200 kHz. This output provides the full-range (0-200m) information.

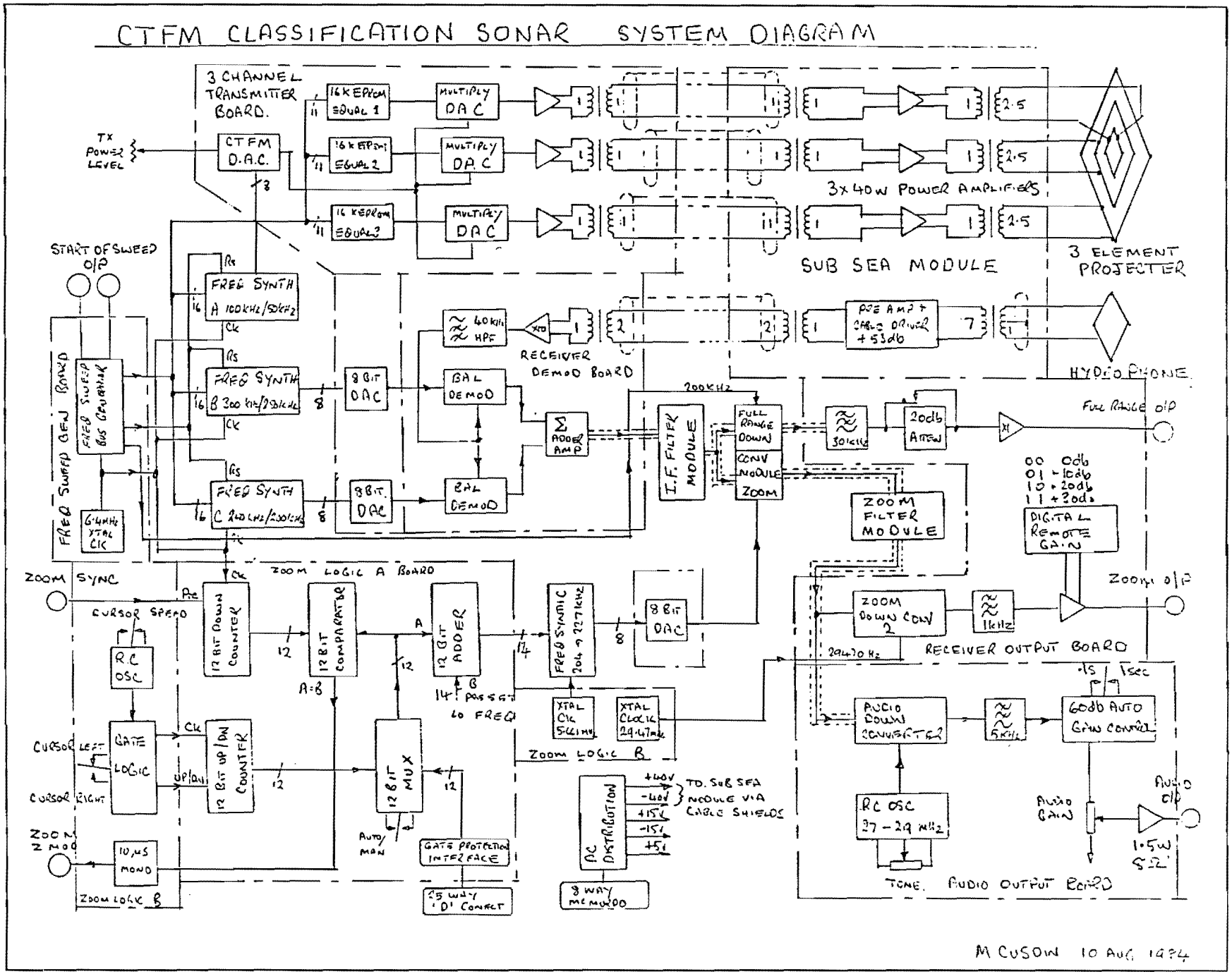

Figure 8.2 : Block diagram of sonar front-end.

Recall from section 3.2 that there may be good reasons for limiting the demodulated bandwidth to less than cT/2, such as phantom target considerations. With the Classification Sonar, the demodulated bandwidth is ultimately limited by the dynamic range available at the output of the demodulators. The demodulators used (LM1496 multipliers) have a quoted wideband dynamic range of 55dB, this figure being limited by harmonic intermodulation components of the local oscillator and input signal. However, in the demodulated band of interest, the amplitudes of the harmonic components are small and comparable to the noise floor, resulting in a much larger useful dynamic range.

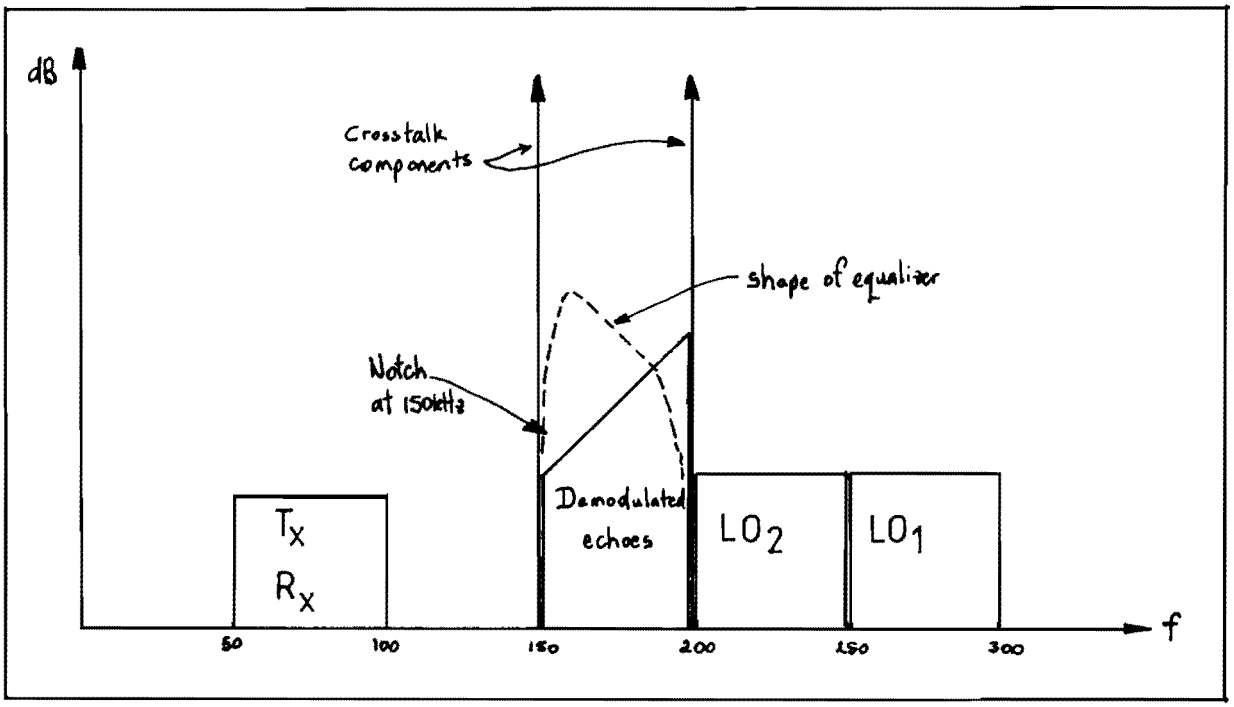

Figure 8.3 : Allocation of frequency bands for transmitter, local oscillators and demodulated signals.

Referring again to Figure 8.3, the two crosstalk components at 150 and 200 kHz set the upper bound of the available dynamic range. The filter used to provide range equalization serves two more purposes: it reduces the amplitudes of these two crosstalk components, and it reduces the noise floor, both of which are important in maintaining as large a signal dynamic range as possible. Note that because of the shape of the equalization filter, the noise floor is more strongly suppressed at short ranges (near the 200 kHz demodulated output), than at the far ranges (near the 175 kHz demodulated

outputs). Now as the proportion of cT/2 used for the demodulated bandwidth is increased (i.e. as the demodulated frequency corresponding to the maximum range approaches 150 kHz), it becomes increasingly difficult to adequately suppress the 150 kHz crosstalk component so as to maintain a useful dynamic range. In the Classification Sonar, the maximum range corresponds to 175 kHz, so that 50% of the available demodulated bandwidth is utilized. The resulting signal dynamic range was measured using the sonar in air (to eliminate reverberation) with a Nicolet Ubiquitous Spectrum Analyzer. Using an analyzer bin width of 125 Hz, a dynamic range of 60dB was recorded. Using realizable filters (such as a 7-pole elliptical filter) it should be possible to suppress the 150 kHz crosstalk component to the level of the range-equalized output signals (thereby retaining the dynamic ranges quoted above) with a demodulated output comprising 75% of cT/2.

Beamwidth compensation (see section 2.2.3) is provided by constructing the transmitting transducer in three concentric sections. At the start of the sweep, only the inner section is activated; as the sweep continues, the centre and finally the outer sections are also activated. Furthermore, to overcome any variation in sensitivity during the sweep, the amplitude of the transmitted waveform applied to each section of the transmitter is carefully tailored to produce a flat overall response out of the receiver hydrophone with changing frequency. Beamwidth and sensitivity compensation are effected by multiplying the 100 - 50 kHz sweep with three waveforms (one for each section) stored in EPROM's using multiplying digital to analogue convertors (MDAC's). The required amplitudes of these waveforms were determined during calibration tests described in Chapter 10. The use of EPROM's and MDAC's instead of analogue filters avoids group delays which would destroy the correct phase relationship between the three concentric sections.

The zoom output is provided by multiplying the output of the IF filter module with a frequency determined by the zoom position select hardware. There are two selection modes: automatic and manual. In the automatic mode, the computer determines the desired zoom position, and sends a 12-bit number to the accumulator feeding a fourth digital frequency synthesizer. The output of this synthesizer is passed through a D/A convertor to be multiplied with the output of the IF filter module. In the manual mode, the operator controls the value of the number fed to the synthesizer by incrementing or decrementing an up/down counter (at a user-selectable normal or fast rate). In either

case, the output of the multiplier is fed to the zoom filter module, which comprises an extremely accurate and stable filter of 1 kHz bandwidth centered at 30 kHz. Thus, the zoom information is extracted by sliding the full range information across a fixed frequency bandpass filter. The zoom information is then brought down to baseband (200 -1200 Hz), filtered, and amplified to provide the zoom output.

The audio output is provided by multiplying the zoom filter module output with a further oscillator (adjustable to vary the pitch) to bring the output to the audio frequency range. This signal is then fed to a 60 dB automatic gain control to compensate the wide variation in echo amplitudes. Since the audio output is derived from the zoom filter module, the audio information always corresponds to the zoom filter position.

The sonar can readily be adapted for use in air, enabling the electronics to be tested in the laboratory and modelling experiments to be performed. In air, one of the three transmitter outputs is connected to an air transducer through an appropriate amplifier; no sensitivity compensation is required, and no beamwidth compensation is provided. The range equalizer is retained as the attenuation underwater over 200m corresponds to that in air over the 3.5m range. Finally, the sweep period is reduced from 533ms to 21ms.

8.3.2 Spectrum Analyzer

The demodulated output of the sonar appears in the frequency domain, and hence a spectrum analyzer is required to discriminate echoes. Various methods of spectral analysis were considered, including digital filtering, digital FFT's, Chirp-Z-Transforms (CZT's), and analogue filter banks. Two banks of contiguous bandpass filters were eventually chosen because of a high performance to cost ratio and previous experience with this form of spectral analysis.

Each filter bank comprises 64 filters. The first bank covers the full range demodulated output from 2,500 to 25,000 Hz (i.e. 20-200m range), with filter bandwidths of 350 Hz, while the second bank covers the zoom-range demodulated output from 200-580 Hz, with filter bandwidths of 6 Hz.

The filters are tunable, 2-pole, active, bandpass filters, with component sensitivities similar to those of the biquad structure (Thomas, 1971) but using only 2 operational amplifiers. The filter circuit is included in Figure 8.4. Bandwidth is determined by

$$\Delta F = 1/(2\pi R_2 C_1) \tag{8.1}$$

while the centre frequency is determined by

$$f_o = 1/\left(2\pi\sqrt{R_9 C_3 (R_3+R_5) C_1}\right). \tag{8.2}$$

Consequently, these filters can easily be trimmed to the desired centre frequency and bandwidth, with the adjustments being independent. The filters have a fixed centre frequency gain. R_1 is adjusted to cancel the negative resistance generated by the network.

Each filter is connected to a detector as shown in Figure 8.4. R_6 is adjusted to cancel any input offsets to op amp A_3 so as to optimize the dynamic range of the detector.

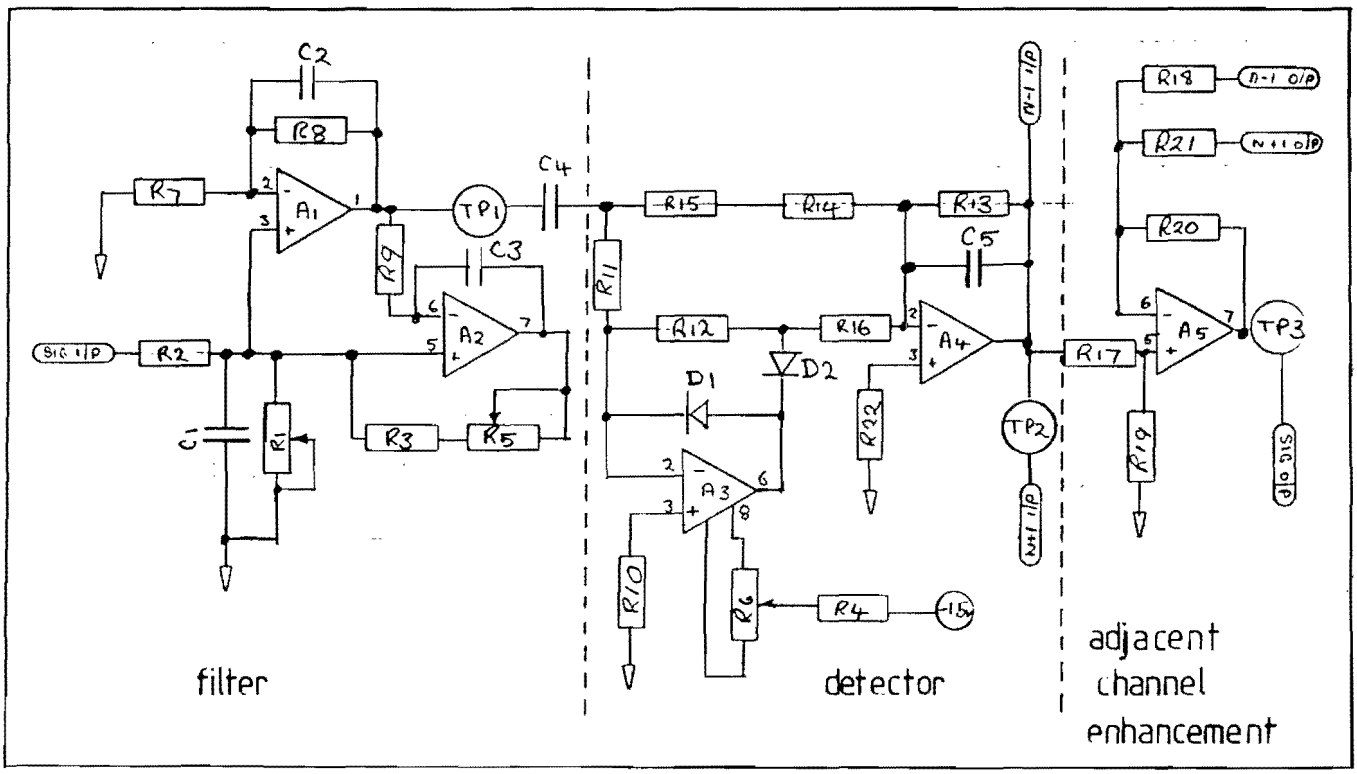

Figure 8.4 : Single channel of filter bank comprising filter, detector, and adjacent channel enhancement circuit.

The selectivity of the filters is improved using adjacent channel enhancement, in which a filter's output is diminished by a portion of the outputs of the two adjacent filters. The enhanced filter output of the nth channel, V_n' is given by

$$V_n' = 4/3\ V_n - 1/3\ V_{n-1} - 1/3\ V_{n+1} \qquad (8.3)$$

where V_n is the non-enhanced output of the nth channel.

The effect of adjacent channel enhancement can be seen in Figure 8.5, where the dotted lines give the independent filter outputs, and the solid lines give the enhanced outputs. For both filter banks, the 3-dB bandwidths of the enhanced filters equal the filter spacing.

The two filter banks each comprise 8 printed circuit boards with 8 filters on each board. The system diagram of one such board is given in Figure 8.6, which shows the cross-over connections required for the adjacent channel enhancement. A 7-bit address derived from the computer module addresses the 128 filters sequentially through a CMOS scanning switch, enabling the filter outputs to be read through a single coaxial cable.

8.3.3 Computer

The computer subsystem provides overall control of the entire sonar, processes the outputs of the spectrum analyzer, and generates the stack plot, probability map and M-mode displays. The computer is controlled via an RS 232C serial port by a terminal, which can also be used to monitor the operation of the system, diagnose faults, and alter program parameters. A block diagram of the computer module is given in Figure 8.7.

The computer module is designed around the Intel Multibus system and comprises 10 multibus boards slotted in a dual card-cage. The heart of the system is an Intel iSBC 86/05 CPU board incorporating a 16-bit 8086-2 CPU running at 8 MHz. Programs are stored in 8K bytes of EPROM. In addition to 8K bytes of on-board high speed RAM, a further 128K bytes of RAM is provided by an iSBC 028A memory board.

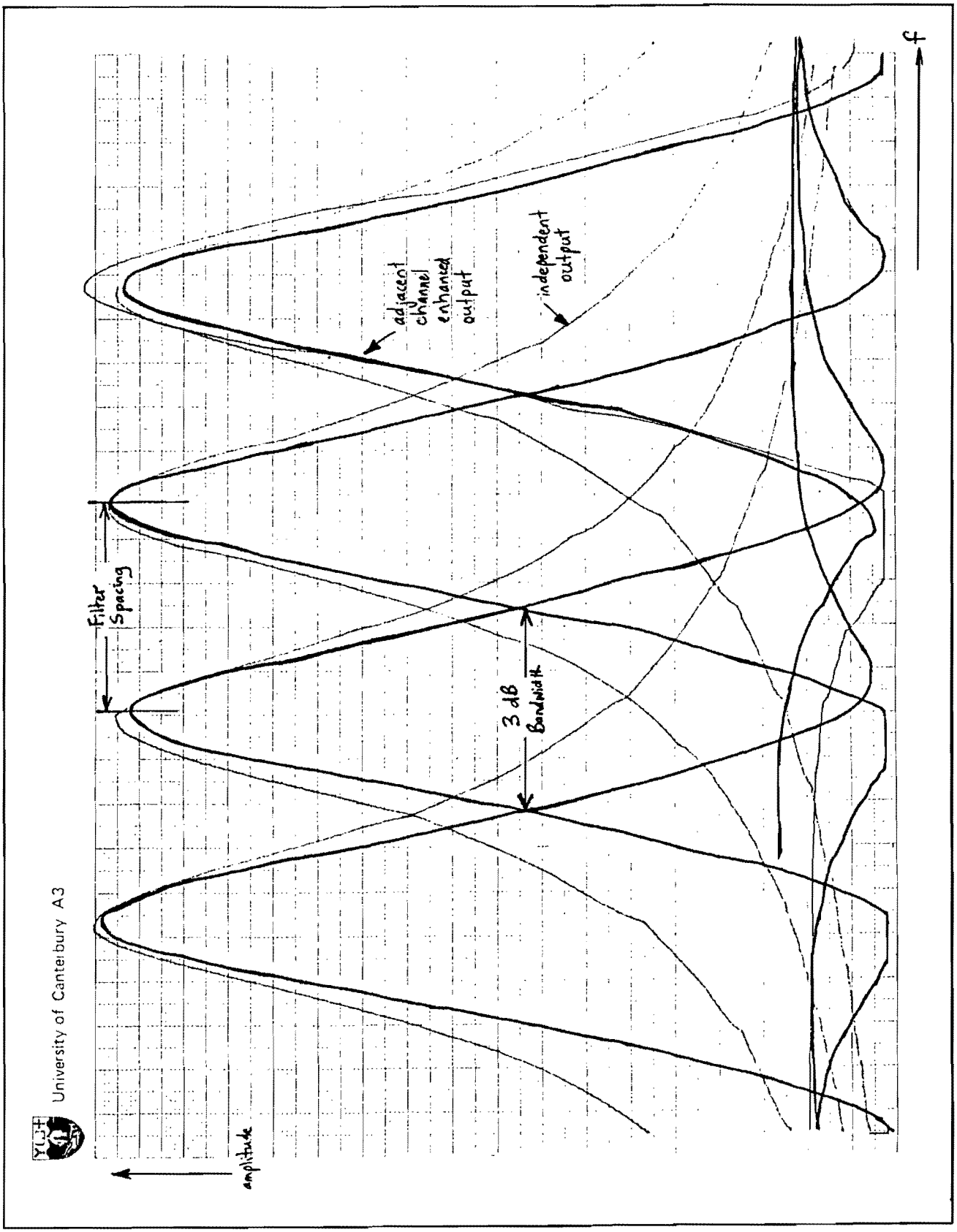

Figure 8.5 : Frequency response of three adjacent filters showing independent filter responses (thin lines) and adjacent channel enhanced responses (thick lines).

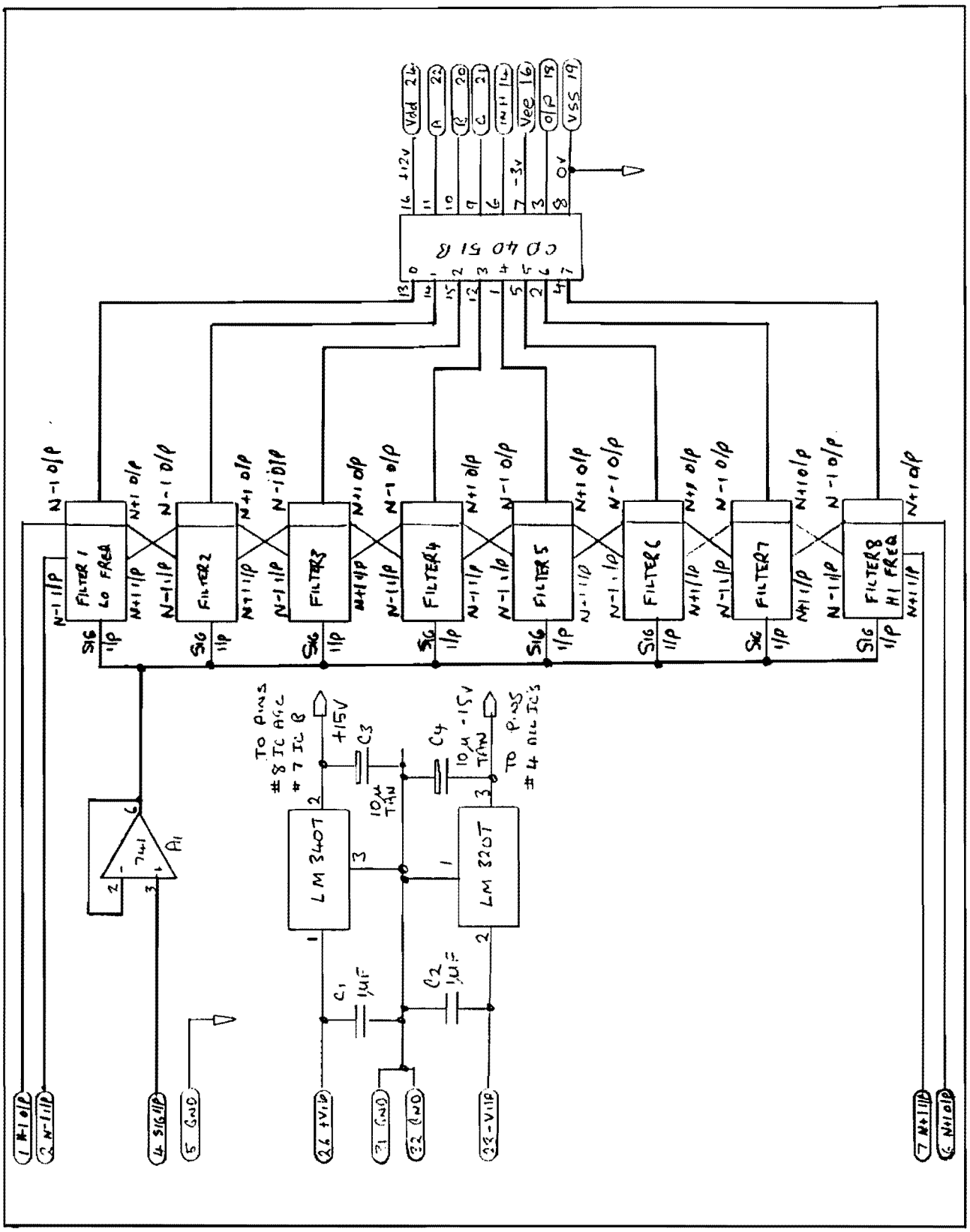

Figure 8.6 : System diagram of one board of filter bank showing cross-over connections between filters for adjacent channel enhancement.

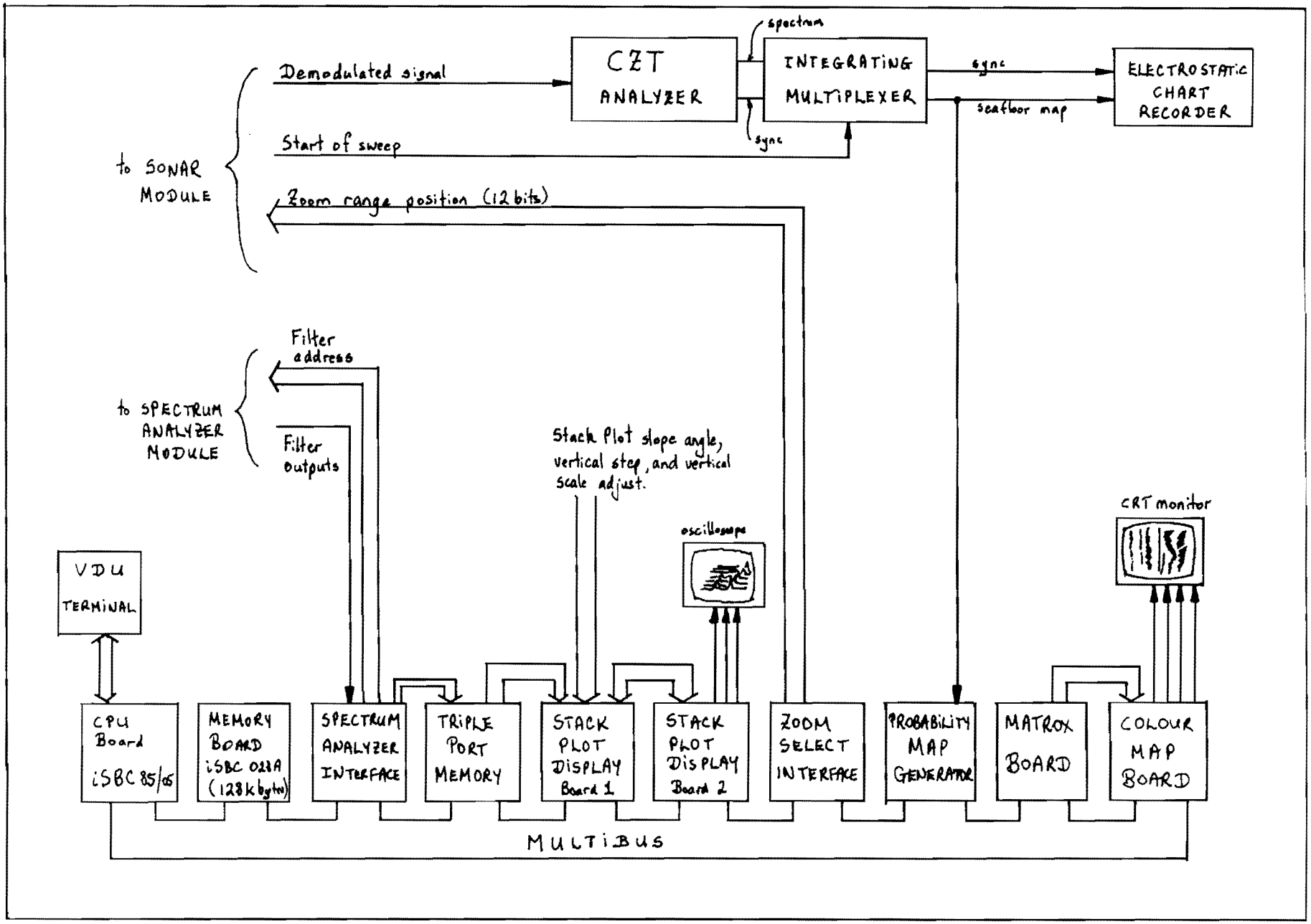

Figure 8.7 : System block diagram of computer module.

The spectrum analyzer interface generates a 7-bit address which is decoded in the spectrum analyzer module to sequentially address each of the 128 filters. The filter outputs are scanned every 1.28ms, and the amplitudes digitized and written to 8K bytes of RAM organized as 1024 16-bit words. The RAM thus records the 8 most recent filter scans. The spectrum analyzer interface also writes the digitized filter outputs via an auxiliary data bus to the triple port memory.

The triple port memory consists of 8K bytes of RAM organised as two 4K byte buffers, each buffer having the dimensions 64 x 64 x 8 bits to match the dimensions of the stack plot display. The three ports of the memory enable data to be written from the auxiliary data bus, read to the stack plot display generator, and both read from and written to the multibus. The latter port is the one used by the automatic detection and classification software. To the software, the triple port memory appears as a contiguous 8K byte block of memory.

A system block diagram of the stack plot display generator (see sections 2.2.7 and 6.3.2) is given in Figure 8.8. Data corresponding to either the full range or zoom output is read from the triple port memory. The 64 filter outputs are then interpolated using a cosine function to provide 1024 points per line displayed. Sixty-four such lines are written to the screen, each line being offset both horizontally and vertically (with user-selectable displacements) to provide a pseudo-3D stack plot. A significant portion of the stack plot hardware serves to provide hidden line elimination, in which the y-deflection of the point about to be written to the screen is compared to the greatest value previously written in the same vertical column (taking due account of the horizontal and vertical line displacements). If the present value is less than a previously written value, the output is blanked. A photograph of the stack plot display generator hardware appears in Figure 8.9. Numerous examples of stack plot displays are given in Chapter 10.

The zoom select interface uses the results of the automatic detection software to generate an address used in the sonar front-end to control zoom placement in the automatic mode.

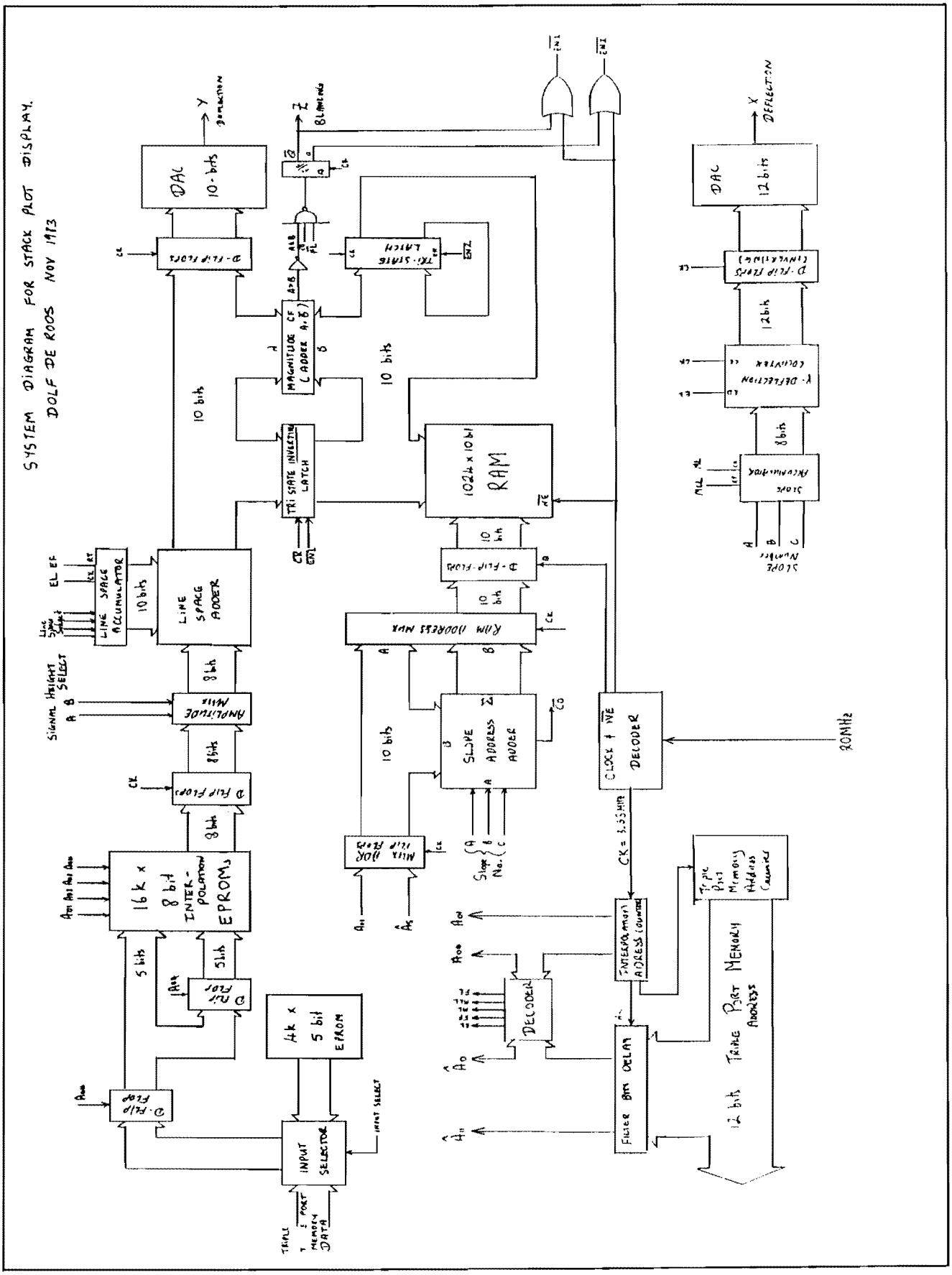

Figure 8.8 : System block diagram of Stack Plot Display Generator.

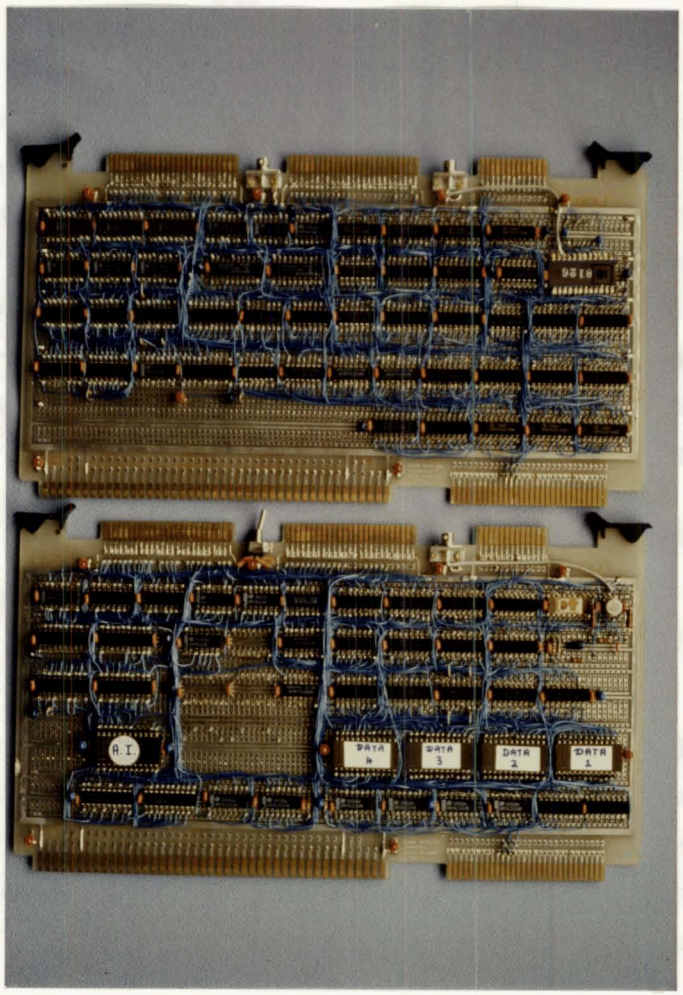

Figure 8.9 : Photograph of Stack Plot Display Generator hardware.

The Probability Map Generator uses the output of the CZT analyzer to generate a side scan map of the seabed, displayed using a 4-bit grey scale on a colour CRT monitor configured as 256 x 256 pixels. Each line (256 x1 pixel) corresponds to a single transmission sweep enabling the 256 most recent sweeps to be displayed on the screen. The results of the automatic detection and classification software are also relayed from the main CPU board to the probability map generator. The probability map generator then superimposes onto the monochrome side scan map coloured markers indicating the probabilities of detected targets being targets sought; if a target is classified as being mine-like, the corresponding location on the side scan map is tagged with a red marker. Various detection criteria and display options may be invoked. For example, the display of probability markers may be suppressed, leaving only the red markers to indicate the presence of classified targets.

The processing of the CZT output and the results of the automatic detection and classification software required to generate the probability map is performed by an Intel 8088 CPU and related hardware. The information to be displayed is written via the multibus to a MATROX RGB-256 image store memory and display controller. The image store memory is configured as 256 x 256 locations each of 4 bits. The contents of this memory are repeatedly read out through the video connector of the MATROX board as four TTL level signals at standard television scan rates. These four outputs are fed to the Colour Map Board which has a translation table memory to convert the 4-bit outputs (as encoded by the Probability Map Generator) into signals which give a pseudo colour image on an RGB-input colour CRT monitor.

8.3.4 Displays

Various displays are incorporated in the Classification Sonar, some of which are included to enable an experimental comparison to be made of their relative effectiveness in analyzing CTFM sonar outputs. In addition to the audio, stack plot, and probability map displays discussed above, the sonar provides the following displays:

1. A-scan (commonly provided on pulsed sonars and radars). Echo strength (y-axis) is plotted against range (x-axis). The signals for this display are taken from the output of the scanning switch in the spectrum analyzer; both the full range and zoom outputs are displayed alternately using a dual trace oscilloscope.

2. M-mode. Echo strength is plotted against range, with the signal strength being used to modulate the z-axis (brightness) of the display. Numerous lines can thus be written side by side (along the y-axis). When each line written to the screen represents one transmission sweep, a side scan map results. In this display, however, each two-dimensional image is generated from a single transmission sweep, with the first lines representing target responses to the high-frequency end of the transmission sweep and the last lines representing the responses to the low frequency end of the sweep. The M-mode display is presented on the colour CRT monitor and

can be selected instead of the probability map. When the M-mode display is selected, both the full range and zoom information are displayed simultaneously.

3. Stack-plot. The stack plot display constructs a pseudo 3-dimensional representation of sonar echoes giving a graphical representation of the frequency signature of targets. Sonar range is plotted along the x-axis, transmit frequency at a diagonal, and signal strength on the y-axis. A complete stack plot shows the position of targets in range and their frequency response. A hidden line facility disables writing to the screen when the trace tries to write over previously written data. Consequently, targets on the screen appear like mountainous ridges, with the ridge height representing target strength at a given transmit frequency. The user has control over the diagonal slope, the separation between lines, and the amplitudes of displayed targets.

4. **Chart Recorder.** The full range output of the CTFM sonar front-end is also processed by a CZT analyzer and integrating multiplexer to drive an Edo 606 electrostatic chart recorder for a hard copy side scan map.

8.4 CONSTRUCTION

The sonar can be divided into two major sections which are physically separate during use : the transducer cluster comprising the transmit and receive transducers and their sub-sea electronics package, and the remaining electronics as described above.

In the normal side scan operating mode, with the transducers towed behind a vessel, the transducer cluster would be housed in a tow fish (stream lined body). For the trials detailed in Chapter 10, however, the transducer cluster was supported by a frame which was mounted on a wharf. The main criteria for this mounting configuration were that the height and bearing of the transducers be readily adjustable. The configuration used is detailed and illustrated in Chapter 10.

The rest of the sonar is housed in five cabinets slotted for 19 inch rack installation. These cabinets, shown in Figure 8.10, contain the sonar front-end, the spectrum analyzer, the processor computing unit, the CZT-hard copy printer interface, and the power supply.

Apart from the 3 OEM boards (iSBC 86/05 CPU, iSBC 028A memory, and MATROX RGB-256) and the computer module switch-mode power supply, all of the sonar electronics was custom designed and built using 868 integrated circuits. The sonar front-end was constructed using prototyping cards and wire pen techniques, while the Spectrum Analyzer filter banks were implemented on 16 printed circuit boards. The electronic components in the computer module were mounted on prototyping multibus boards and interconnected using wire-wrap techniques.

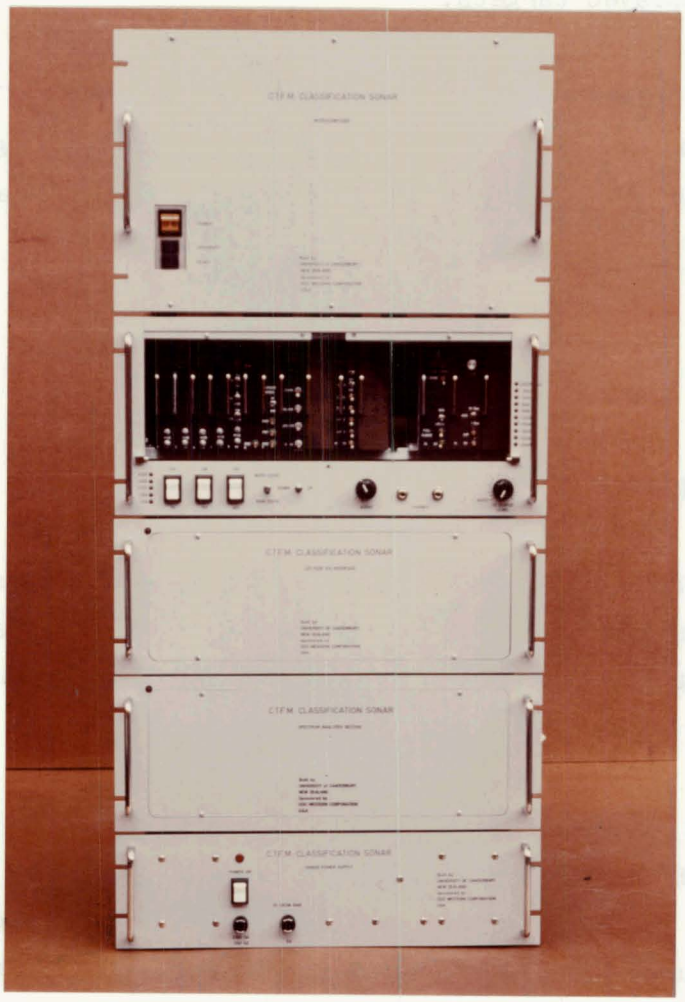

Figure 8.10 : Photograph of cabinets housing the Classification Sonar.

The remaining equipment required for a fully functioning sonar were two oscilloscopes (one for the A-scan display and one for the stack plot display), a colour monitor (for the probability map and M-mode displays), a paper chart recorder, and a loudspeaker or headphones (for the audio output).

8.5 OPERATOR CONTROLS

During use, the operator has control over the following functions:

1. **Output Power Level.** This can be varied from 0 to 100 % of the full output power for each of the three transmitters independently. The correct operation of each transmitter can thus be checked by turing off the remaining two transmitters.

2. **Receiver Gain Control.** The gain of the full range output can be increased by a single 20 dB increment, while that of the zoom output can be increased by 10, 20 or 30 dB.

3. **Zoom versus Full Range Select.** While the A-scan display always presents both the zoom and full range information, either one or the other is presented by the stack plot and M-mode displays.

4. **Zoom Select.** The operator can choose between automatic and manual selection of the low resolution filter which will be range expanded. In the auto mode, this selection is determined by software (see next chapter). In the manual mode, the operator steps the zoom filter bank through the full range.

5. **Audio Output.** The auditory display always presents the zoomed output; the operator can control the volume and pitch, while the time constant of the automatic gain control can be changed from 1s to 0.1s for use in air.

6. **Data Recording.** Various means exist for recording the sonar outputs. A CZT spectrum analyzer is used to drive an Edo 606 electrostatic

paper chart recorder, giving a hard copy of the full range outputs. A Revox taperecorder is used to record the full range demodulated output and the zoom output. These recordings can subsequently be played back to the sonar processor to recreate the displayed information. Alternatively, photographs or video recordings can be made of the displays whenever features of interest appear.

7. **Image Freeze.** An additional operator facility is the visual display freeze, whereby the M-mode and/or stack plot displays can be frozen for further operator evaluation or to facilitate photography. Such a facility is becoming common on digital memory-mapped displays (Milne, 1983).

8.6 CONCLUSIONS

An experimental CTFM side scan sonar has been constructed with the aim of providing classification capability. The design is highly modular. Various displays (both visual and auditory) are incorporated, while the operator has control over a large number of sonar parameters and operating conditions. The following chapter details the automatic detection and classification software, and Chapter 10 presents the results of sea trials.

CHAPTER 9

DETECTION AND CLASSIFICATION SOFTWARE

9.1 INTRODUCTION

The software described in this chapter was written for the Classification Sonar detailed in Chapter 8 to provide automatic target detection and classification. The automation of these processes may draw an operator's attention to suspect objects, substantiate or refute an operator's interpretation of objects, or obviate the need for an operator altogether.

Since the performance of the sonar in an oceanic environment remained uncertain until the trials, the algorithms were developed heuristically on the basis of results from air modelling experiments (see Chapter 4) and modified according to the results of early sea trials. During the trials, optimum strategies and parameters were derived. To facilitate this optimization, algorithms and parameters could be changed in the field through a computer terminal. This flexibility has been retained in the sonar, enabling operators to further change parameters to suit particular targets and environments.

Echo processing takes place in two stages. Firstly, the outputs of the low resolution filters are rapidly analyzed to detect possible targets of interest. Secondly, if targets are present in any of the low resolution cells, then these cells are examined in greater detail by directing the high resolution filter bank over these cells and analyzing the outputs with the classification software.

Finally, because of the continually varying nature of the environment being sensed, rugged software must adapt itself to any changing conditions. Such environmental changes may occur temporally (e.g. the level of sea-state noise) or spatially (e.g. the amount of seabed backscatter from different ranges). Effective adaptability cannot be provided with "add-on" routines; rather, adaptability must be an inherent design objective. The software described below automatically adapts itself to a wide variety of conditions.

9.2 EVALUATING SOFTWARE PERFORMANCE

The performance of any software is limited amongst other things by the power of the computer in use, the efficiency and ingenuity of the program being run, and the time available to collect and analyze data. While these factors are fixed for any particular sonar trial, other factors are sufficiently variable that an accurate assessment of a program's performance is difficult at best. These variable factors include short term changes in the position of targets and possibly the sonar (caused for instance by tidal currents) and longer term variations in the experimental setup, such as changes in seabed structure (e.g. after dredging) resulting in a different backscatter, and an inability to accurately reposition targets and transducers. Consequently, due consideration must be made when repeating experiments or comparing results using specific software programs.

Nonetheless it is desirable to estimate the performance of the detection and classification software. Two probabilities are commonly used to measure the ability of any searching mechanism to find what it is looking for: the probability of a successful find, and the probability of a false alarm (see Chapter 6).

In the Classification Sonar, a man-made target must be both detected and classified for the software to record a "find". Let the combined probability of detection and classification be called the probability of a find, P_{find}. Then the acceptable levels of P_{find} and P_{fa} will be determined by the task at hand. For instance, a mine hunting sonar will tolerate a relatively high P_{fa} in an effort to ensure an almost certain P_{find}, while a sonar searching for a pipeline may accept a lower P_{find} to reduce the number of false alarms.

For the trials of the Classification Sonar, the system was configured to look for man-made objects on the harbour floor. A design objective of $P_{find} = 0.8$ and $P_{fa} = 0.05$ was seen as an acceptable compromise between finding man-made objects and rejecting false alarms. These probabilities are graphically illustrated in Figures 9.1 (a), (b) and (c).

Figure 9.1(a) refers to a man-made object, and shows the probability of detection and subsequent classification. Since the probability of a find equals the probability of detection given the object was man-made, multiplied by the probability of classification given the objects was man-made and detected, i.e.

$$P_{find} = P_{d\,|\text{man-made}} \times P_{cl\,|\text{man-made and detected}} \tag{9.1}$$

then the condition

$$P_{find} = 0.8 \tag{9.2}$$

will be satisfied with the conditional probabilities

$$P_{d\,|\text{man-made}} = 0.9 \tag{9.3}$$

and

$$P_{cl\,|\text{man-made and detected}} = 0.9. \tag{9.4}$$

Figure 9.1(b) refers to naturally occurring objects, some of which will be erroneously detected as if they were man-made objects. Let $P_{d\,|\text{natural}} = 0.9$. The classification software should reject these objects; the probability of a naturally occurring object being detected and classified has been limited to:

$$P_{cl\,|\text{natural and detected}} = 0.055. \tag{9.5}$$

Finally, Figure 9.1(c) refers to the outputs of all range cells not encompassing any objects, be they man-made or naturally occurring. The probability of detecting a phantom target should be low ($\approx$0.05), and similarly the probability of classifying a phantom target given it was supposititiously detected should also be low ($\approx$0.05). Hence, the probability of a false alarm for a phantom target will be small ($\approx$0.0025).

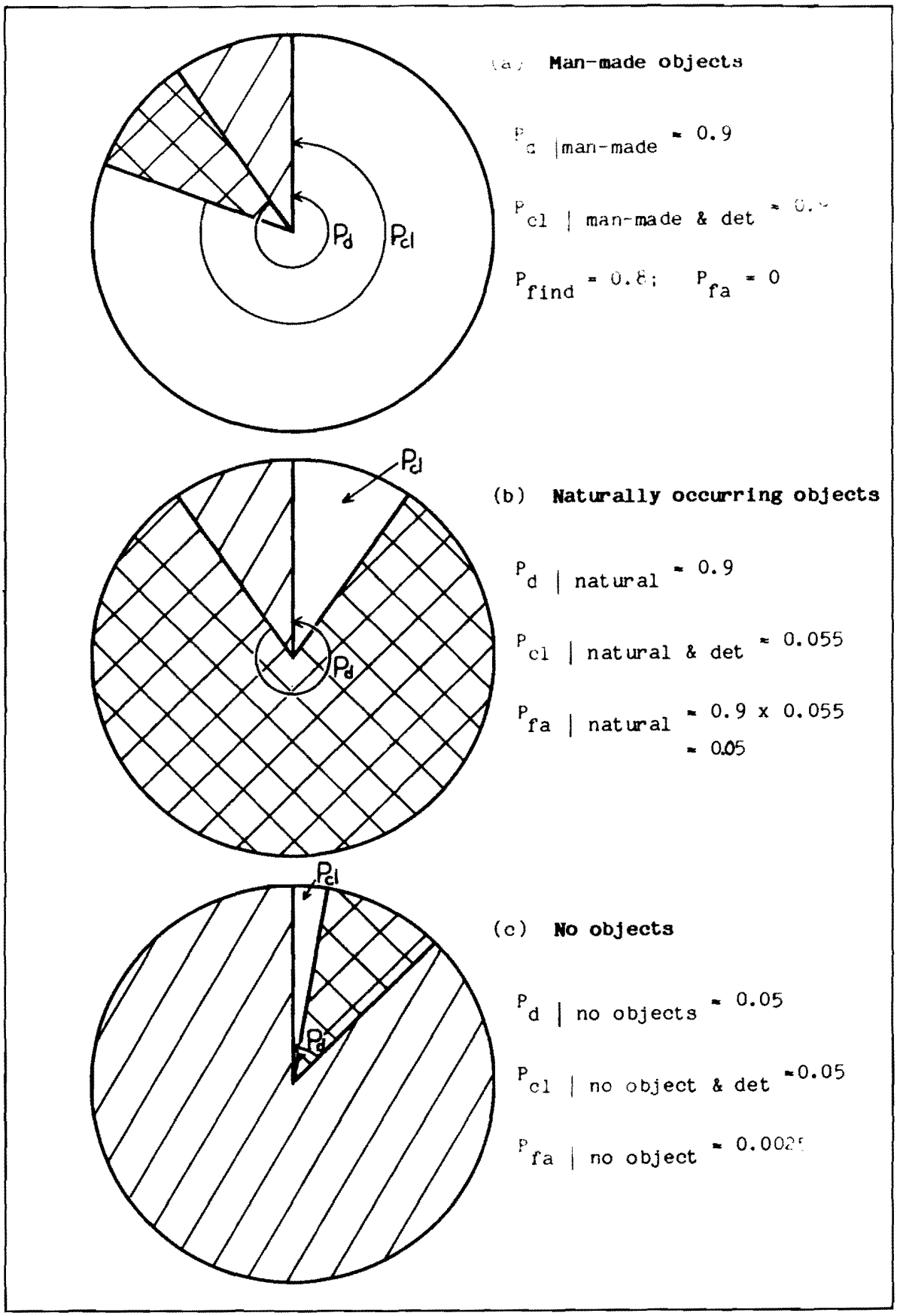

Figure 9.1 : Probabilities of detection, classification, "find", and false alarms for (a) man-made objects; (b) naturally occurring objects; and (c) no objects.

As mentioned above, the software was designed to result in a P_{find} of 0.8, and a P_{fa} of 0.05. During all trials, the performance of the different algorithms was monitored and their parameters altered to achieve these probabilities. Where these probabilities could easily be achieved, the number of samples taken by a routine was reduced to allow the software to work more rapidly. Hence the term "optimum parameters" refers to those values for parameters which would meet the desired P_{find} and P_{fa} in the shortest time possible.

9.3 DETECTION ROUTINES

The target detection algorithms process the outputs of the low resolution filter bank. This filter bank comprises 64 filters covering the full demodulated bandwidth of 2.5 - 25kHz, corresponding to 20 - 200m of range. Each filter has a bandwidth of 390Hz, and thus a response time of 2.5ms. This rapid response time has been achieved by trading off range resolution (see section 2.2.5) - each filter corresponds to around 3m of range, compared to the minimum possible range cell size for this sonar of 5cm. Of course, the S/N from a 3m range cell will be lower than that from a 5cm range cell. However, the S/N may be improved by utilizing the many samples which are now available for processing, using either integration or probability density analysis techniques (see section 6.2). A 3m range resolution is too poor to provide any structural information of expected targets and therefore prevents any form of target classification. Instead, the filter outputs are analyzed to detect the presence of targets; if any are found, these can subsequently be examined in greater detail using a high resolution filter bank.

The processing time required for target classification is longer than that required for detection, as the response times of the high resolution filters are longer. Furthermore, targets may be detected in the low resolution filter bins simultaneously, whereas classification can only be invoked on one target at a time. Thus the advantage of the two stage approach is that no effort is wasted attempting to classify the outputs of range cells that contain no targets. If it were not possible to scan the low resolution filters with the detection software prior to classification, then the full

range would have to be analyzed using classification routines and high resolution filters. This would require considerably more processing time or hardware, depending on whether the range cells were analyzed sequentially or simultaneously. For example, the detection software may detect 5 targets in the sonar's range within 250ms. If classification of each target takes 500ms, then the five targets will be classified after 2.5s, giving a combined detection and classification time of 2.75s. If detection were not possible, each range cell would have to be processed using the classification software, which would require 64 x 500ms = 32s.

Several possible detection strategies are reviewed in Chapter 6. Some of the strategies considered for the Classification Sonar, such as the Maximum Likelihood Estimator, were computationally too demanding to be attempted using the hardware installed in the sonar. Others, which seemed reasonable in theory and using air models, were found not to work as reliably or consistently as expected. Conversely, strategies which seem reasonable if not obvious in hindsight did not always appear so initially.

The simplest detection strategy is to establish a single, fixed threshold and to consider a target to be detected when this threshold is exceeded. Such a strategy is inadequate for the Classification Sonar because the outputs of the 64 filters will be different even in the absence of targets. Firstly, the arc width of a range annulus increases with range as the ultrasonic beams spread, so that a considerably larger band of seabed and volume of reverberant water is intercepted at longer ranges. Secondly, any phantom backscatter or reverberation resulting from range ambiguities (cf. section 3.2) will have a markedly greater effect near the maximum range than near the minimum range. Thirdly, the level of backscatter in any range cell will depend on the terrain of the seabed being intercepted, and this will often vary over the range of the sonar. Consequently, a single, fixed threshold for all range cells is inappropriate for the present task.

The two most successful detection algorithms, described below, incorporate different methods of dynamically establishing the threshold for each filter during every sweep. These algorithms (and several others) are stored in the computer and can be selected by the operator.

9.3.1 Local Dominance Of A Peak

Although there may be considerable variation of backscatter over the entire range, the variation tends to be gradual from one cell to the next. Hence, the dominance of any one cell may not be significant globally, but could well have localized significance. The basis of using a localized average is illustrated in Figure 9.2. A single, fixed threshold, as indicated by the dashed line, would miss peak A, and erroneously detect many targets in addition to peak B. Using the criterion that a peak must stand proud of a local average by some factor or amount enables both peaks A and B to be detected with no false alarms.

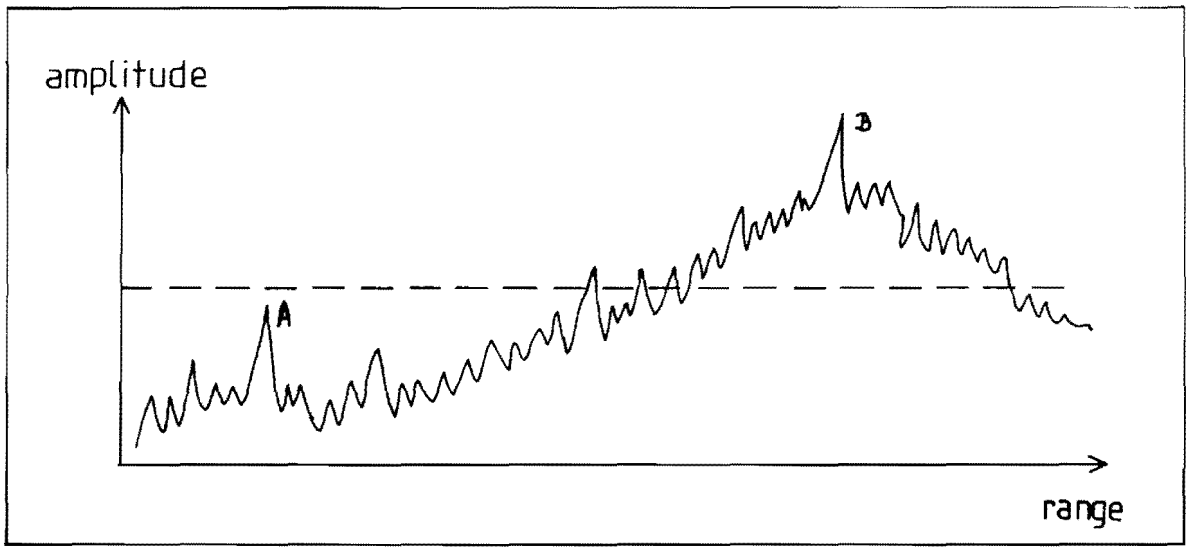

Figure 9.2 : Target detection using a localized threshold.

Optimum parameters (as defined in section 9.2 above) for this algorithm were found to be:

1. 120 low resolution samples from each range cell must be integrated;

2. Each local average is to comprise 5 adjacent cells;

3. The amplitude of the central cell must exceed that of the local average by at least 20%.

9.3.2 Hole Detection

The principle of hole detection is described in Chapter 6. Recall that for each low resolution range cell, a low threshold is established, and the number of times filter outputs fall below this threshold is noted. Range cells with none or few samples below the threshold tend to contain targets.

Experiments with a single, fixed hole threshold for the entire range suffered from analogous problems to those encountered with local peak detection. Here the problems are overcome by establishing the threshold level for each filter during each sweep on the basis of initial samples from that filter alone. The threshold is established by taking a proportion of the average amplitude of initial samples from a filter.

Optimum parameters were found to be:

1. 32 samples required to determine the average;

2. Set the threshold at 1/3 of the average;

3. Take a further 64 samples and count the number of samples that fall below this threshold;

4. Allow no more than 8 samples below the threshold to accept a target as being suspect and worthy of classification.

Note that this strategy selects targets according to the size of a hole, and not the average amplitude. Thus, a small, highly specular reflector such as a sphere may be classified as being man-made, while a larger, more diffuse reflector with a greater average echo strength may not.

9.4 CLASSIFICATION ROUTINES

When a target has been detected in a low resolution filter bin, the target may be analyzed by the classification software. Classification is effected by mixing the output of the relevant low resolution filter bin with a local oscillator, so that the signals within the low resolution filter fall over the fixed high resolution filter bank. The high resolution filter bank comprises 64 filters, each being 6Hz wide and therefore having a response time of 167ms.

As with the detection routines, various different classification strategies are stored in the computer and can be invoked by the operator. All strategies are based on an observation initially made during air modelling experiments, namely that the echoes from man-made objects tended to have one or two peaks with an amplitude considerably greater than the average amplitude of the outputs of the high resolution filter bank. However, because some targets exhibit a distinct frequency response, a peak which is dominant during part of the sweep will not necessarily be dominant for the duration of the sweep. Such a target is illustrated in Figure 9.3, where the target has a considerable response at an ultrasonic frequency of around 65kHz, yet no visible response at either end of the ultrasonic sweep. Consequently, if the outputs of the 6Hz filters are sampled only once, the peak may not be captured, and hence the cell will be deemed not to contain a target. To ensure that the peaks of targets exhibiting a fluctuating frequency response are detected, three separate samples are needed, requiring three response times of 167ms, or one full sweep period. The three samples from each high resolution filter are peak-detected, i.e. the greatest value of the three samples is used by the classification software.

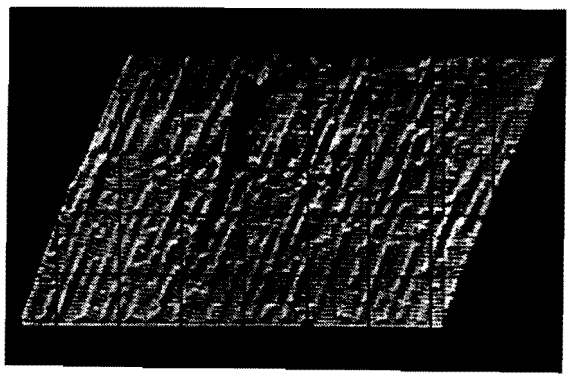

Figure 9.3 : Target with a highly frequency selective response.

9.4.1 Primary And Secondary Peak Dominance Over Average

In this algorithm, the outputs of the 64 high resolution filters are processed to determine the average amplitude and the positions and amplitudes of the two major peaks. If the primary and secondary peaks exceed the average by pre-selected factors or amounts, and further, if the separation between these two peaks falls within certain constraints, then a man-made target is considered to be present. Although some ideal man-made targets can be expected to have a single reflecting point (e.g. a sphere or tri-plane), practical targets used during the trials had at least two. The second reflecting point was usually the shackle used to suspend or retrieve the target.

Optimum parameters were found to be:

1. The primary peak must exceed the average by a factor of at least 4;

2. The secondary peak must exceed the average by a factor of at least 2;

3. The separation between the primary and secondary peaks must be at least 2 bins (otherwise the secondary peak is just part of the slope leading to the primary peak) but no more than 7 bins (thereby placing a limit on the physical size of targets).

9.4.2 Threshold Transgressions

A similar strategy to the preceding one consists of establishing a threshold by taking some proportion of the peak amplitude of the whole filter bank. The greater the number of filter outputs which exceed or transgress this threshold, the smaller the likelihood of an object being man-made. Optimum parameters were found to be:

1. Threshold is set to 0.6 of the peak amplitude;

2. Accept 5 violations before deciding the target is not man-made.

9.4.3 Mean Versus Median

The presence of a small number of high amplitude filter outputs associated with man-made objects is likely to affect the mean value more than the median value of the high resolution filter bank outputs. This feature is exploited by comparing the mean to the median, and considering a target to be man-made if the mean is greater than the median by some factor. The optimum ratio for acceptance of a target as man-made was found to be 1.1.

9.4.4 Multiple Invocations

In many situations it will be vital not to miss any man-made objects. To reduce the chances of missing a target, the sonar operator may invoke several or all of the classification algorithms to simultaneously process the outputs of the high resolution filter bank. The sonar will then consider a target to be man-made if any one algorithm indicates this.

Alternatively, more than one classification algorithm may be invoked, and the sonar programmed to indicate the presence of a man-made object if all invoked algorithms agree the target is man-made. While some man-made objects may now be missed, the chances of any target picked up by the sonar being man-made will be very high.

Thus the operator has two methods at his disposal for trading the probability of a false alarm against the probability of missing a man-made target: he may invoke several routines simultaneously and logically combine the outputs, or he may alter the parameters listed above for each individual algorithm.

9.5 SERIAL VERSUS PARALLEL OPERATION

There are two user-selectable modes of software operation : serial and parallel processing of the low resolution filter outputs. In the serial mode, each low resolution filter is analyzed sequentially. If the detection

software indicates the presence of a target, the high resolution filter bank is directed to that low resolution cell, and the classification software is invoked to determine whether the target is man-made. The sonar operator can observe the operation of the software, as the bright-up pulse on the A-scan display will jump from bin to bin in the absence of detected targets, hesitate where targets have been detected (indicating that the classification software is being invoked), and lock onto a bin if a target is classified as being man-made. Hence, serial operation allows an operator to observe the functioning of the software, and, more importantly, forces the sonar to invoke the classification software on every detected target.

However, under normal side scan operating conditions, (i.e. with forward vessel motion) serial implementation of the software will be impractical, as there will be insufficient time to effect sequential processing on a given area of seabed. Instead, parallel processing may be selected, in which the outputs of the low resolution filter bank are analyzed simultaneously. Since each classification algorithm requires a full sweep period for reliable operation, no more than one detected target can now be classified for each sector of seabed examined by the sonar using the present hardware (as the high resolution filter bank can only analyze the output of one low resolution cell at a time). Consequently, some measure of the likelihood of a target being man-made is required of the detection algorithms, so that the most likely target can be analyzed by the classification software.

The likelihood of detected targets being man-made can be derived from the detection software. For instance, in the first of the two detection algorithms described above, the extent to which a local peak exceeds a local average will give a measure of this likelihood. Similarly, using hole detection, the number of times the hole threshold is exceeded will indicate the likelihood. Thus, in the parallel mode, the 64 low resolution outputs are analyzed simultaneously, and the detected target that is most likely to be man-made (if there are any detected targets at all) will be analyzed by the classification software for confirmation. On the A-scan display, the operator will see the bright-up pulse jump to whichever bin has the most likely target.

9.6 PROBABILITY MAP

In addition to detecting and classifying targets, the software can generate a probability map of the sea bed. This map writes a grey-scale image of the seabed onto a colour monitor, with one axis representing sonar range, and the other axis representing time (such that it takes 2 minutes to completely fill the display). Superimposed on this grey-scale are coloured markers which tag suspected targets of interest. For example, the five most likely targets (as determined by the the detection algorithms) may be tagged with markers coloured respectively orange, yellow, green, blue, and violet. In addition, the most likely target is analyzed by the classification software, and if this process confirms that the target is indeed man-made, the tag associated with this target is changed to red. Alternatively, the colours indicating likelihood may be suppressed, leaving only red markers to indicate where targets have been classified as being man-made. A probability map is reproduced in the following chapter.

9.7 DISCUSSION

The automatic detection and classification software for the Classification Sonar described in Chapter 8 was written on an Intel Microcomputer Development System (MDS) in PLM-86, and occupies just under 5 kilobytes of program memory. An operator can choose between two general modes: serial and parallel processing.

Using serial processing, each of the 64 low resolution range cells is analysed sequentially; if a target is detected, that cell is further processed by the classification software to confirm or refute the presence of a man-made target. Using parallel processing, the 64 low resolution range cells are analysed simultaneously; the positions of the five range cells most likely to contain targets (as determined by the detection routines) are displayed on a probability map using coded colours, while the most likely target is further analysed by the classification software to confirm or refute the presence of a man-made target.

The software adapts itself to variations in backscatter, both within the 200m range, and from one side scan sector to the next. The desired detection and classification strategies can be selected by the operator in the field, while the individual parameters of each strategy can be adjusted to suit the particular environment in which the sonar is being used. Furthermore, up to five classification algorithms can be invoked simultaneously and their outputs logically combined.

Overall, the software has the flexibility to adapt itself to a wide variety of conditions and targets. The automation of target detection and classification enables operators to be relieved of these tasks. Operators may then monitor and veto software decisions, or alternatively, the sonar may be operated without human supervision.

CHAPTER 10

POOL AND HARBOUR TRIALS

10.1 INTRODUCTION

Initial trials of the Classification Sonar were conducted in an olympic sized diving pool measuring 30 x 21 x 4.5 m. Such a pool provides a controlled environment for calibration and measurement without the vagaries of the ocean (seabed backscatter, sea-state-noise, etc.). Nonetheless, a pool imposes its own limitations of a severely restricted range, and, for CTFM sonars, multiple and continuous backscatter from the pool walls. Consequently, most trials were conducted in a harbour environment. This chapter describes the experimental procedures used and presents the results of trials using as targets, amongst other things, spheres, tri-planes, tubes, drums, scuba divers and snorkel divers. These results are then compared to those attainable with other sonars.

10.2 POOL TRIALS

10.2.1 Constant Beamwidth And Frequency Response

Once the correct functioning of the sonar front-end (transmitter, receiver and demodulator sections) had been established in the pool, it was desired to equalize the frequency response while maintaining constant horizontal beamwidth throughout the transmitted sweep. Equalizing the

frequency response of the transmitter-receiver chain normally involves varying the power level of the transmitter during a sweep so that the output of the demodulator corresponding to a particular target remains constant. Such equalization is usually implemented independently of any constant beamwidth adjustment.

However, since beamwidth is dependent on wavelength, the beamwidths of CTFM sonars vary during a transmission sweep (see section 2.2.3). For the Classification Sonar, the one octave frequency variation results in a 2:1 ratio of beamwidths at opposite ends of the transmit sweep. To overcome any wavelength dependent variation in beamwidth, the transmit transducer was constructed out of three concentric arrays, each array being dimensioned to provide the desired beamwidth over a portion of the sweep. The aim of one pool trial was thus to establish the power levels required for each transmitting array during the transmit sweep to provide a constant beamwidth and a constant amplitude at the output of the demodulators.

To determine the required power levels, the transmit and receive transducers were mounted facing each other at opposite sides of the pool, the direct path eliminating any frequency dependent effects of any reflector. The sonar was manually stepped through its operating frequency band in 2kHz steps; at each frequency, the relative power levels required by the three transmit arrays to provide constant beamwidth were selected (based on data supplied with the transducer). Subsequently, these power levels were varied in fixed proportion to provide a reference amplitude at the output of the demodulator. The required power levels at these 2kHz steps were later interpolated to provide data for PROMs. These PROMs are read every 250μs during a sweep to enable the appropriate power level to be applied to each array in the transducer. (A different set of PROMs has to be used to operate the sonar in air.) Note that for the present application, constant vertical beamwidth was not considered necessary.

10.2.2 Crosstalk

A further pool trial set out to determine the separation required between the transmit and receive transducers and/or the need for acoustic baffles to keep the crosstalk to an acceptable level. The crosstalk component at the output of the demodulator was monitored while the position of the receive transducer was moved relative to that of the transmit transducer. Crosstalk resulting in a demodulated output not exceeding that of the specified minimum detectable target was considered acceptable on the basis that anything larger may impinge on the dynamic range. Under these conditions, the receiver could be positioned to within 12cm of the transmitter. The mounting configuration is discussed in the next section.

10.3 HARBOUR TRIALS

10.3.1 The Environment

The sea trials were conducted in a natural harbour of volcanic origin (Lyttelton Harbour, Christchurch, New Zealand). A gantry supporting the transducers was mounted on the side of the main wharf (Cashin Quay) so that the transducers faced the opposite side of the harbour, about 2km distant, as shown in Figure 10.1. The height of the transducers above the seabed was adjusted using a ratchet drive on the right side of the gantry. The gantry and transducer supporting frame are shown in Figures 10.2 and 10.3. The two transducers and their hydraulic steering mechanism were mounted on a substrate which was attached to the transducer support frame with hinges so that the transducers could be folded out for underwater use and folded in to facilitate retrieval. Transducer elevation angle was manually adjusted while the transducers were out of the water; bearing was adjusted remotely through the hydraulic steering mechanism, as shown in Figures 10.4 and 10.5.

The transmitter transducer power amplifier and receiver transducer pre-amplifier are shown in Figure 10.2 housed in two metal cylinders clamped onto the transducer supporting frame above the transducers. The receive transducer was connected to the larger transmit transducer by a section of rubber tubing to minimise microphony. A multi-core cable connected the

transducers and their respective amplifiers to the remaining electronics, which were housed in a caravan situated on the wharf. All adjustments to the sonar could be made from within the caravan, with the exception of transducer height and transducer elevation angle.

Figure 10.1 : Lyttelton Harbour from Cashin Quay.

The depth of the water at the transducers varied between 13m and 16m with the tide. To optimize detection at various ranges, the height of the transducers could be varied from just below the water line to 2m above the sea bed. Further optimisation was possible by varying the elevation angle of the transducers.

The seabed in front of the transducers and extending out for some 300m was frequently dredged in a line parallel to the wharf, resulting in channels up to several metres deep being dug in the mud. Consequently care had to be taken to ensure targets were not positioned in such a channel, as detection could then be prevented.

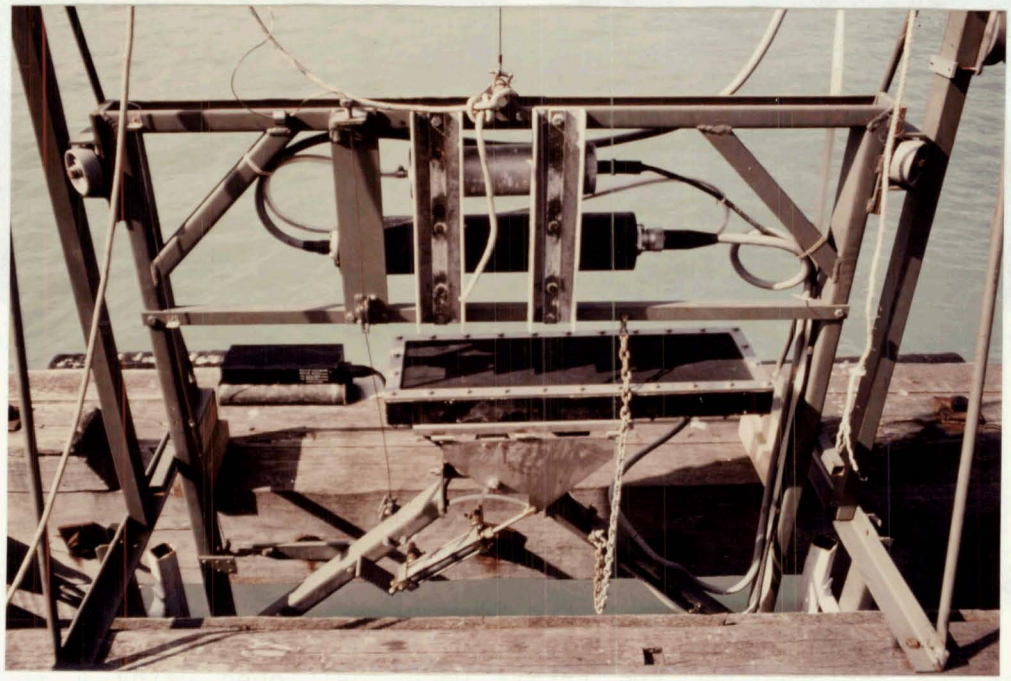

Figure 10.2 : Gantry and transducer support frame. Note the two canisters containing the transmitter power amplifier and the receiver pre-amplifier.

Figure 10.3 : View of gantry with transducers just entering the water.

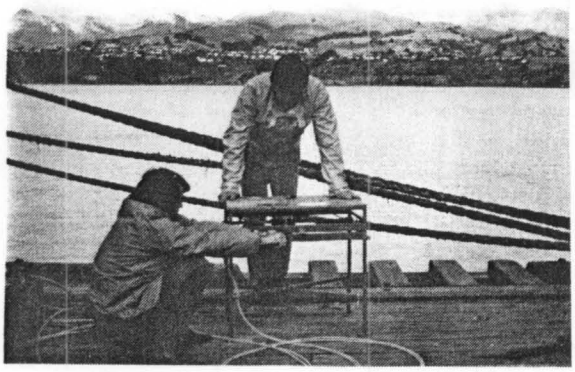

Figure 10.4 : Hydraulic control of bearing.

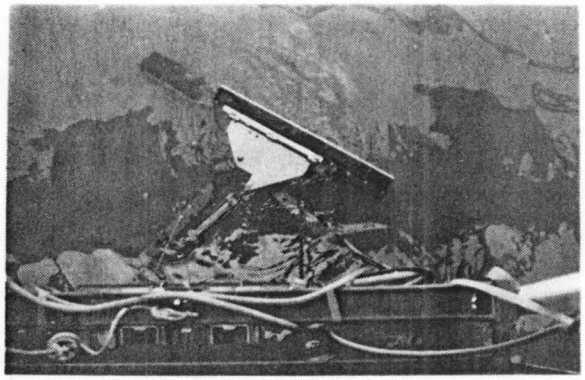

Figure 10.5 : Maximum deflection to the right.

10.3.2 Operational Procedure

Targets deployed for the trials were positioned using a motorboat. Many targets were negatively buoyant, and these were placed on the seabed, thereby eliminating most target movement caused by currents and tidal swells. Such targets were attached to marker buoys by ropes for later retrieval. Some targets (either positively or negatively buoyant) were suspended between the seabed and the surface by using anchors and buoys. The buoys, anchors, and connecting ropes frequently appeared on the sonar displays, and care had to be taken not to confuse their echoes with those of the target per se.

The elevation angle of the transducers was adjusted prior to the lowering of the transducers into the water. The transducers were then lowered to the desired depth (i.e. height above the seabed). All subsequent adjustments were implemented from within the mobile laboratory.

The A-scan and M-mode displays always showed the full range information and the zoom range information simultaneously. Upon power-up, the stack plot displayed the full range output, although the zoom range output could subsequently be selected by the operator. The audio display was always centred on the zoom information. The portion of the full range which was expanded by the zoom facility was determined either manually or automatically. In the manual mode, an up/down switch was used to effectively place the high resolution filter bank anywhere in the full range; in the automatic mode, the detection software (see Chapter 9) assumed control of the zoom placement.

An operator could steer the beam by means of an hydraulic linkage to the transducers. Furthermore, the transmitted power output level could be varied to optimize the display of echoes.

Various means existed for recording either or both of the full range and zoom range information. A CZT spectrum analyzer was used to drive an Edo 606 electrostatic paper chart recorder, while a 4-track Revox tape recorder was used to record the full range demodulated output and the zoom output. These recordings could subsequently be played back to the sonar processor to recreate the displayed information. Alternatively, photographs or video recordings could be made of the displays whenever features of interest appeared.

An additional operator facility was the visual display freeze, whereby the M-mode and/or stack plot displays could be frozen for further operator evaluation or to facilitate photography. Such a feature is becoming standard on modern memory mapped sonar displays (Milne, 1983).

Manual detection of targets was usually attempted while observing the full range A-scan display and listening to the audio output. As soon as a target had been detected, attention was usually shifted to the zoom stack plot and the zoom A-scan displays in an effort to classify the targets.

Numerous trials were conducted over a period of three months to test and modify various parts of the sonar. In particular, the detection and classification software was modified to incorporate knowledge gained about the spectral and temporal characteristics of targets and other sources of echoes.

10.3.3 Backscatter From The Seabed

Early investigations into the backscattering of sound from a harbour bottom (Urick, 1954) showed that the echo strength is largely determined by seabed roughness. However, McKinney & Anderson (1964) concluded that a knowledge of the particle structure of the bottom is useful in estimating the backscatter strength. The backscatter strength is conventionally defined in terms of reverberation strength per unit area of bottom (Martin, 1966). This

definition is analogous to the target strength definition for single targets. The resultant measure of backscatter strength is thus dimensionless and independent of the size of the range annulus.

An extensive compilation of measured backscatter (Wong & Chesterman, 1968) and a theoretical treatment of backscatter (Urick, 1979) suggest that for the composition and roughness of the seabed at the test site in Lyttelton Harbour, and the elevation angles used, the backscattered strength should vary between approximately -25 and -35 dB. During the trials, a -21 dB sphere had an echo strength greater than the surrounding seabed of between 6 and 19 dB depending on conditions.

The backscatter received by the sonar is illustrated in Figure 10.6. Figure 10.6(a) shows the backscatter on the full range stack plot, while Figure 10.6(b) shows the same information on the full range M-mode display. Figure 10.6(c) shows an A-scan of both the full range (upper trace) and zoom expansion (lower trace) of the backscatter at a range of 42m.

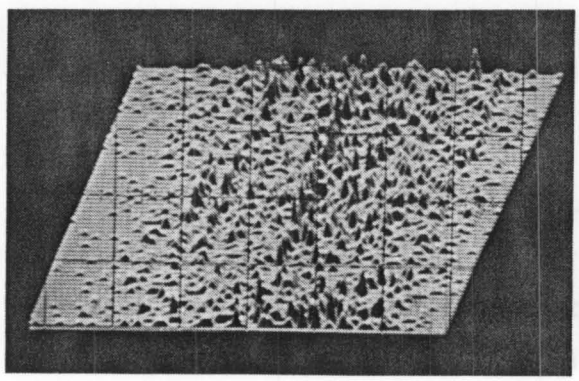

Fig. 10.6(a): Backscatter, full range.

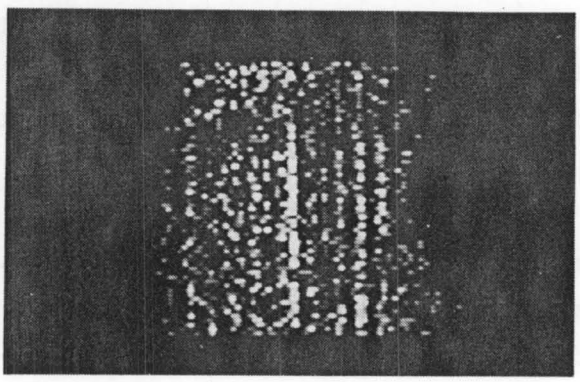

Fig. 10.6(b): Backscatter, full range.

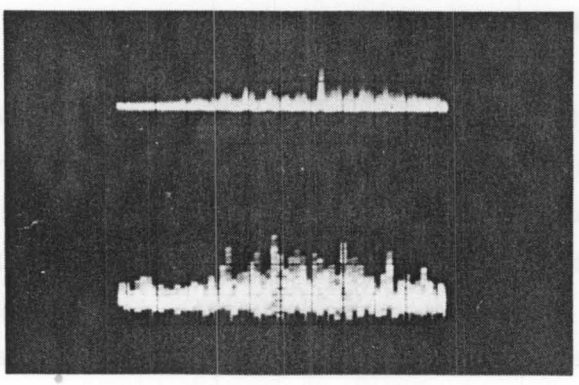

Fig. 10.6(c) : Backscatter, full range (top), zoom (bottom).

Figures 10.6 (d) and (e) show zoom expansions of the backscatter on the stack plot display at 42m and 190m respectively. Figures 10.6 (f) and (g) show the same information on the M-mode display. Note that the backscatter is frequency dependent, i.e. the amplitude of each echo component varies during the sweep.

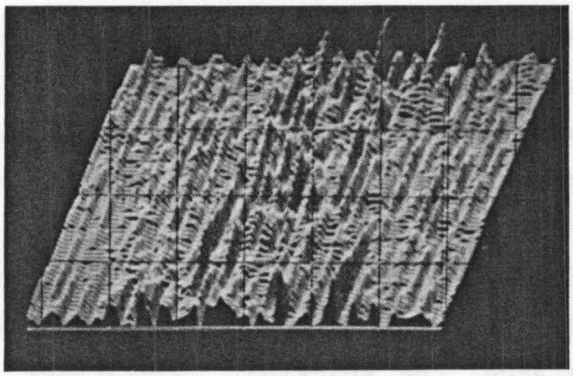

Fig. 10.6(d): Backscatter, zoom range, at 42m.

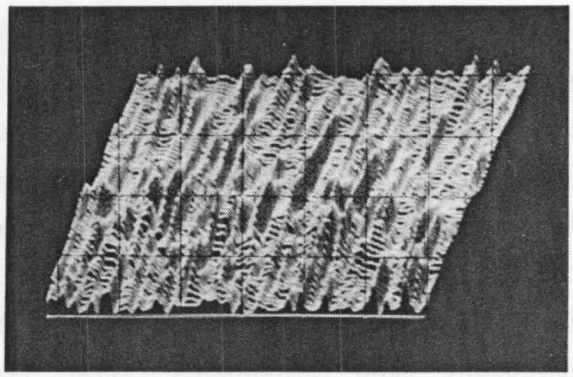

Fig. 10.6(e): Backscatter, zoom range, at 190m.

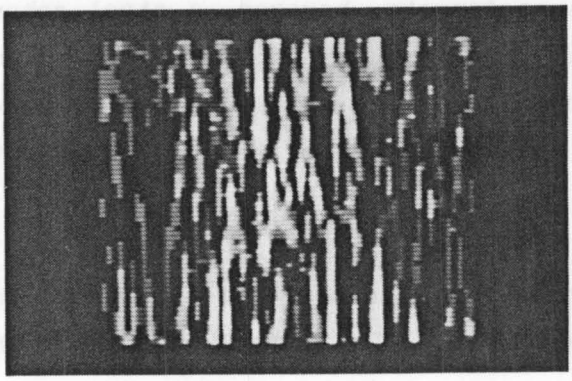

Fig. 10.6(f): Backscatter, zoom range, at 42m.

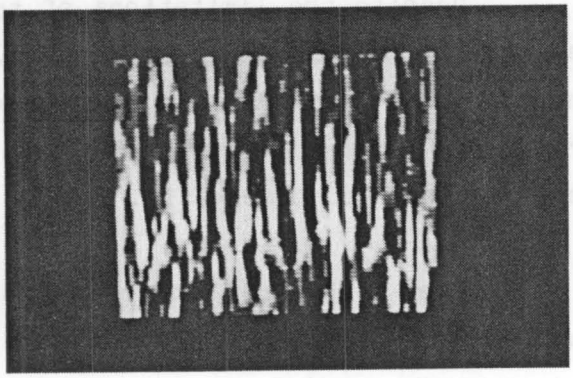

Fig. 10.6(g): Backscatter, zoom range, at 190m.

10.3.4 Spheres

Large, air-filled metal spheres are often used as reference targets to calibrate underwater sonars. This is because the echo from a sphere is independent of aspect, and also because, assuming the sphere to be large in terms of wavelengths and its surface to be rigid, the backscattering cross section is known and is independent of frequency.

In practice, spheres used as reference targets may depart appreciably from the idealised bodies they are assumed to be. These deviations result from welding seams, imperfections in manufacture, dents, and suspension fittings (e.g. eyebolts, shackles and ropes). In a detailed examination of the target strengths of spheres, Freedman (1964) found that there could be a variation in target strength of up to 20 dB with aspect, and that the first echo (from the front face of the sphere) could actually be smaller than subsequent echo components (from, for instance, the shackle). Variations in the echo strengths from spheres have also been noted with changes in pulse length (Hampton & McKinney, 1961), shell thickness and internal composition (Diercks & Hickling, 1967), and illuminating frequency (Hickling & Means, 1968).

Despite the limitations of spheres as targets, however, a steel sphere was used as one of the test targets. The sphere measured 445mm in diameter, and had two antipodal eyebolts protruding 110mm and made of 10mm diameter iron. The sphere, being air-filled, was very buoyant, so that heavy weights were required to submerge it.

The high resolution capability of the Classification Sonar (5cm) enabled many reflecting points on the sphere to be recorded. Although the primary echo amplitude and ratio of primary to secondary echoes did vary, depending on conditions, many stable and recognisable echoes were received from the sphere. Figures 10.7 (a) to (e) show respectively the full range stack plot, full range M-mode, zoom stack plot, zoom M-mode, and full range and zoom A-scans of the sphere at a range of 50m. From the zoom stack plot and zoom M-mode displays it can be seen that the primary echo is almost independent of frequency, while the secondary echo, presumably from the eyebolt and shackle, varies with transmitted frequency. Note that this difference in frequency stability is not evident on the zoom A-scan.

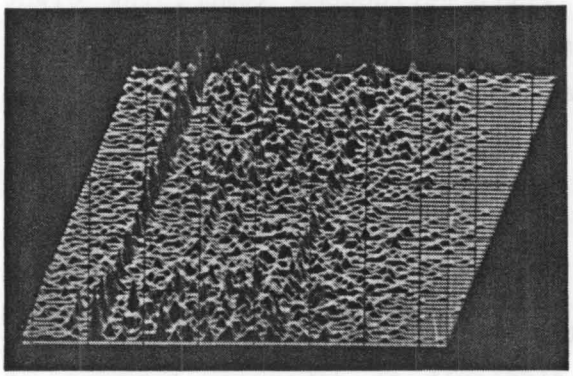

Fig. 10.7(a): Sphere, full range.

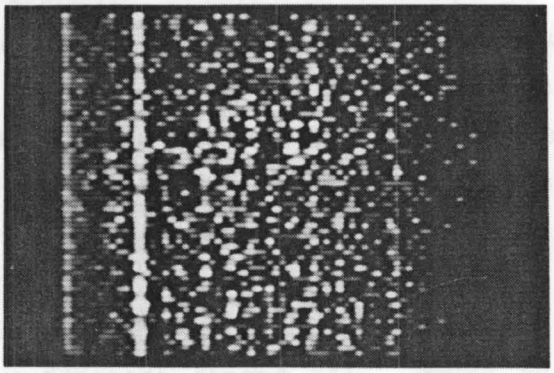

Fig. 10.7(b): Sphere, full range.

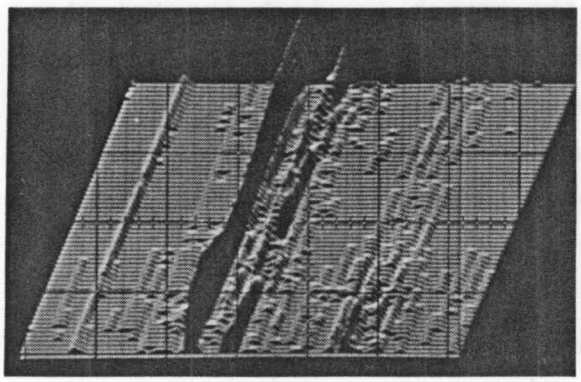

Fig. 10.7(c): Sphere, zoom range.

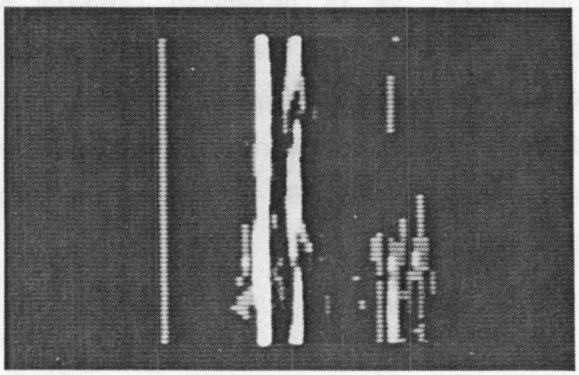

Fig. 10.7(d): Sphere, zoom range.

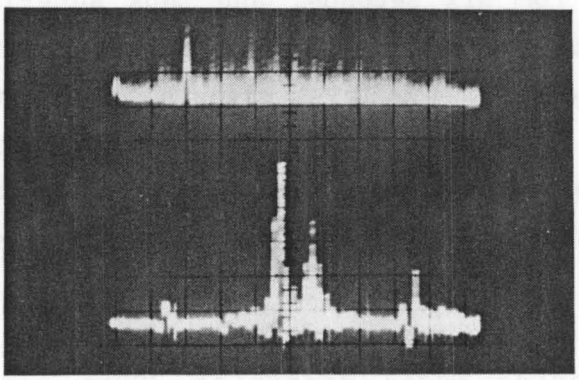

Fig. 10.7(e): Sphere, full range (top), zoom (bottom)

10.3.5 Tri-planes

Tri-planes are three dimensional retro-reflectors comprising eight triangular corner reflectors. Their large ratio of target strength to cross-sectional area allows them to be readily detected, and they are often used as reference points in underwater positioning systems. (In air, tri-planes are mounted on the masts of small vessels to greatly enhance detection of the vessel by radar.)

The largest tri-plane employed in the sonar trials had leading edges measuring 450mm. Its target strength was difficult to determine because of the non-rigidity of the sheet-metal sides and imperfections in manufacture, but assuming an ideal construction, the target strength was calculated to be 15 dB. Furthermore, this target strength was difficult to confirm experimentally, as it depended largely on the manner in which the tri-plane rested on the seabed: if placed on a firm, smooth surface, the seabed acted like a mirror and increased the effective cross-sectional area, whereas if placed on a soft surface, the tri-plane would partially sink into the mud, thereby reducing the effective cross-sectional area and decreasing the echo strength.

Nonetheless, the large tri-plane was easily recognisable because of its strong echo. Figures 10.8 (a) to (e) show the full range stack plot, full range M-mode, zoom stack plot, zoom M-mode and A-scans respectively of the tri-plane at near the maximum range. The full range A-scan of Figure 10.8(e) illustrates the mechanism of hole detection described in Chapter 6. The photograph was exposed for six seconds, and thus superimposes the filter outputs for 12 consecutive transmit sweeps. At the position of the target, there is a complete absence of low level signals, giving the impression of a hole on the display. In this example, the target could readily have been detected using peak-amplitude or even average-amplitude techniques, but in many situations hole detection offers distinct advantages (see section 6.2.2).

A more complex target was constructed using two small tri-planes. Each triplane had leading edges measuring 200mm and a target strength calculated to be 1.2 dB. They were attached to opposite ends of a rod so that their centres were spaced 1m apart. Figures 10.9 (a) to (e) show the full range stack plot, full range M-mode, zoom stack plot, zoom M-mode, and A-scans

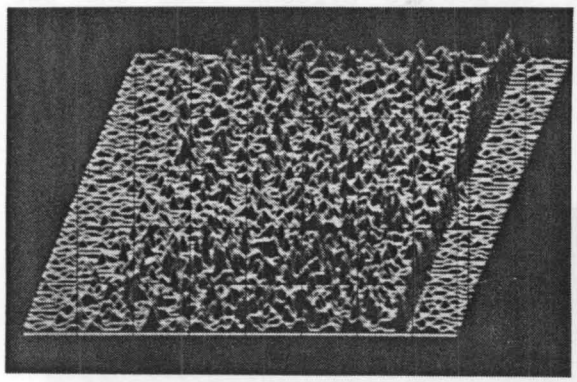

Fig. 10.8(a): Tri-plane, full range.

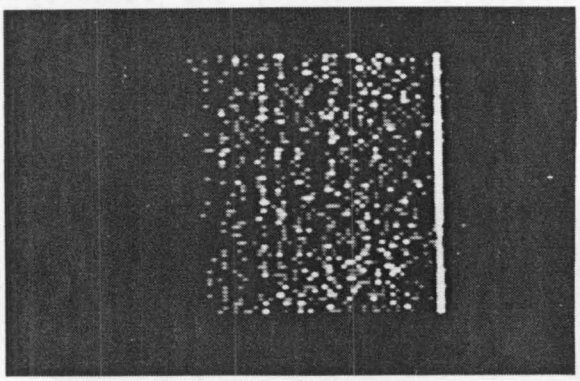

Fig. 10.8(b): Tri-plane, full range.

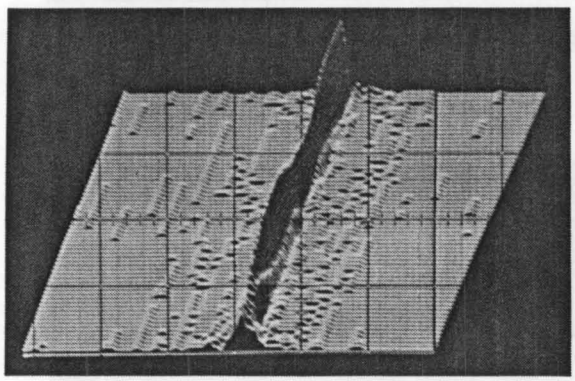

Fig. 10.8(c): Tri-plane, zoom range.

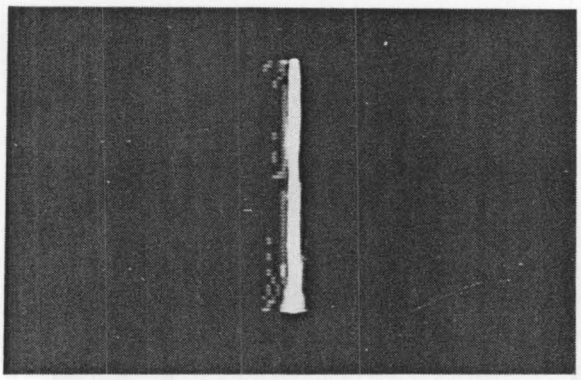

Fig. 10.8(d): Tri-plane, zoom range.

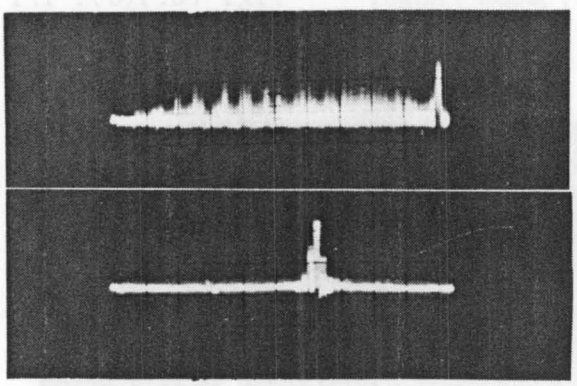

Fig. 10.8(e): Tri-plane, full range (top), zoom (bottom)

respectively of this double tri-plane at 90m range. Although it is difficult to visually detect this target on the full range displays, once a zoom expansion is obtained, the identity of the target is evident from the two frequency independent echoes.

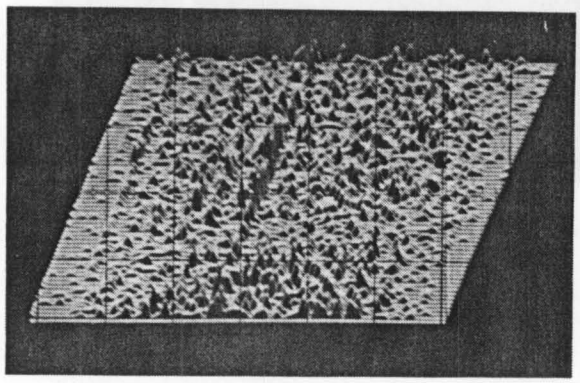

Fig. 10.9(a): Tri-planes, full range.

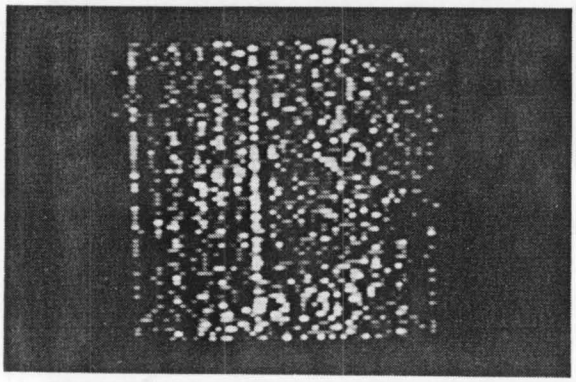

Fig. 10.9(b): Tri-planes, full range.

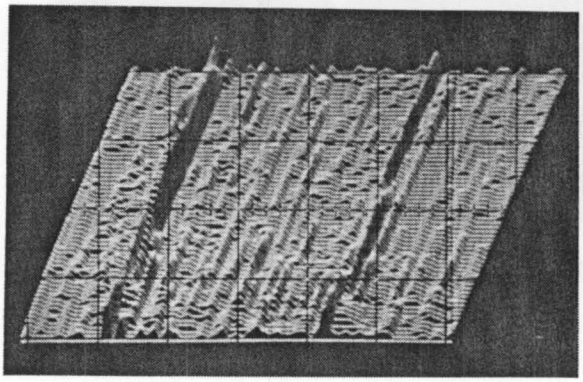

Fig. 10.9(c): Tri-planes, zoom range.

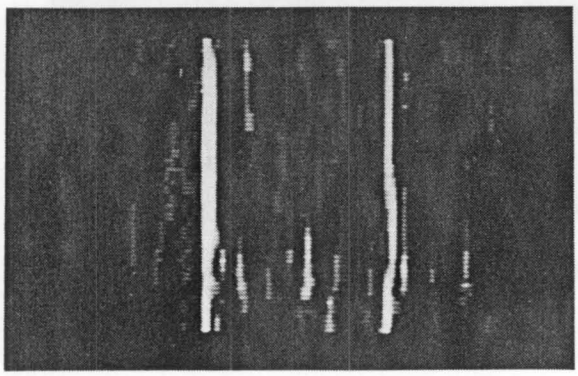

Fig. 10.9(d): Tri-planes, zoom range.

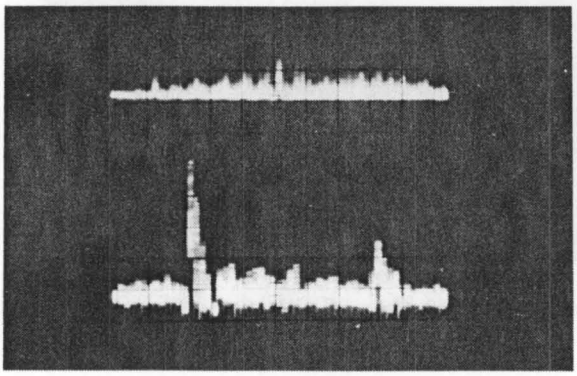

Fig. 10.9(e): Tri-planes, full range (top), zoom (bottom)

10.3.6 Drums

A complex target was made by modifying three 20-gallon drums. All the end discs were cut away, leaving tubular sections. Inner walls were then welded to these tubes with a spacing of 20mm between the inner and outer walls. Air filled the space between the walls. Each modified drum had an outer diameter of 385mm and a length of 590mm. The drums had lugs welded at their ends so that they could be used individually or bolted together to form a longer target.

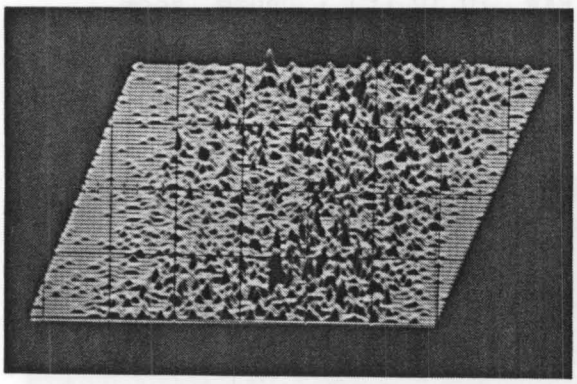

Fig. 10.10(a) : Drums, full range.

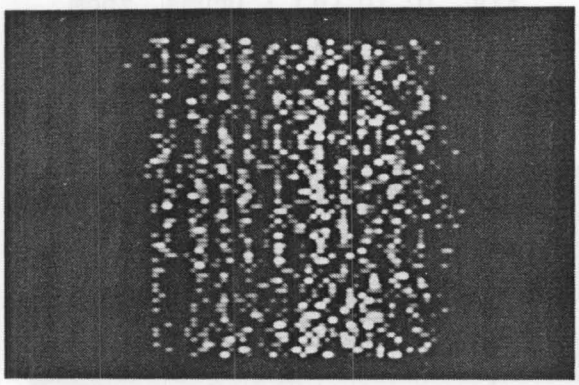

Fig. 10.10(b) : Drums, full range.

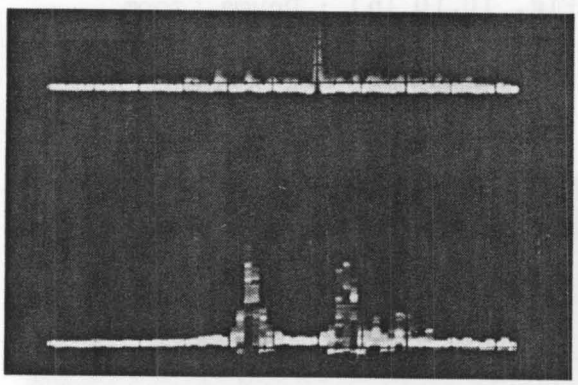

Fig. 10.10(c) : Drums, A-scans.

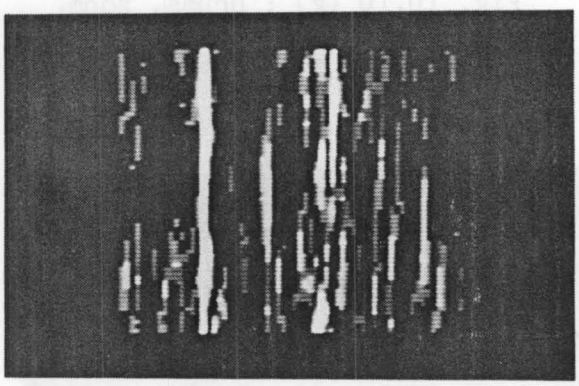

Fig. 10.10(d) : Drums, zoom range.

Of all the inanimate targets deployed, the drums exhibited the greatest variation in echo structure. This is not surprising, since in addition to the connecting lugs, each drum had two circumferential protrusions

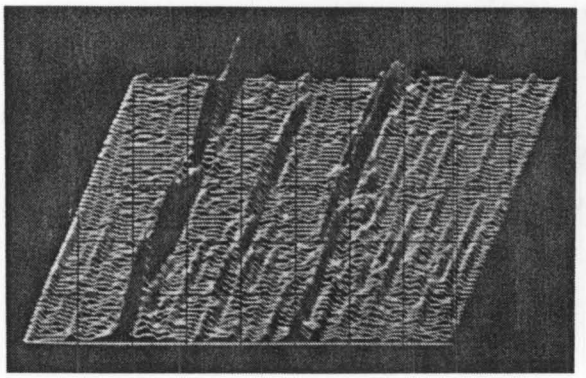

Fig. 10.10 (e) : Drums, zoom.

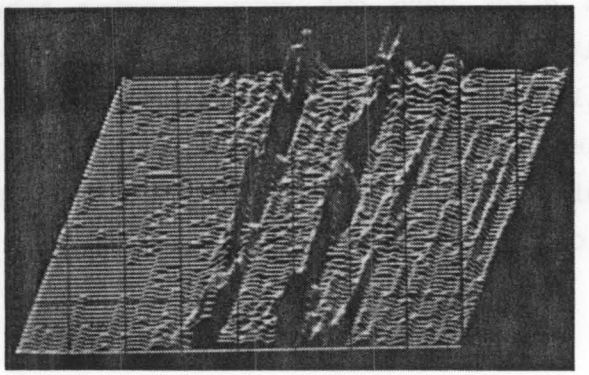

Fig. 10.10 (f) : Drums, zoom.

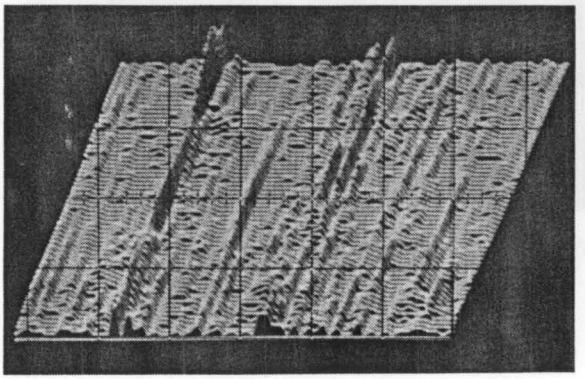

Fig. 10.10 (g) : Drums, zoom.

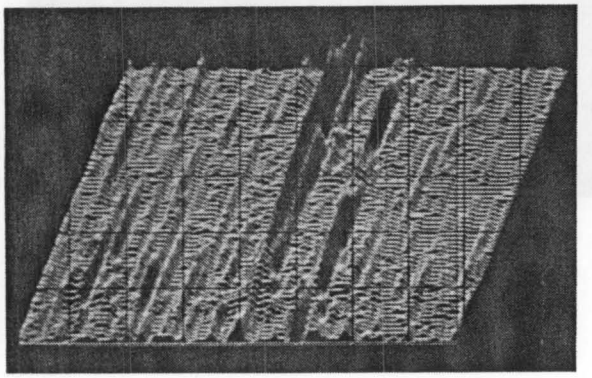

Fig. 10.10 (h) : Drums, zoom.

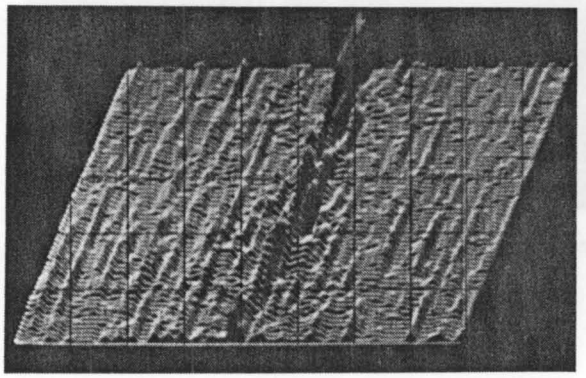

Fig. 10.10 (i) : Drums, zoom.

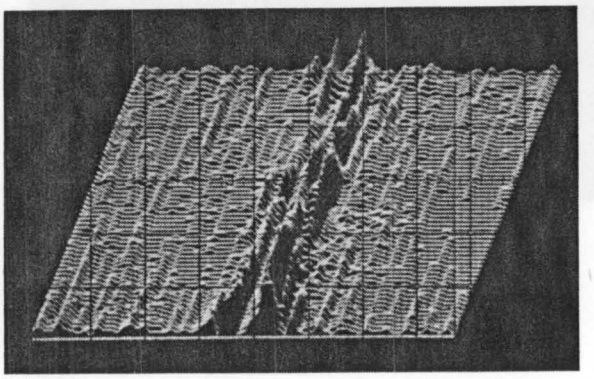

Fig. 10.10 (j) : Drums, zoom.

embossed on the outer shell. Hence, with the three sections bolted together, there were many reflecting points, and the echoes could be expected to vary considerably with aspect. Figures 10.10 (a) to (d) show the full range stack plot, full range M-mode, A-scans, and zoom M-mode respectively for the three drums at 120m range. To illustrate the variability of the echo from the three drums with aspect, Figures 10.10 (e) to (j) show six different zoom stack plots of the drums with different aspect.

Frequently, there would be 3 main echoes, of which two were usually stronger than the third, as in Figures 10.10 (e), (f) and (g). With other aspects, however, there were only one or two main echoes, as in Figures 10.10 (h), (i) and (j), and identification of the drums was difficult.

10.3.7 Scuba And Snorkel Divers

During the trials, surface swimmers and submerged divers were monitored on the sonar. Unlike the targets described above which were tethered and moved only in response to tidal currents, the human targets were continually mobile. Consequently, the echoes varied considerably from sweep to sweep.

The air tanks carried by scuba divers gave a strong echo that made these divers easy to detect and track. Figures 10.11 (a) to (d) show four zoom stack plots of a submerged scuba diver. Note that in all cases the main echo exhibits strong (albeit not predictable) frequency dependence. Furthermore, in three of the four stack plots, the main echo is also the only appreciable echo.

This contrasts with echoes received from snorkel divers, as shown in Figures 10.12 (a) and (b). There are many echo components, none of which is frequency independent, suggesting reflections from many reflecting points which interfere with each other.

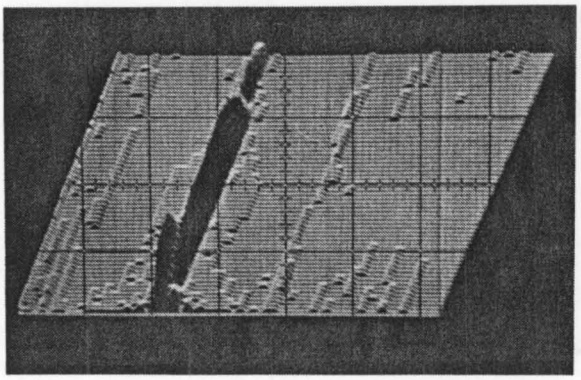

Fig. 10.11(a) : Scuba Diver.

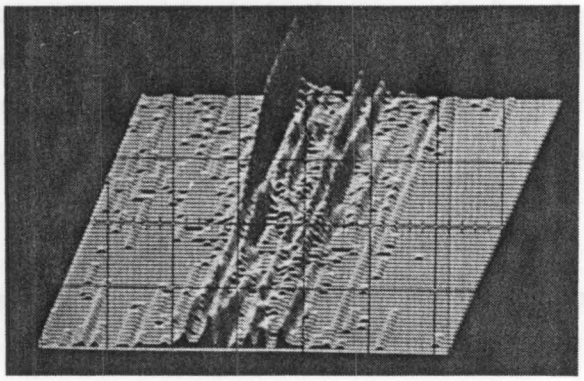

Fig. 10.11(b) : Scuba Diver.

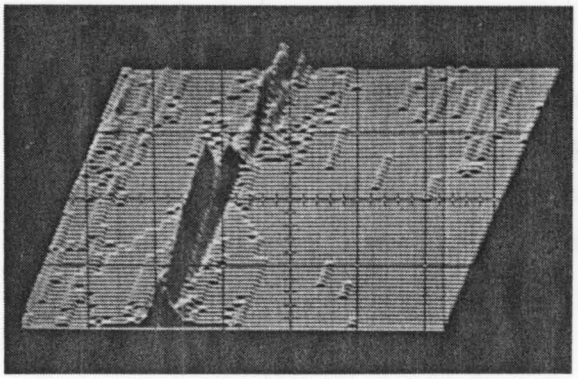

Fig. 10.11(c) : Scuba Diver.

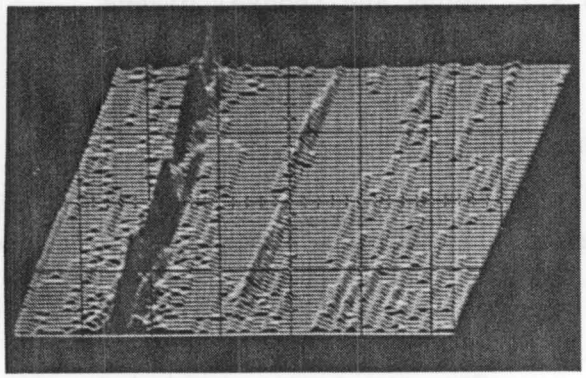

Fig. 10.11(d) : Scuba Diver.

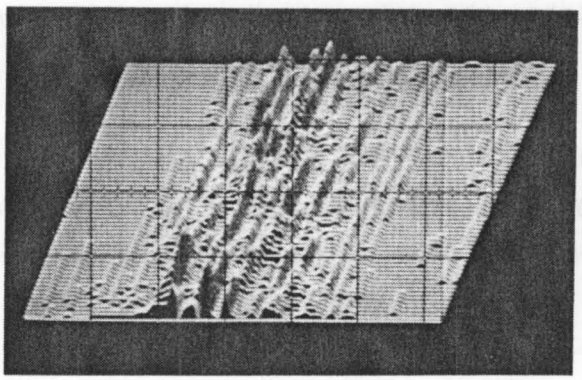

Fig. 10.12(a) : Snorkel Diver.

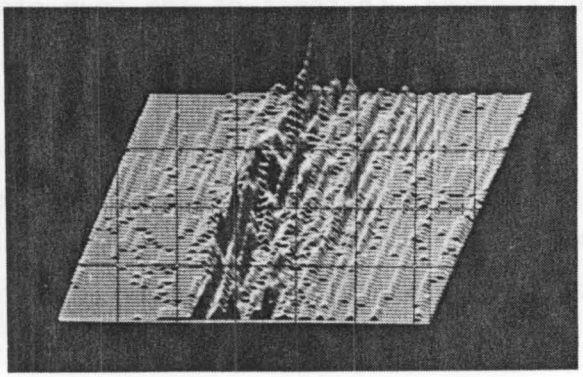

Fig. 10.12(b) : Snorkel Diver.

10.3.8 Unidentified Targets

In addition to examining deployed targets with the sonar, other objects were found and examined on the sonar displays. Most notable among these was a small, highly frequency dependent object at around 40m range that was detected on each day of trials, the trials lasting several months. This object was so small that visual detection on the full range displays was impossible, even with the a priori knowledge of target range and when the target was in the sonar's field of view. Similarly, the zoomed outputs of the A-scan and M-mode displays did not suggest a target. However, in the automatic detection mode, the hole detection algorithm only rarely failed to detect this target, even after missing other objects which to the operators seems more obvious. The zoom stack plot display revealed that there was an object in that range annulus with a very distinct frequency signature. The signature had a strong response at around 80 kHz (+6dB with respect to the noise) but disappeared into the noise at around 90 kHz and 70 kHz. The object giving rise to this signature was never retrieved for identification. However, it is assumed from the low average S/N that the object was relatively small. The low S/N also explains why detection and classification were difficult using many of the displays, since these displays and the manner in which they are perceived are subject to temporal integration. The algorithms in use at the time, however, did not average the outputs, but peak-detected for the duration of the sweep, thereby enabling detection and classification. Thus, a target that would under normal operating conditions have been missed by human operators, was consistently detected and classified by the computer. A zoom stack plot of this target is reproduced in Figure 10.13.

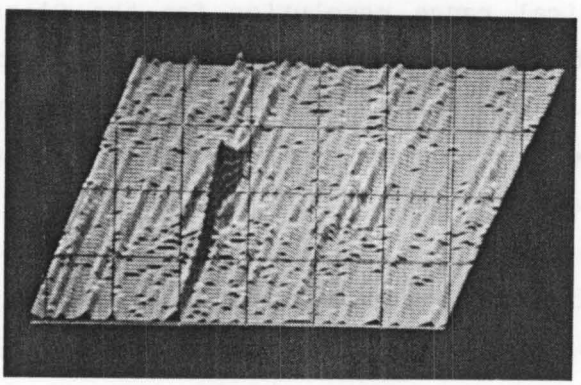

Fig. 10.13 : Small unidentified target.

Other unknown targets were also detected by the software or an operator, which is merely indicative of the debris typically found in all harbours. Zoom stack plots of two such targets are reproduced in Figures 10.14 (a) and (b). While it is difficult to draw any conclusive inferences from these stack plots, it seems that the first object extended about 40cm in range and comprised two or three main reflecting points, and that the second object extended about 120cm and comprised many reflecting points. These objects were not recovered to confirm the characterizations.

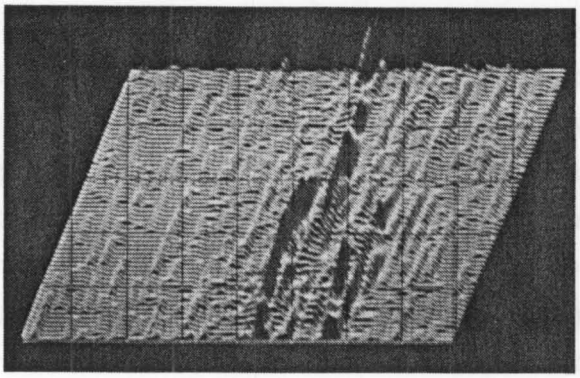

Fig. 10.14(a) : Unidentified target.

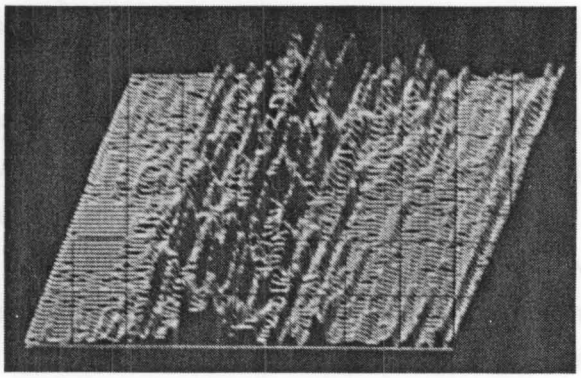

Fig. 10.14(b) : Unidentified target.

10.3.9 Range Resolution

In Chapter 2, the range resolution attainable with a CTFM sonar was shown to be $c/\Delta F$, where c is the speed of sound, and ΔF is the bandwidth. This suggests a theoretical range resolution for the Classification Sonar of 3cm. Confirmation that this range resolution is attainable in practice requires a spectrum analyzer with a cell width corresponding to 1.5cm (see section 2.2.6). The spectrum analyzer in use had a cell width corresponding to 5cm, so that this analyzer could not be used to confirm the theoretical resolution. However, experiments conducted in air with an air model of the sonar, where the theoretical range resolution was 6.6mm, resulted in a measured range resolution of 6.0 +/- 1.4mm (Gough et al., 1984a). This result suggests that the underwater sonar should also be able to achieve the theoretical resolution so long as there are no significant medium

fluctuations. Numerous researchers give practical results indicating that over a 200m range and a time span of several minutes, the fluctuations due to the medium should not result in variations in the depicted range of a stationary target of more than 3mm (e.g. Lee, 1979).

To confirm that the range resolution dictated by the spectrum analyzer could be achieved, an aluminium tube 75mm in diameter was positioned vertically on the seabed. Figure 10.15(a) shows an A-scan of this target. Both the front and rear walls of the tube are visible, and the dip between their respective echoes is well in excess of the 3dB required for resolution. Figures 10.15 (b) and (c) show two different zoom stack plots of the tube and indicate that the medium fluctuations are not sufficient to cause the echoes to jump from bin to bin.

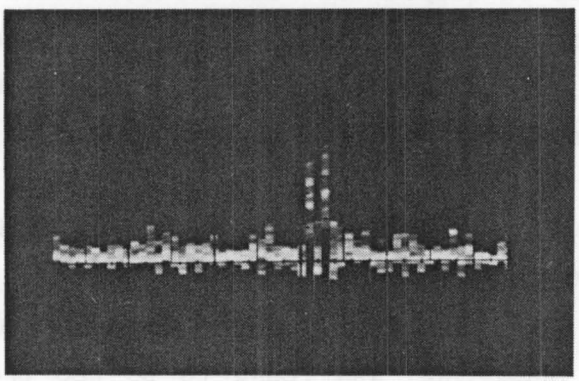

Fig. 10.15(a) : A-scan shown resolving a 75mm diameter tube.

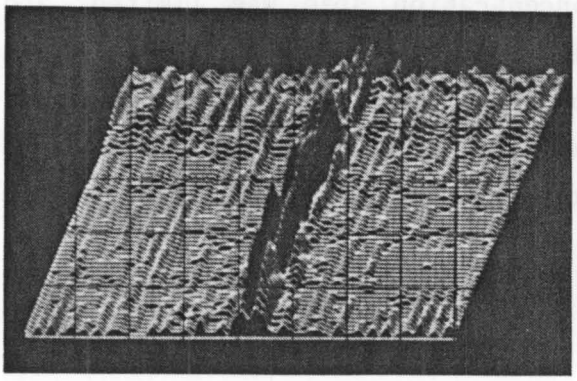

Fig. 10.15(b) : 75mm tube.

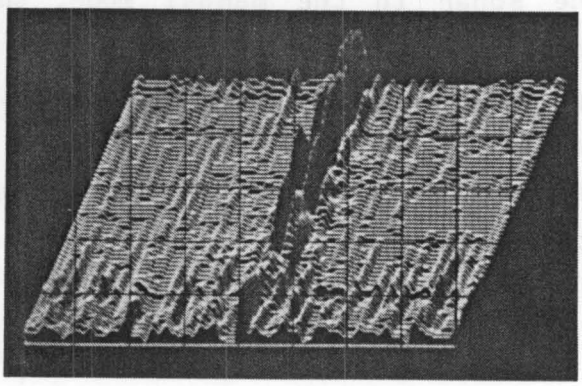

Fig. 10.15(c) : 75mm tube.

10.3.10 Automatic Detection And Classification

Two probabilities are used to measure the effectiveness of detection (or classification) systems : P_d, the probability of detection (or classification) and P_{fa}, the probability of a false alarm. If a target, the presence and position of which is known, is not detected, then certainly the "miss" degrades the P_d. However, if objects other than known targets are detected, it is presumptuous to assume a false alarm has occurred. The seabed in a harbour environment is likely to be littered with a variety of debris, and unknown detected objects may well conform to the specification of the types of target being sought. Thus it is difficult to accurately determine the P_{fa} without retrieving all detected targets from the seabed.

While the classification algorithms invoked depended on the objects being sought, the same detection principle was used throughout, viz. "hole detection" as detailed in Chapter 6. The effectiveness of this technique was highlighted by "unknown" targets being detected (as confirmed by subsequent zoom expansion) even though no discernible energy was apparent on any of the visual displays corresponding to that low resolution filter bin.

As explained in Chapter 9, the software was designed to give a P_d and P_{cl} of approximately 0.9, giving an overall P_{find} of 0.8, with a P_{fa} of 0.05. The initial criterion for classifying targets (namely that they are man-made as opposed to naturally occurring) was found to be too broad: echoes from the targets described above show wide albeit consistent differences. Hence the software selected will depend on the particular kind of target being sought.

While operators became adept at rapidly finding man-made targets using the sonar in the manual mode, their concentration span was limited, and performance dropped off with time. In the automatic mode, the sonar could function without operator interaction, or alternatively with the operator confirming the software decisions. In the latter case, the software would remove the tedium and pressure from the operator, and greatly lengthen his concentration span.

10.3.11 Probability Map

The Classification Sonar is intended to be used as a side scan sonar. Side scan sonars usually generate maps of the seabed, with the sonar range as one axis and the vessel position as the other. Two such maps can be generated by the Classification Sonar. One is generated by a CZT-interface and printed on an Edo 606 electrostatic chart recorder, while the other is generated by software using the outputs of the bank of filters spectrum analyzer and displayed on a colour monitor.

Additional software was written to enable the results of the automatic detection and classification software to be added to the side scan map. The automatic detection software gives an indication of the likelihood of a target being man-made; the five most likely detected targets can thus be displayed on the map, with different colours indicating the likelihood of the target being of interest. Alternatively, the indication of detected targets can be suppressed. In either case, the most likely target is analyzed using the automatic classification software; if this software determines that the target is man-made, its position is marked on the side scan map with a red marker. Such a probability map is shown in Figure 10.16.

10.4 DISCUSSION

The photographs included in this chapter are static reproductions of display images which frequently exhibited considerable temporal variations. Although the backscatter fluctuated randomly, these fluctuations were not distracting to operators. However, some target echoes fluctuated (when the target was slightly moved by tidal swells, for instance). The observation of these temporal variations provided a further basis for classifying or identifying targets that is not evident from the photographs.

Recall from Chapter 5 that the human visual and auditory perception mechanism can integrate displays to extract weak signals from noise. In a practical side scan sonar with a 3 degree beam and operating at a forward vessel speed of 20 knots, a target at a range of 200m will be in the sonar's field of view for some 600ms, or just more than one pulse repetition period or sweep period. Under these conditions, further (visual) integration is

impossible and the photographs will provide as much information as the original displays. However, if the vessel speed is reduced to enable a longer examination of the targets, the effect of target fluctuations on the displays may provide additional information useful for classification. During the trials of the Classification Sonar, the transducers were fixed to the wharf, and consequently targets could be examined for lengthy periods.

Photographs of visual displays can approximate visual integrations. For example, a photograph of an A-scan where the exposure time is much longer than the response time of the analyzer bins may reveal a peak amplitude or a hole in the baseline (e.g. Figure 10.6(e) above) that would not be discernible with a short exposure. Similarly, a photograph of a stack plot enables visual integration along the slanted y-axis to detect a target that may not be apparent if only a small portion of the stack plot were visible (e.g. Figure 10.6(a) above). However, the extent of integration possible with photographs is limited by practical exposure times for A-scans, and to one sweep for stack plots, while operators may view the displays for longer periods. Consequently, some information may be lost when viewing the photographs compared to the original, dynamic displays.

A further source of information available to the operator but impossible to reproduce in print is the auditory display. However, while an auditory output forms a useful and important part of many CTFM sonars (see Section 2.2.10), operators found that the audio output of the Classification Sonar did not significantly aid target classification or identification. Operators familiar with the auditory displays of other CTFM sonars found that there was insufficient audio information to discern useful differences between targets.

The audio output did prove to be very useful as an aid to manual target detection. Many smaller targets were difficult if not impossible to detect on the full range visual displays, while their presence was frequently apparent from the auditory display, which would produce a discernible tone whenever the zoom function was centred on the relevant cell. Hence, although an auditory output does not contribute to automatic detection and classification, such a display is a worthwhile feature if any manual target detection is to be carried out. Furthermore, an auditory display has the advantage of any audio warning device over a visual warning: the operator can be alerted to the presence of a target without consciously paying attention to any displays.

The Classification Sonar had a theoretical range resolution of $c/\Delta F$, or 6.6mm in air and 3cm in water. This range resolution was confirmed in air; measurement of the range resolution underwater was limited by the spacing of the spectral lines of the spectrum analyzer in use to 5cm. Nonetheless this represents a significant improvement over pulsed sonars with comparable maximum ranges. Flemming et al. (1982) list a selection of modern commercial side scan sonars, for which the shortest pulse length is 0.1ms, which seems to be a lower limit determined by cavitation constraints. Such a pulse length limits the range resolution to around 7.5cm underwater. High frequency pulsed sonars can operate with shorter pulse lengths, but the maximum range attainable is then reduced. The Klein Hydroscan, for example, operates at 500 kHz, but its pulse length is still 0.1ms to enable operation out to 100m. The Classification Sonar, on the other hand, can operate with its 5cm resolution out to the maximum range of 200m. Furthermore, this resolution may be sacrificed to obtain a faster filter response time. The trade-off between range resolution and response time enables the sonar to be operated according to conditions, and represents a feature no pulsed sonar can match.

Air modelling experiments indicated that the Classification Sonar should be able to detect and classify a variety of man-made objects. This prediction was confirmed during the sea trials. The real-time spectrum analyzer enables received echoes to be presented on several displays, enabling operators to continuously appraise incoming data in real-time. Classification may thus be based on operator judgement, or may occur independently of an operator using the automatic detection and classification software. This software also operates in real-time, a feature not matched by other attempts at underwater classification (e.g. Martin & Au, 1978; and Deuser et al., 1979).

Apart from these advantages over pulsed systems, the Classification Sonar represents a significant advance over previous underwater CTFM sonars. The largely digital implementation of the sonar ensures a high degree of flexibility, and more importantly, enables the detection and classification software to be incorporated. This software can be adapted (manually or automatically) to suit particular environmental conditions or targets. Overall, the sonar is a powerful tool for underwater target classification, and its flexibility makes the sonar suitable for a wide variety of tasks.

Fig. 10.16 (facing page) : Photograph taken from the colour monitor showing a scan of the seabed on which two man-made targets had been placed. The red markers indicate that the targets have been detected and subsequently classified as being man-made. The target on the right gives a strong echo (as indicated by the grey-scale); detection and classification can therefore be expected. Note however that the target on the left has a very weak echo (weaker in fact than much of the backscatter from the seabed). Nonetheless the software detects and correctly classifies this target.

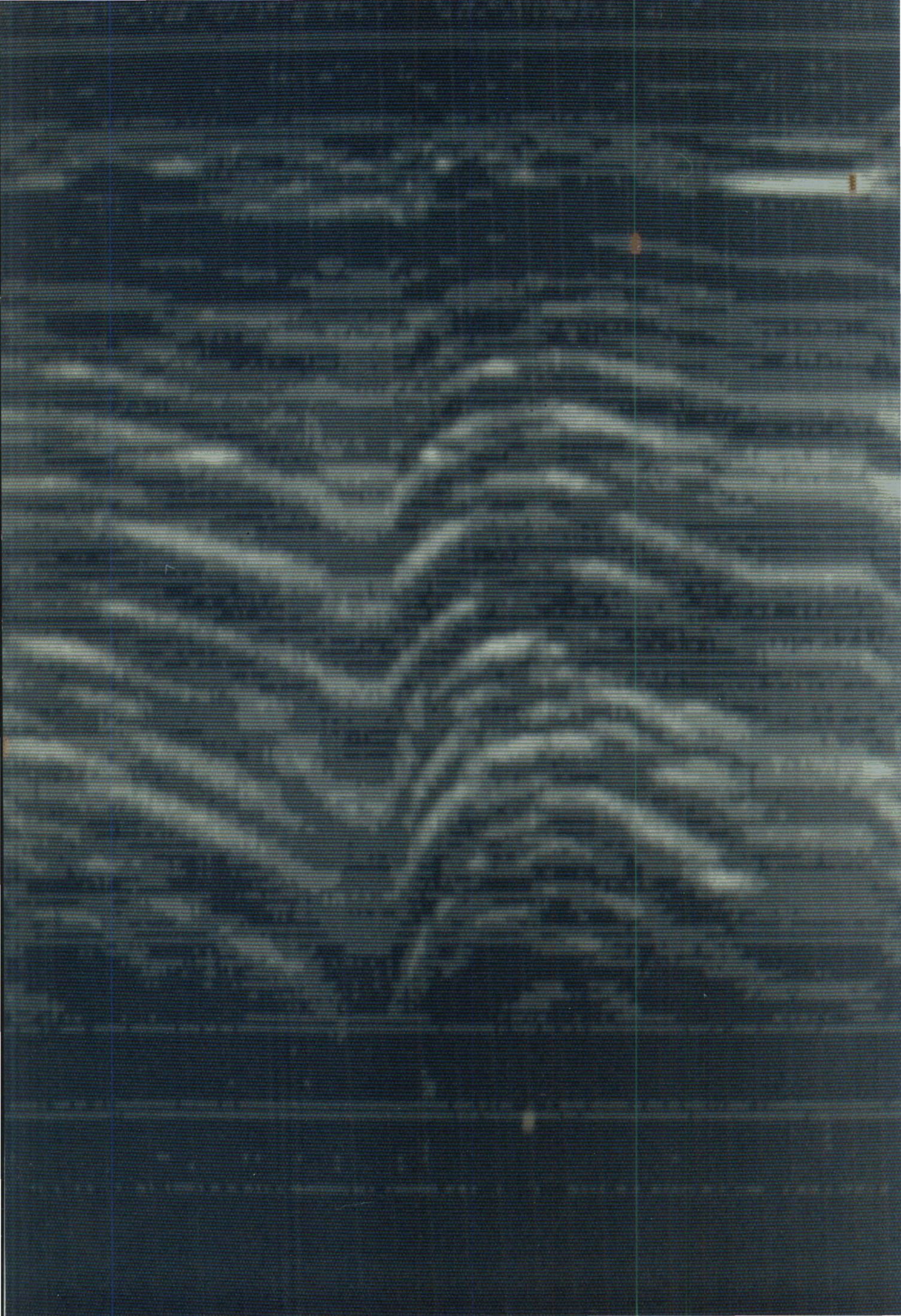

CHAPTER 11

CONCLUSIONS

Conclusions relating to specific areas of research covered in this thesis have been discussed at the ends of the relevant chapters. In this final chapter, conclusions relating the research as a whole are given, along with suggestions and recommendations for further research.

11.1 SONAR TECHNOLOGY

It has been seen that given identical system parameters such as time-bandwidth products and transmitted energies, pulsed and CTFM sonars can achieve identical performance (e.g. range resolution and maximum range attainable). However, in operation, there are practical differences between pulsed and CTFM sonars which can result in considerably different performance capabilities. For example, range resolution can be traded for response time in CTFM sonars, something pulsed sonars cannot do once the maximum range has been established. Similarly, CTFM outputs may be effectively processed aurally, and the greater energy output generally available with CTFM sonars results in a greater maximum range capability compared to pulsed sonars.

Particular applications of CTFM technology may capitalize on only one or several of these advantages. For example, the Diver's Sonar capitalizes on the convenient auditory display available with CTFM sonars, enabling a diver to operate his sonar even in murky waters. The Classification Sonar, on the

other hand, mainly capitalizes on the trade-off between range resolution and response time to classify targets: a fast response time is used (with a poor range resolution) to locate potential targets, and then a high resolution analysis is invoked (with a correspondingly slower response time) to classify the target.

Of course, the development of a particular CTFM sonar need not be motivated by a single feature of CTFM sonars. For example, it has been shown that the inclusion of an auditory display as an adjunct to a visual output increases the channel capacity of an operator interpreting the sonar's output. Thus, the addition of the auditory display is a bonus available using CTFM technology.

A practical and viable technique of eliminating blind time has been developed, thereby improving the quality of auditory displays, and enabling the full range resolution as determined by the transmitted bandwidth to be attained. Furthermore, air modelling has been seen to be an effective means of rigorously testing, evaluating, and modifying system concepts and parameters. In particular, the statistical basis of the software incorporated in the Classification Sonar was developed using an air model of the underwater sonar.

More generally, the elimination of blind time, the incorporation of digital frequency synthesis into CTFM sonar front ends, and the digital signal processing of sonar outputs has resulted in a new generation of CTFM sonars capable of tasks previously not attempted. For example, all operating parameters (sweep rate, equalization function, etc.) may be under computer control. A sonar designed for use underwater can thus rapidly be adapted for use in air by changing the transducers, their associated amplifiers, and a few parameters such as the sweep rate. Similarly, with the outputs of the spectrum analyzer in digital form, the echoes can be analyzed by a variety of software, the parameters of which may be changed during operation.

The Diver's Sonar and Classification Sonar detailed in this thesis are examples of a technology providing features not found on contemporary sonars. The quality of the auditory output (the only display on the Diver's Sonar) enables the diver the locate and classify a wide variety of targets. Similarly, the high resolution A-scan and stack plot displays on the

Classification Sonar enable considerable target classification, while the sonar outputs may also be processed by software to provide automated target detection and classification. These features represent significant advances in classification technology.

11.2 FUTURE DEVELOPMENTS

Despite the technological advances discussed in this dissertation, there is much scope for further development. For example, the development of the detection and classification software required feedback from sea trials, so that most of the software was written towards the end of the project as the trials progressed. Consequently, many improvements should be possible. Similarly, all processing after the spectrum analyzer takes place digitally; as electronic technology advances, additional stages may progressively be converted to digital form, so that demodulation and spectrum analysis may be entirely performed digitally. Full digital control of the system will greatly facilitate development of new sonar systems such as sophisticated robot sonars or forward looking scanning sonars.

The Classification Sonar described in this dissertation was designed as a side scan sonar providing one dimension of spatial information, (i.e. range), and target frequency signature. (The second dimension on a side scan map results from the forward vessel motion.) An interesting progression would be a forward looking scanning sonar providing three dimensions of spatial information (bearing, elevation, and range) in addition to target frequency signature. Range would still be coded using the demodulated frequency, and bearing and elevation could be provided by using a two-dimensional phased array.

The information conveyed to an operator by such a sonar would be limited by the display mechanism used. The Stack Plot display used in the Classification Sonar has three dimensions (range, echo amplitude, and ultrasonic illuminating frequency), but only presents one spatial dimension. It would be challenging to develop a display that would present all three spatial dimensions simultaneously as well as target frequency response. Such a display can be envisaged using a high definition colour monitor: the x-axis

would correspond to bearing, the y-axis would correspond to elevation, and range could be coded in one of several manners such as colour and/or size of markers indicating the positions of targets. If sufficient screen resolution were available, stack plots could be displayed next to or instead of the target markers; the size of a stack plot could be made inversely proportional to the target's range, and its colour could be coded by classification software to give an idea of the "importance" of the target.

The sonar and display mechanism described above would be ideally suited to Remote Operated Vehicle (ROV) applications - the operator controlling the ROV could look "into" the screen and perceive the environment in front of the submersible as if he were on board.

Whether this technology is used as an integral part of a forward looking scanning sonar, a side scan imaging sonar, or a robot imaging system, the unique properties of CTFM sonars make them eminently suitable for further development.

APPENDIX I

DIVER'S SONAR SPECIFICATIONS

Transmitted bandwidth :	65 kHz
Centre frequeny :	197.5 kHz
Beam widths (3-dB) :	
vertical (all transducers)	14°
horizontal (centre channel receiver)	7°
horizontal (transmitter & side channels)	53°
Directivity Index of transmitter :	17 dB
SPL @ 1m :	65 dB re 1μbar/V
Splay angle :	15°
Maximum range :	40 m
Sweep period :	100-800 ms
Audio output bandwidth :	5 kHz
Battery life (per charge) :	9 hr

APPENDIX II

CLASSIFICATION SONAR SPECIFICATIONS

Transmitted bandwidth :	50 kHz
Centre frequeny :	75 kHz
Beam widths (3-dB) :	
transmitter (horizontal)	3°
transmitter (vertical)	20°
receiver (horizontal)	10°
receiver (vertical)	30°
Transmitter response :	175 dB re 1μPa/V
Approximate receiver sensitivity :	-190 dB re 1V/μPa
Maximum operating range :	200 m
Sweep period :	533 ms
Display bandwidth (demodulator output) :	25 kHz
Range resolution :	5 cm
Low resolution filter bandwidth :	350 Hz
High resolution filter bandwidth :	6 Hz

APPENDIX III

MINIMUM TARGET STRENGTH REQUIREMENTS FOR THE CLASSIFICATION SONAR

Assume the system is reverberation limited. Then

$$TS(min) = S/N(min) + \{ 10 \log(area) + Ss \} - IF$$

where TS(min) is the minimum target strength required for target detection;
S/N(min) is the minimum signal to noise ratio required for target detection;
Ss is the backscatter strength per square metre;
IF is the integration improvement factor.

At 200m, a low resolution range cell is 3m x 7m = 21m. Assume further that we require a S/N(min) of 10 dB for detection and that the filter outputs are independent so that IF = 5 log N, where N is the sweep period multiplied by the filter bandwidth, i.e.

area = $21m^2$
S/N = 10
Ss = -40 dB for mud
Ss = -20 dB for rock
N = 533ms x 350 Hz

Then $TS(min) = 10 + \{10\log(21) - 40\} - 5\log(0.533 \times 350)$
$= -28$ dB for mud

Similarly, TS(min) = -8 dB for a rock seabed.

When using the high resolution filters, the resolution range cell at 200m is 5cm x 7m = 0.35m^2. Hence for the high resolution filters,

$$TS(min) = 10 + 10\log(0.35) - 40 - 5\log(0.533 \times 6)$$

$$= -37 \text{ dB for a mud seabed,}$$

and $TS(min) = -17$ dB for a rock seabed.

REFERENCES

Abramowitz, Milton & Stegun, Irene A. (1972) "Handbook of Mathematical Functions", Dover Publications.

Altes, R.A. & Titlebaum, E.L. (1970) "Bat Signals as Optimally Doppler Tolerant Waveforms", JASA, Vol. 48, No. 4 (Part 2), pp 1014-1020.

Altes, R.A. & Reese, W.D. (1975) "Doppler Tolerant Classification of Distributed Targets - a Bionic Sonar", IEEE Transactions on Aerospace and Electronic Systems, Vol. AES-11, No. 5, Sept., pp 708-723.

Altes, Richard A. (1976) "Sonar for Generalized Target Description and its Similarity to Animal Echolocation Systems", JASA, Vol. 59, No. 1, Jan., pp 97-105.

Altes, Richard A. (1980) "Detection, Estimation and Classification with Spectrograms", JASA, Vol. 67, No. 4, April, pp 1232-1246.

Altes, Richard A. (1981) "Review of Animal Sonar Systems", Technical Memorandum No. TM-186, Orincon Corp., June, 43 pp.

Altes, Richard A. (1982) "Radar/Sonar Signal Design for Bounded Doppler Shifts", IEEE Transactions on Aerospace and Electronic Systems, Vol. AES-18, No. 4, July, pp 369-380.

Anderson, Victor C. (1972) "The First Twenty Years of Acoustic Signal Processing", JASA, Vol. 51, No. 3 (Part 2), pp 1062-1065.

Au, Whitlow W.L. & Hammer, Clifford E. (1980) "Target Recognition via Echolocating by Tursiops Truncatus", in 'Animal Sonar Systems', edited by Busnel & Fish, Plenum Press, pp 855-858.

Bach-y-Rita, P., Collins, C.C., Saunders, F.A., White, B. & Scadden, L. (1969) "Vision Substitution by Tactile Image Projection", Nature, Vol. 221, pp 963-964.

Bailey, W.N., Buss, D.D., Hite, L.R. & Whatley, M.W. (1975) "Radar Video Processing Using the CCD Chirp Z Transform", CCD '75 Proceedings, San Diego, Oct., pp 283-290.

Barton, D.K. (1978) "Detection and Measurement", in 'Radar Technology' edited by Eli Brookner, Artech Publications, pp 69-79.

Bates, R.H.T. (1964) "Graphical Presentation of the Statistics of Fluctuating Target Detection by Pulse Radar", Mitre Corporation, Research note SR-120, Nov.

Bates, R.H.T. (1966) "Statistics of Fluctuating Target Detection", IEEE Transactions on Aerospace and Electronic Systems, Vol. AES-2, No. 1, Jan., pp 137-138.

Bates, R.H.T. (1971) "A Theorem for Wide Bandwidth Echo-location Systems", J. Sound Vib., Vol. 16, No. 2, pp 223-230.

Bauer, B.B. & Torick, E.L. (1965) "Calibration and Analysis of Underwater Earphones by Loudness-Balance Method", JASA, Vol. 37, No 6, June, p 1210.

Benjamin, R. (1966) "Modulation, Resolution and Signal Processing in Radar, Sonar and Related Systems", Pergamon Press, 184pp.

Bergland, G.D. (1969) "A Guided Tour of the Fast Fourier Transform", IEEE Spectrum, Vol. 6, No. 7, July, pp 41-52.

Beuter, Karl (1985) "Sound Pattern Recognition Supports Automatic Inspection", Sensor Review, Jan., pp 13-17.

Bird, John S. (1982) "Calculating Detection Probabilities for Systems Employing Noncoherent Integration", IEEE Transactions on Aerospace and Electronic Systems, Vol. AES-18, No. 4, July, pp 401-409.

Boys, J.T., Mason, J.L. & Hodgson, R.M. (1978) "Improved Continuous Wave Frequency Modulated Sonars with Aural Displays", Ultrasonics, Vol. 16, No. 3, May, pp 123-126.

Boys, J.T., Strelow, E.R. & Clark, G.R.S. (1979) "A Prosthetic Aid for a Developing Blind Child", Ultrasonics, Vol. 17, No. 1, Jan., pp 37-42.

Brabyn, J.A., Sirisena, H.R. & Clark, G.R.S. (1978) "Instrumentation System for Blind Mobility Aid Simulation and Evaluation", IEEE Transactions on Biomedical Engineering, Vol. BME-25, No. 6, Nov., pp 556-559.

Brabyn, J.A. (1978) "Laboratory Studies of Aided Blind Mobility", Ph.D. Thesis, University of Canterbury, New Zealand.

Brabyn, J.A., Collins, C.C. & Kay, L. (1981) "A Wide Bandwidth CTFM Scanning Sonar with Tactile and Acoustic Display for Persons with Impaired Vision", Ultrasonics International '81 Conference Proceedings, IPC Science and Technology Press, pp 348-353.

Brown, Michael K. (1985) "Feature Extraction Techniques for Recognizing Solid Objects with an Ultrasonic Range Sensor", IEEE Journal of Robotics and Automation, Vol. RA-1, No. 4, Dec., pp 191-205.

Bruel & Kjaer (1980) "Introduction to Underwater Acoustics", Bruel & Kaer, Naerum, Denmark.

Busnel, Rene-Guy & Fish, James F. (editors) (1980) "Animal Sonar Systems", Proceedings of the 2nd International Interdisciplinary Symposium on Animal Sonar Systems, NATO Advanced Study Institute Series A, Life Sciences, Vol. 28, Plenum Press.

Buss, D.D., Veenkant, R.L., Brodersen, R.W. & Hewes, C.B. (1975) "Comparison Between the CCD CZT and the Digital FFT", CCD '75 Proceedings, San Diego, Oct., pp 267-281.

Cable, P.G. (1977) "Maximum Likelihood Detection of Signals in Noise of Unknown Level", in 'Aspects of Signal Processing, Part 1', G. Tacconi (ed.), pp 229-250, Reidel Publishing Co.

Cady, Walter G. (1949) "A Theory of the Crystal Transducer for Plane Waves", JASA, Vol. 21, No. 2, March, pp 65-73.

Carr, A.E., Cuthbert, L.G. & Olver, A.D. (1981) "Digital Signal Processing for Target Detection in FMCW Radar", IEE Proceedings, Vol. 128, Part F, No. 5, Oct., pp 331-336.

Chesterman, W.D., Clynick, P.R. & Stride, A.H. (1958) "An Acoustic Aid to Seabed Survey", Acustica, Vol. 8, pp 285-290.

Chestnut, Paul C., Landsman, Helen & Floyd, Robert W. (1979) "A Sonar Target Recognition Experiment", JASA, Vol. 66, No. 1, July, pp 140-147.

Chestnut, Paul C. & Floyd, Robert W. (1981) "An Aspect Independent Sonar Target Recognition Method, JASA, Vol. 70, No. 3, Sept., pp 727-734.

Clarricoats, P.J.B. (1977) "Portable Radar for the Detection of Burried Objects", in 'Radar 77', IEE Conference Publication No. 155, 25-28 Oct., pp 547-550.

Colldeweih, I.R., Walls, E.L. & Lee, R.D. (1961) "Portable Sonar for Frogmen", Electronics, 29th Dec., pp 37-39.

Cook, Charles E. (1960) "Pulse Compression - Key to More Efficient Radar Transmission", Proc. I.R.E., Vol. 48, No. 3, March, pp 310-316.

Cook, Charles E. & Bernfeld, Marvin (1967) "Radar Signals - an Introduction to Theory and Application", Academic Press, New York.

Cox, D.R. & Hinkley, D.V. (1978) "Problems and Solutions in Theoretical Statistics", Chapman & Hall.

Cram, L.A. & Staveley, J.R. (1977) "Recent Developments in Scale Modelling of Radar Reflections By Radar and Sonar Methods", in 'Radar 77', IEE Conference Publication No. 155, 25-28 Oct., pp 473-475.

Cusdin, Michael J. & de Roos, Adolf (1984) "CTFM Sonar Enhances Diver's Eyes with Sound", Sea Technology, Vol. 25, No. 9, Sept., pp 44-46.

Cusdin, M.J., de Roos, A., Gough, P.T. & Sinton, J.J. (1984) "A New Type of CTFM sonar with no Blind Time and a One Octave Bandwidth", New Zealand National Electronics Conference Proceedings, Vol. 21, pp 59-64.

Cusdin, M.J., de Roos, A., Gough, P.T. & Sinton, J.J. (1985) "A New Type of CTFM sonar with no Blind Time and a One Octave Bandwidth", New Electronics, April, pp 31-33.

Cutrona, Louis J. (1975) "Comparison of Sonar System Performance Achievable using Synthetic-aperture Techniques with the Performance Achievable by more Conventional Means", JASA, Vol. 58, No. 2, August, pp 336-348.

Deley, G.W. (1970) "Waveform Design", Chapter 3 of 'Radar Handbook', edited by M.I. Skolnik, McGraw Hill.

de Roos, A., Kay, L., Cusdin, M.J. & Vernon, A.N. (1981) "A Sonar Aid for Divers using Binaural Displays", Ultrasonics International '81 Conference Proceedings, IPC Science and Technology Press, pp 171-175.

de Roos, Dolf, Cusdin, M.J., Kay, L. (1983) "A Diver's Sonar with Auditory Display", Transactions of the Institution of Professional Engineers of New Zealand, Vol. 10, No. 2, July, pp 55-58.

Deuser, Larry M. & Middleton, David (1979) "On the Classification of Underwater Acoustic Signals. I. An Environmentally Adaptive Approach", JASA, Vol. 65, No. 2, Feb., pp 438-443.

Deuser, Larry M., Middleton, David, Plemons, Terry D. & Vaughan, J. Kenneth (1979) "On the Classification of Underwater Acoustic Signals. II. Experimental Applications Involving Fish", JASA, Vol. 65, No. 2, Feb., pp 444-455.

Diercks, K. Jerome & Hickling, R. (1967) "Echoes from Hollow Aluminium Spheres in Water", JASA, Vol. 41, No. 2, pp 380-393.

Diercks, K.J. & Goldsberry, T.G. (1970) "Target Strength of a Single Fish", JASA, Vol. 48, No. 1 (Part 2), pp 415-416.

Di Franco, J.V. & Rubin, W.L. (1968) "Radar Systems", Prentice-Hall, 654 pp.

Dijkgraaf, S. (1943) "Over een merkwaardige functie van den gehoorsin bij vleermuizen", Verslagen Nederlandische Akademie van Wetenschappen Afdeling Naturkunde, Vol. 52, pp 622-627.

Dijkgraaf, S. (1946) "Die Sinneswelt der Fledermause", Experientia, Vol. 2, pp 438-448.

Dix, J.F. & Palmer, H.N.C. (1984) "Study of the Relative Sonar Performance of Incoherent and Coherent Processing against Echo Fading in Shallow Water", IEE Proceedings, Vol. 131, Part F, No. 3, June, pp 308-314.

Do, M.A. & Kay, L. (1976) "Resolution in an Artificially Generated Multiple Object Auditory Sensations Space using New Auditory Sensations, Acustica, Vol. 36, No. 1, pp 9-16.

Do, M.A. (1977) "Perception of Spatial Information in a Multiple Object Auditory Space", Ph.D Thesis, University of Canterbury, New Zealand.

Do, M.A. & Surti, A.M. (1982) "Accumulative Uncertainties in the Quantitative Evaluation of Signals from Fish", Ultrasonics, Vol. 20, No. 5, Sept., pp 217-223.

Dreher, John J. (1966) "Bistatic Target Signatures and their Acoustic Recognition - A suggested Animal Model", Douglas Advanvced Research Laboratories Paper No. 3900, Communication No. 3, Feb., 34 pp.

Dybedal, J., Ingebrigtsen, K.A. & Lovik, A. (1985) "A High Resolution Sonar for Sea-bed Imaging", Ultrasonics, Vol. 23, No. 2, March, pp 71-76.

Dziedzic, Zdzislaw-Albin (1978) "Experimental Study of the Sonar Emissions of Certain Delphinids", Doctoral Thesis, University of Paris, published by Applied Research Laboratories, University of Texas at Austin.

Engelson, Morris (1969) "Spectrum Analyzer Circuits", Tektronix Inc.

Escudie, E. & Hellion, A. (1975) "Etude Bionique des Systemes Sonar Animaux a l'aide du Traitement du Signale et de la Theorie des Communications par le Laboratiore Traitement du Signal de l'I.C.P.I.", Revue - Cethedec, Vol. 12, Part 44, pp 77-88.

Fay, Richard R. (1974) "Auditory Frequency Discrimination in Vertebrates, JASA, Vol. 56, No. 1, July, pp 206-209.

Flatte, Stanley M. (ed.) (1979) "Sound Transmission through a Fluctuating Ocean", Cambridge University Press.

Flemming, B.W., Klein, M. & Denbigh, P.N. (1982) "Recent Developments in Side Scan Sonar Techniques", edited & published by W.G.A. Russel-Cargill, Central Acoustics Laboratory, Cape Town.

Flemming, M.A., Mulling, F.H. & Watson, A.W.D. (1977) "Harmonic Radar Detection Systems", in 'Radar 77', IEE Conference Publication No. 155, 25-28 Oct., pp 552-554.

Freedman, A. (1964) "An Experimental Examination of Acoustic Echo Structure", Acustica, Vol. 14, No. 2, pp 89-104.

Fung-I. Tseng & Tapan K. Sarkar (1982) "Enhancement of Poles in Spectral Analysis", IEEE Transactions on Geoscience and Remote Sensing, Vol. GE-20, No. 2, April, pp 161-168.

Gammel, P.M. (1981a) " Improved Ultrasonic Detection using the Analytic Signal Magnitude", Ultrasonics, Vol. 19, No. 2, March, pp 73-76.

Gammel, P.M. (1981b) "Analogue Implementation of Analytic Signal Processing for Pulse-echo Systems", Ultrasonics, Vol. 19, No. 6, Nov., pp 279-283.

Gardner, Mark B. (1968) "Historical Background of the Haas and/or Precedence Effect", JASA, Vol. 43, No. 6, pp 1243-1248.

Garner, W.R. & Miller, G.A. (1947) "The Masked Threshold of Pure Tones as a Function of Duration", J. Exptal. Psych., Vol. 37, pp 293-303.

Gjessing, Dat T. (1981) "Adaptive Techniques for Radar Detection and Identification of Objects in an Ocean Environment", IEEE Journal on Oceanic Engineering, Vol. OE-6, No. 1, Jan., pp 5-17.

Glisson, Tildon H., Black, Charles I. & Sage, Andrew P. (1970) "On Sonar Signal Analysis", IEEE Transactions on Aerospace and Electronic Systems, Vol. AES-6, No. 1, Jan., pp 37-49.

Gnanalingam, S. (1954) "An Apparatus for the Detection of Weak Ionospheric Echoes", Proc. IEE, Part III, Vol. 101, pp 243-248.

Gough, P.T., de Roos, A., Cusdin, M.J. (1984a) "Continuous Transmission F.M. Sonar with One Octave Bandwith and No Blind Time", IEE Proceedings, Vol. 131, Part F, No. 3, June, pp 270-274.

Gough, P.T., Cusdin, M.J., de Roos, A. & Sinton, J.J. (1984b) "A High Speed Side Scan Sonar based on Wide Band CTFM", Proceedings International Conference on Developments in Marine Acoustics, (Sydney, 4-6th Dec.), Australian Acoustical Society, pp 225-230.

Grace, O.D. & Pitt, S. (1968) "Quadrature Sampling of High-Frequency Waveforms", JASA, Vol. 44, No. 5, pp 1453-1454.

Green, J.R. & Margerison, D. (1979) "Statistical Treatment of Experimental Data", Elsevier.

Green, M.D. (1980) "The Detectability of a Mine using Replica Correlation (RC) and Echo-Echo Correlation (EEC)", Technical Report No. 535, Naval Oceans System Centre, April, 42 pp.

Griffin, D.R. & Galambos, R. (1941) "The Sensory Basis of Obstacle Avoidance in Flying Bats", Journal of Experimental Zoology, Vol. 86, pp 481-506.

Griffin, D.R. (1944) "How Bats Guide their Flight by Ultrasonics", American Journal of Phys., Vol. 12, p 342.

Griffin, D.R. (1950a) "The Navigation of Bats", Scientific American, Vol. 183, No. 2, August, pp 52-55.

Griffin, D.R. (1950b) "Measurement of the Ultrasonic Cries of Bats", JASA, Vol. 22, p 247.

Griffin, D.R. (1954) "Bird Sonar", Scientific American, Vol. 190, No. 3, March, pp 78-88.

Griffin, D.R. (1958a) "Listening in the Dark: the Acoustic Orientation of Bats and Men", Yale University Press, New Haven.

Griffin, D.R. (1958b) "More about Bat Radar", Scientific American, Vol. 199, No.1, July, pp 40-44.

Griffiths, J.W.R. (1953) "Signal/Noise Performance of Modified Detector Circuits", U.D.E. Pamphlet No. 161, April.

Griffiths, J.W.R., Pratt, A.R. & Stevens, P.J. (1978) "High Resolution Sonar Systems", Proc. Oceanology International '78, Technical Session J, pp 3-7.

Griffiths, J.W.R. (1983) "Adaptive Array Processing", IEE Proceedings, Vol. 130, Parts F & H, No. 1, Feb., pp 3-10.

Gudimetla, V.S. Rao & Holmes, J. Fred (1982) "Probability Density Function of the Intensity for a Laser-Generated Speckle Field after Propagation through the Turbulent Atmosphere, Journal of the Optical Society of America, Vol. 72, No. 9, Sept., pp 1213-1218.

Haber, Ralph Norman & Wilkinson, Leland (1982) "Perceptual Components of Computer Displays", IEEE Computer Graphics and Applications, Vol. 2, No. 3, May, pp 23-35.

Hald, A. (1960) "Statistical Theory with Engineering Applications, Wiley.

Hampton, L.D. & McKinney, C.M. (1961) "Experimental Study of the Scattering of Acoustic Energy from Solid Metal Spheres in Water", JASA, Vol. 33, No. 5, May, pp 664-673.

Hancock, John C. & Wintz, Paul A. (1966) "Signal Detection Theory", McGraw Hill.

Harris, Frederick J. (1978) "On the Use of Windows for Harmonic Analysis with the Discrete Fourier Transform", Proc. IEEE, Vol. 66, No. 1, Jan., pp 51-83.

Helstrom, Carl W. (1968) "Statistical Theory of Signal Detection", 2nd edn, Pergamon Press.

Hickling, R. & Means, R. W. (1968) "Scattering of Frequency-modulated Pulses by Spherical Elastic Shells in Water", JASA, Vol. 44, No. 5, pp 1246-1252.

Hicks, James W. Jr. & Hollien, Harry (1983) "Diver Navigation by Sound", Sea Technology, March, pp 37-45.

Hodgson, R.M. & Boys, J.T. (1977) "A Novel Prosthetic Sonar", Ultrasonics, Vol. 15, No. 3, May, pp 99-100.

Hoffman, J.F. (1971) "Classification of Spherical Targets Using Likelihood Ratios and Quadrature Components", JASA, Vol. 49, No. 1 (Part 1), Jan., pp 23-30.

Holliday, D.V. (1972) "Resonance Structure in Echoes from Schooled Palegic Fish", JASA, Vol. 52, No. 4 (Part 2), pp 1322-1332.

Holliday, D.V. (1974) "Doppler Structure in Echoes from Schools of Palegic Fish", JASA, Vol. 55, No. 6, June, pp 1313-1322.

Howes, M.J. & Morgan, D.V. (editors) (1979) "Charge-Coupled Devices and Systems", Wiley.

Hulst, A.P. (1973) "On a Family of High Powered Transducers", Ultrasonics International 1973 Conf. Proc., pp 285-293.

Hunt, F.V. (1972) "The Past Twenty Years in Underwater Acoustics: an Introductory Retrospection", JASA, Vol. 51, No. 3 (Part 2), pp 992-993.

Jarvis, R.A. (1983) "A Perspective on Range Finding Techniques for Computer Vision", IEEE Transactions on Pattern Analysis and Machine Intelligence, Vol. PAMI-5, No. 2, March, pp 122-139.

Jobst, William J. & Talivaldis, I. Smits (1974) "Mathematical Model for Volume Reverberation: Experiment and Simulation", JASA, Vol. 55, No. 2, Feb., pp 227-236.

Johnson, Norman L. & Leone, Fred C. (1977) "Statistics and Experimental Design in Engineering and the Physical Sciences", Vol. 1, 2nd edn, Wiley.

Johnson, Richard A. & Titlebaum, Edward L. (1976) "Energy Spectrum Analysis: a Model of Echolocation Processing", JASA, Vol. 60, No. 2, August, pp 484-491.

Kanciruk, Paul (1982) "Hydroacoustic Biomass Estimation Techniques", Oak Ridge National Laboratory TM-8304, Nureg CR-2838, Environmental Sciences Division Publication No. 2019.

Kay, L. (1959) "A Comparison between Pulse and Frequency Modulation Echo-Ranging Systems", Journal of the British I.R.E., Vol. 19, No. 2, Feb., pp 105-113.

Kay, L. (1960) "An Experimental Comparison between a Pulse and a Frequency-Modulation Echo-Ranging System", Journal of the British I.R.E., Vol. 20, No. 10, Oct., pp 785-796.

Kay, L. (1962a) "A Plausible Explanation of the Bat's Echo-Location Acuity", Animal Behaviour, Vol. 10, Nos. 1-2, January-April, pp 34-41.

Kay, L. (1962b) "Auditory Perception and its Relation to Ultrasonic Blind Guidance Aids", Journal of the British I.R.E., Vol. 24, No. 4, Oct., pp 309-317.

Kay, L. & Pickvance, T.J. (1963) "Ultrasonic Emissions of the Lesser Horseshoe Bat Rhinolophus Hipposideros (Bech.)", Proc. Zoological Society of London, Vol. 141, Part 1, July, pp 163-171.

Kay, L. (1964) "An ultrasonic Sensing Probe as a Mobility Aid for the Blind", Ultrasonics, April-June, pp 53-59.

Kay, L. & Bishop, M.J. (1965) "The Effect of a Linear Phase Taper on the Near Field of an Ultrasonic Multi-Element Array", The Radio and Electronic Engineer, Vol. 29, No. 4, April, pp 207-212.

Kay, L. (1974) "A Sonar Aid to Enhance Spatial Perception of the Blind : Engineering Design and Evaluation", Radio and Electronic Engineer, Vol. 44, No. 11, Nov., pp 605-627.

Kay, L. & Do, M.A. (1976) "An Artificially Generated Multiple Object Auditory Space for Use where Vision is Impaired", Acustica, Vol. 36, No. 1, pp 1-8.

Kay, L., Boys, J., Clark, G. & Mason, J. (1977) "The Echocardiophone: a new means for Observing Spatial Movement of the Heart", Ultrasonics, Vol. 15, No. 3. May, pp 136-141.

Kay, L., Bui, S.T., Brabyn, J.A. & Strelow, E.R. (1977) " Single Object Sensor: A Simplified Binaural Mobility Aid", Journal of Visual Impairment and Blindness, May.

Kay, L. & Strelow, E.R. (1977) "Blind Babies Need Specially Designed Aids", New Scientist, June 23, pp 709-712.

Kay. L. (1980) "Air Sonar with Acoustical Display of Spatial Information", in 'Animal Sonar Systems', edited by R. Busnel & J. Fish, Plenum Press, pp 769-816.

Kay, L. (1981) U.S. Patent No. 4292678.

Kay, L., Kay, N., Sinton, J.J., de Roos, A. (1981) "Characterization of Surface and Volume Structure using an Air Sonar with Auditory Display for the Blind", Ultrasonics International '81 Conference Proceedings, IPC Science and Technology Press, pp 38-42.

Kay, L. (1985) "Airborne Ultrasonic Imaging of a Robot Workspace", Sensor Review, Jan., pp 8-12.

Kay, Steven M. & Marple, Stanley Lawrence (1981) "Spectrum Analysis - a Modern Perspective", Proc. IEEE, Vol. 69, No. 11, Nov., pp 1380-1419.

Knight, William C., Pridham, Roger G. & Kay, Steven M. (1981) "Digital Signal Processing for Sonar", Proc. IEEE, Vol. 69, No. 11, Nov., pp 1451-1506.

Kock, W.E. (1973) "Radar, Sonar and Holography", Academic Press, 140 pp.

Kramer, Stuart A. (1967) "Doppler and Acceleration Tolerances of High-Gain, Wideband Linear FM Correlation Sonars", Proc. IEEE, Vol. 55, No. 5, May, pp 627-636.

Kuhl, W., Schodder, E.R. & Schroder, F.K. (1954) "Condenser Transmitters and Microphones with Solid Dielectric for Airborne Ultrasonics", Acustica, Vol. 4, pp 519-532.

Kurie, F.N.D. (ed.) (1946) "FM Sonar Systems", Prepared by the Sonar Devices Division, University of California Division of War Research at the United States Navy Electronics Laboratory, San Diego, under U.S. Navy Contract NObs 2074 Task 3.

Lee, Henry E. (1979) "Extension of Synthetic Aperture Radar (SAR) Techniques to Undersea Applications", IEEE Journal on Oceanic Engineering, Vol. OE-4, No. 2, April.

Lindstrom, K., Mauritzon, L., Benoni, G., Svedman, P. & Willer, S. (1982) "Application of Air-borne Ultrasound to Biomedical Measurements", Medical and Biologiocal Engineering and Computing, May, pp 393-400.

Love, Richard H. (1975) "Predictions of Volume Scattering Strengths from Biological Trawl Data", JASA, Vol. 57, No. 2, Feb., pp 300-306.

Luyendyk, Bruce P., Hajic, Earl J., and Simonett, David S. (1983) "Side-scan Sonar Mapping and Computer-aided Interpretation in the Santa Barbara Channel, California", Marine Geophysical Researches, Vol. 5, pp 365-388.

Maginness, M.G. (1972) "The Reconstruction of Elastic Wave Fields from Measurements over a Transducer Array", Journal of Sound and Vibration, Vol. 20, No. 2, pp 219-240.

Manasse, R. (1960) "Summary of Maximum Theoretical Accuracy of Radar Measurements", Mitre Technical Series Report No. 2, SR-11, April.

Manes, G.F., Gerli, D., Tortoli, P. & Atzeni, C. (1983) "An Analogue Hilbert Transformer for Complex Waveform Detection", Ultrasonics, Sept., pp 211-214.

Marcum, J.I. (1960) "A Statistical Theory of Target Detection by Pulsed Radar", IRE Transactions on Information Theory, Vol. IT-6, No. 2, April, pp 59-267; originally published as research memorandum RM-754 for the U.S.A.F. Project Rand on 1 Dec., 1947 and reissued 25 April, 1952; ASTIA Document No. AD 101287.

Margolin, Jerome & McHugh, Paul G. (1981) "Radar Signal Processing: Digital, Charge-coupled Device (CCD) or Surface Acoustic Wave (SAW)?", Optical Engineering, Vol. 20, No. 5, Sept/Oct., pp 795-800.

Marsh, Henry W. Jr. (1975) "Progress in Underwater Acoustics", Part III of 'Underwater Sound - A Review', IEEE Transactions on Sonics and Ultrasonics, Vol. SU-22, No. 5, Sept., pp 333-335.

Marsh, K.A., Richardson, J.M., Schoenwald, J.S. & Martin, J.F. (1984) "Acoustic Imaging in Robotics Using a Small Set of Transducers", Proc. 4th International Conference on Robotic Vision and Sensory Controls, Oct., IFS Publications, pp 261-268.

Martin, Douglas W. & Au, Whitlow W.L. (1978) "Aural Discrimination of Target Echoes by Human Observers using Broadband Sonar Pulses", Naval Ocean Systems Center.

Martin, Douglas W. & Au, Whitlow W.L. (1978) "Aural Discrimination of Target Echoes in White Noise by Human Observers using Broadband Sonar Pulses", Naval Ocean Systems Center.

Martin, G. (1969) "Electronics and Transducers for an Ultrasonic Blind Mobility Aid", M.E. Thesis, University of Canterbury, New Zealand, March.

Martin, J.J. (1966) "Sea-surface Roughness and Acoustic Reverberation - an Operational Model", JASA, Vol. 40, No. 3, pp 697-710.

McCue, J.J.G. (1966) "Aural Pulse Compression by Bats and Humans", JASA, Vol. 40, No. 3, pp 545-548.

McKinney, C.M. & Anderson, C.D. (1964) "Measurements of Backscattering of Sound from the Ocean Bottom", JASA, Vol. 36, No. 1, Jan., pp 158-163.

Meyer, Charles R. (1982) "Preliminary Results on a System for Wide-band Reflection-mode Ultrasonic Attenuation Imaging", IEEE Transactions on Sonics and Ultrasonics, Vol. SU-29, No. 1, Jan., pp 12-17.

Miller, George A. (1956) "The Magical Number Seven, Plus or Minus Two: Some Limits on our Capacity for Processing Information", The Psychological Review, Vol. 63, No. 2, March, pp 81-97.

Miller, G.L., Boie, R.A. & Sibilia, M.J. (1984) "Active Damping Ultrasonic Transducers for Robotic Applications", IEEE Robotics Conference Proceedings, March.

Milne, P.H. (1980) "Underwater Engineering Surveys", E. & F.N. Spon Ltd, London.

Milne, P.H. (1983) "Underwater Acoustic Positioning Systems", E. & F.N. Spon Ltd, London.

Moore, David R. (1983) "Binaural Maps in the Brain", Nature, Vol. 301, 10th Feb., pp 463-465.

Neininger, Geunter (1977) "An FM/CW Radar with High Resolution in Range and Doppler; Application for Anti-collision Radar for Vehicles", in 'Radar 77', IEE Conference Publication No. 155, 25-28 Oct., pp 526-530.

Neppiras, E.A. (1973) "The Pre-stressed Piezoelectric Sandwich Transducer", Ultrasonics International '73 Conference Proceedings.

Neuweiler, G., Bruns, V. & Schuller, G. (1980) "Ears Adapted for the Detection of Motion, or How Echolocating Bats Have Exploited the Capacities of the Mammalian Auditory System", JASA, Vol. 68, No. 3, Sept., pp 741-753.

Newhouse, V.L., Bilgutay, N.M., Saniie, J. & Furgason, E.S. (1982) "Flaw-to-grain Echo Enhancement by Split-spectrum Processing", Ultrasonics, Vol. 20, No. 2, March, pp 59-68.

Ohman, Gunnar P. (1960) "Getting High Range Resolution with Pulse Compression Radar", Electronics, 7th Oct., pp 53-57.

Pierce, G.W. & Griffin, D.R. (1938) "Experimental Determination of Supersonic Notes Emitted by Bats", J. Mammal., Vol. 19, pp 454-455.

Plomp, R. (1964) "The Ear as a Spectrum Analyzer", JASA, Vol. 36, No. 9, Sept., pp 1628-1636.

Pye, J.D. (1960) "A Theory of Echo-location by Bats", J. Laryng. Otol., Vol. 74, p 718.

Pye, J.D. (1971) "Bats and Fog", Nature, Vol. 229, 19th Feb., pp 572- 574.

Pye, J.D. (1981) "Ultrasound and the Animal World", Ultrasonics International '81 Conference Proceedings, IPC Science and Technology Press, pp 1-9.

Pyketr, C.E. (1977) "Automatic Estimation of the Number of Radar Targets in a Resolution Cell", in 'Radar 77', IEE Conference Publication No. 155, 25-28 Oct., pp 164-167.

Rice, S.O. (1944) "Mathematical Anaysis of Random Noise, Part III, Statistical Properties of Random Noise Currents", Bell System Technical Journal, Vol. 23, pp 282-332, and Vol. 24, pp 46-156.

Richardson, L.F. (1912) British Patent Office patent no. 0074619.

Robertson, G.H. (1980) "Signal Characterization using Spectral Microanalysis", JASA, Vol. 67, No. 5, May, pp 1663-1669.

Roederer, Juan G. (1975) "Introduction to the Physics and Psychophysics of Music", 2nd edn., Springer-Verlag.

Ross, C.W. (1977) "A Miniature Air Sonar Altimeter", Ultrasonics International '77 Conf. Proc., IPC Science & Technology Press, pp 448-455.

Rowell, D. (1970) "Auditory Display of Spatial Information", Ph.D thesis, University of Canterbury, N.Z.

Russo, Donato M. & Bartberger, Charles L. (1965) "Ambiguity Diagram for Linear FM Sonar", JASA, Vol. 38, No. 2, August, pp 183-190.

Schroeder, Manfred R. (1971) "Models of Hearing", Proc. IEEE, Vol. 63, NO. 9, Sept., pp 1332-1350.

Schuller, G. (1979) "Coding of Small Sinusoidal Frequency and Amplitude Modulations in the Inferior Colliculus of 'CF-FM' Bat, Rhinolophus Ferrumequinum", Experimental Brain Research, Vol. 34, pp 117-132.

Schuller, G. (1977) "Echo Delay and Overlap with Emitted Orientation Sounds and Doppler-shift Compensation in the Bat, Rhinolophus Ferrumequinum", Journal of Comparative Physiology, Vol. 114, pp 103-114.

Schusterman, Ronald J. (1974) "Low False-alarm Rates in Signal Detection by Marine Mammals", JASA, Vol. 55, No. 4, April, pp 845-848.

Scorer, M. (1977) "An Advanced Man Portable Surveillance Radar", in 'Radar 77', IEE Conference Publication No. 155, 25-28 Oct., pp 29-32.

Shearman, E.D.R. (1980) "Remote Sensing of the Sea-surface by Dekametric Radar", Radio and Electronic Engineer, Vol. 50, No. 11/12, Nov/Dec., pp 611-623.

Sherman, Charles H. (1975) "Underwater Sound Transducers", Part I of 'Underwater Sound - A Review', IEEE Transactions on Sonics and Ultrasonics, Vol. SU-22, No. 5, Sept., pp 281-290.

Sherwin, Chalmers W., Kodman, Frank, Jr., Kovaly, John J., Prothe, Wilbert C. & Melrose, Jay (1956) "Detection of Signals in Noise : A Comparison Between the Human Detector and an Electronic Detector", JASA, Vol. 28, No. 4, July, pp 617-622.

Shorrock, G. & Woodward, B. (1984) "A Multiple Function Sonar Rangefinder for Divers", Ultrasonics, Vol. 22, No. 1, Jan., pp 16-24.

Sibul, L.H. & Titlebaum, E.L. (1981) "Volume Properties for the Wideband Ambiguity Function", IEEE Transactions on Aerospace and Electronic Systems, Vol. AES-17, No. 1, Jan., pp 83-86.

Simmons, James A. (1971) "Echolocation in Bats: Signal Processing of Echoes for Target Range", Science (AAAS), Vol. 171, No. 3974, 5th March, pp 925-928.

Simmons, James A. (1973) "The Resolution of Target Range by Echolocating Bats", JASA, Vol. 54, pp 157-173.

Simmons, James A., Lavender, W.A., Lavender, B.A., Doroshow, C.A., Kiefer, S.W., Livingston, R. & Scallet, A.C. (1974) "Target Structure and Echo Spectral Discrimination by Echolocating Bats", Science (AAAS), Vol. 186, No. 4169, 20th Dec., pp 1130-1132.

Skinner, D.P., Altes, R.A. & Jones, J.D. (1977) "Broadband Target Classification using a Bionic Sonar", JASA, Vol. 62, No. 5, Nov., pp 1239-1246.

Skolnik, Merrill I. (1980) "Introduction to Radar Systems", McGraw Hill.

Slaymaker, Frank H. & Meeker, Willard F. (1948) "Blind Guidance by Ultrasonics", Electronics, Vol. 21, May, pp 75-80.

Smith, D.J. (1981) "The Maximum Entropy Method", The Marconi Review, Vol. XLIV, No. 222, Third Quarter, pp 137-158.

Smith, J.M. (1977) "Problems Solved and Unsolved in Radar Detection Theory", in 'Radar 77', IEE Conference Publication No. 155, 25-28 Oct., pp 263-265.

Smith, R.P. (1972) "Transduction and Audible Displays for Broad Band Sonar Systems", Ph.D. thesis, University of Canterbury, N.Z.

Somers, M.L. & Stubbs, A.R. (1984) "Sidescan Sonar", IEE Proceedings, Vol. 131, Part F, No. 3, June, pp 243-256.

Swerling, P. (1960) "Probability of Detection for Fluctuating Targets", IRE Transactions on Information Theory, Vol. IT-6, No. 2, April, pp 269-308; originally published as research memorandum RM-1217 for the U.S.A.F. Project Rand on 17 March, 1954; ASTIA Document No. AD 80638.

Swets, John A., Green, David M., Getty, David J. & Swets, Joel B. (1977) "Identification and Scaling of Complex Visual Patterns", Technical Report No. 3536, Engineering Psychology Program, Office of Naval Research, Nov., 39 pp.

Tanner, Wilson P. Jr. & Swets, John A. (1954) "A Decision Making Theory of Visual Detection", Psych. Review, Vol. 61, No. 6, pp 401-409.

't Hoen, P.J. (1982) "Aperture Apodization to Reduce the Off-axis Intensity of the Pulsed-mode Directivity Function of Linear Arrays", Ultrasonics, Vol. 20, No. 5, Sept., pp 231-236.

Thomas, L.C. (1971) "The Biquad: Part I - Some Practical Design Considerations", IEEE Transactions on Circuit Theory, Vol. CT-18, pp 350-357.

Tucker, D.G. & Griffiths, J.W.R. (1953) "Detection of Pulse Signals in Noise", Wireless Engineer, Vol. 30, Nov., pp 264-273.

Tucker, D.G., Welsby, V.G., Kay, L., Tucker, M.J., Stubbs, A.R. & Henderson, J.G. (1959) "Underwater Echo-ranging with Electronic Sector Scanning: Sea Trials on R.R.S. Discovery II", Journal of the British I.R.E., Vol. 19, No. 11, Nov., pp 681-696.

Tucker, D.G. (1966) "Underwater Observation using Sonar", Fishing News Books Ltd.

Tucker, D.G. (1967) "Sonar in Fisheries - A Forward Look", Fisheries News Books Ltd.

Tucker, D.G. & Gazey, B.K. (1967) "Applied Underwater Acoustics", Pergamon, London.

Tucker, M.J. & Stubbs, A.R. (1961) "Narrow-beam Echo-ranger for Fishery and Geological Investigations", Brit. J. Appl. Physics, Vol. 12, No. 3, March, pp 103-110.

Urick, R.J. (1954) "The Backscattering of Sound from a Harbor Bottom", JASA, Vol. 26, No. 2, March, pp 231-235.

Urick, R.J. (1975) "Principles of Underwater Sound", 2nd edn., McGraw-Hill.

Urick, R.J. (1979) "Sound Propagation in the Sea", Defence Advanced Research Projects Agency publication number 008-051-00071-2.

Urkowitz, H., Hauer, C.A. & Koval, J.F. (1962) "Generalized Resolution in Radar Systems", Proceedings of the I.R.E., Oct., pp 2093-2105.

Voglis, G.M. & Cook, J.C. (1966) " Underwater Applications of an Advanced Acoustic Scanning Equipment", Ultrasonics, Vol. 4, Jan., pp 1-9.

von Biel, H.A. (1981) "A Statistical Assessment of Synoptic D-Region Partial Reflection Data", Journal of Atmospheric and Terrestrial Physics, Vol. 43, No. 3, pp 225-230.

von Schlachta, K. (1977) "A Contribution to Radar Target Classification", in 'Radar 77', IEE Conference Publication No. 155, 25-28 Oct., pp 135-137.

Wagner, Robert F., Smith, Stephen W., Sandrik, John M. & Lopez, Hector (1983) "Statistics of Speckle in Ultrasound B-Scans", IEEE Transactions on Sonics and Ultrasonics, Vol. SU-30, No. 3, May.

Wainstein, L.A. & Zubakov, V.D. (1962) "Extraction of Signals from Noise", translated from the Russian by R.A. Silverman, Prentice-Hall, 382 pp.

Wallerus, Heinz (1980) "Blindenorientierungshilfe mit Ultraschallsonargssystem und akustischer Anzeige", Acustica, Vol. 46, No. 2, Oct., pp 193-200.

Ward, Harold R. (1969) "The Effect of Bandpass Limiting on Noise with a Gaussian Spectrum", Proc. IEEE, Nov., pp 2089-2090.

Weast, Robert C. (ed.) (1981) "Handbook of Chemistry and Physics", 60th edn., 3rd printing, CRC Press.

Williams, Ross E. (1976) "Creating an Acoustic Synthetic Aperture in the Ocean", JASA, Vol. 60, No. 1, July, pp 60-73.

Willis, W.P. & Kay, L. (1970) "An Ultrasonic Position Sensor for Automatic Control", Radio & Electronic Engineer, Vol. 40, No. 6, Dec., pp 305-307.

Winder, Alan A. (1975) "Sonar System Technology", Part II of 'Underwater Sound - A Review', IEEE Transactions on Sonics and Ultrasonics, Vol. SU-22, No. 5, Sept., pp 291-332.

Wong, H. & Chesterman, W. (1968) "Bottom Backscattering Strengths Near Grazing Incidence in Shallow Water", JASA, Vol. 44, p 1713.

Woodward, P.M. (1964) "Probability and Information Theory, with Applications to Radar", 2nd edition, Pergamon Press.